

Assembly and detection of viruses and biological molecules on inorganic surfaces.

By Asher Keeling Sinensky

B.S. Materials Science and Engineering
University of California at Berkeley, 2002

Submitted to the Department of Materials Science and Engineering in partial fulfillment of the requirements for the degree of:

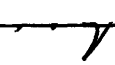
Doctorate of Philosophy (Ph.D.) in
Materials Science and Engineering at the
Massachusetts Institute of Technology

September, 2007,

Signature of Author: _____


Asher K. Sinensky
Dept. of Materials Science and Engineering
Submitted for Consideration on July 23rd, 2007

Certified By: _____


Prof. Angela M. Belcher
Germehausen Professor of Materials Science and Engineering and Biological Engineering
Thesis Supervisor

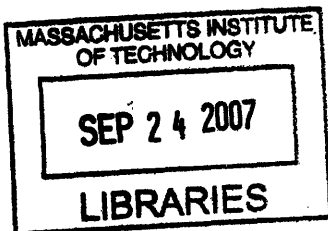
Accepted By: _____


Prof. Samuel M. Allen
POSCO Professor of Physical Metallurgy
Chair, Departmental Committee on Graduate Students

Thesis Committee Members:

Prof. Lionel C. Kimerling
Thomas Lord Professor of Materials Science and Engineering

Prof. Francesco Stellacci
Finmeccanica Assistant Professor of Materials Science and Engineering



ARCHIVES

Assembly and detection of viruses and biological molecules on inorganic surfaces.

By Asher Keeling Sinensky

Submitted to the Department of Materials Science and Engineering on July 23rd, 2007 in
partial fulfillment of the requirements for the degree of Doctorate of Philosophy in
Materials Science and Engineering.

Abstract

This work is composed of three distinct, albeit related, projects. Each project is an exploration of the ways in which interactions between inorganic surfaces and biological molecules can be advantageously exploited.

The first project entitled, *Biomolecular Recognition of Crystal Defects* extended the phage display technique to the detection of crystal defects. The system used is based on the M13 bacteriophage with 7-residue constrained random sequence on protein III. After considerable experimentation a procedure described as 'Diffuse Selection' was developed for selecting defects on crystal surfaces. Challenges occur because it is difficult to drive phage display towards the selection of particular surface features as opposed to whole surfaces. After multiple iterations, diffuse selection was optimized and consensus sequences were achieved. Virus binding was characterized using Atomic Force Microscopy, Fluorescence Microscopy and Titration. Using a simple bimolecular model, the binding sequence identified through this work is shown to have a binding constant 100,000 times better than a random peptide sequence.

The second project entitled, *Surface Patterning of Genetically Programmed Viruses*, developed a generalizable approach to patterning viruses regardless of the genetic modification made to the virus. Genetic modifications are made in order to create viruses which will construct inorganic materials on their bodies in the appropriate chemical environment. Three generalizable virus patterning approaches were developed based on hydrophobic, electrostatic and covalent binding approaches respectively. This work showed successful patterning using all three approaches, but only the covalent approach was shown to be an effective way to actually construct materials on the genetically programmed viruses.

The third and final project is entitled, *A Kelvin Probe Biosensor*. This project devised a label-free high-resolution scanning probe approach for detecting target biomolecules on nano-scaled features. In analogy to modern fluorescence microarrays, biological probes were patterned on a gold substrate. When the probes were exposed to a target analyte, the target would bind the probe and change the local surface potential. This change in surface potential could then be measured using Kelvin Probe Force Microscopy. This work represented the first example of detecting biological molecules on surface using KPFM at the nanoscale.

Acknowledgments

Firstly, I must acknowledge my family: Dr. Marita J Keeling (mother), Dr. Michael S Sinensky (father) Tamara K Sinensky (sister), Dr. Christine Keeling (Aunt), Mr. Curt Taylor (Uncle), Dr. John Keeling (Grandfather), Mrs. Marita Keeling (Grandmother) as well as my cousins and other family for the support throughout the years without which none of this would have been possible.

I would also like to acknowledge my fiancée, Amy E Mugg, for providing me with emotional support and an occasional respite from the rigors of graduate student life.

I would like to acknowledge my advisor, Prof. Angela M Belcher, for providing me with advice and guidance throughout my research and for ensuring that I always had the resources and freedoms necessary to pursue my projects wherever they may lead. Thank you for always having an open door.

I would like to thank my Thesis Committee, Professors Lionel C Kimerling and Francesco Stellacci, for providing insightful counsel on my research.

I would like to thank my lab mates and friends, particularly Peter Freed, Marshall Jung, Joseph Collins, Lewis Hyatt, Scott Litzelman, Carl Dohrman, Tim Mueller, Chris Fischer, Michelle Barron, Sreekar Bhaviripudi, Chung-Yi Chiang, David Gray, Rana Ghosh, Jennifer Hsieh, Ahmed 'Mo' Khalil, Steve Kottman, Eric Krauland, Andrew Magyar, Ki Tae Nam, Dr. Yun, Roberto Barbero, Dan Solis, and Brian Reiss for their friendship and help with whatever problems I encountered in my research.

I would like to acknowledge the Department of Homeland Security and the National Science Foundation for supplying me with fellowship support throughout my graduate career. Without this support, I don't know that I would have had the same freedom to pursue my goals.

I would like to thank the Materials Science Departments at the University of California at Berkeley and the Massachusetts Institute of Technology for providing me with an education that I will cherish for the rest of my life.

Finally, I would like to thank all the teachers who have given me so much throughout my life without receiving the reward or recognition that they truly deserve.

To all of you, there is nothing I can really do to repay you for what you have done for me. The best I can do is promise that I will use the gifts you have given me to the best of my abilities.

Thank you!

-Asher Keeling Sinensky

Author's Note

This is my dissertation thesis submitted for consideration of the award of Doctor of Philosophy (Ph.D.) from the Massachusetts Institute of Technology Department of Materials Science and Engineering. Included in this document is a detailed recounting of the major research projects I undertook while at MIT. This is in no way a complete account of everything I have accomplished during my graduate student career; rather it is an attempt to allow my most successful projects to be accessible to future generations.

This work is divided up into five sections; an introduction, three chapters on my research products and a short concluding section with closing remarks. The chapters are broken up thematically, but there are cases where a protocol is relevant to more than one chapter. In general, protocols are placed in appendices following each chapter and are referenced in the text where appropriate. Figures are placed at the end of each section and are referenced throughout the text. A full table of contents and listing of figures provide good reference points for finding material in the text.

Table of Contents

Title Page	1
Abstract.....	3
Acknowledgments	4
Author's Note	5
Table of Contents	6
Listing of Figures	9
Listing of Acronyms.....	11
Biographical Note.....	12
Introduction.....	15
• <i>Structure of this Dissertation</i>	16
<i>Int.1: My Work</i>	17
• <i>Biomolecular Defect Recognition</i>	17
• <i>Surface Patterning of Genetically Programmed Viruses</i>	18
• <i>Kelvin Probe Biosensor</i>	19
<i>Int.2: Experimental Techniques</i>	21
• <i>Phage Display</i>	21
• <i>Dip Pen Nanolithography</i>	23
• <i>Kelvin Probe Microscopy</i>	25
• <i>Figures for Section Int.2</i>	27
<i>Appendix I.A: Phage Display Protocol</i>	34
• <i>Figures for Appendix I.A</i>	36
<i>Appendix I.B: Mathematical Treatment of Vibrating Capacitor</i>	38
<i>Int.Ref: References</i>	39
Chapter 1: Biomolecular Recognition of Crystal Defects: A Diffuse Selection Approach	41
<i>1.1: Introduction</i>	41
• <i>Figures for Section 1.1</i>	43
<i>1.2: The First Iteration</i>	44
• <i>Figures for Section 1.2</i>	47
<i>1.3: Diffuse Selection</i>	48
• <i>Complementary substrates</i>	48
• <i>Combinatorial selection</i>	50
• <i>Positive and negative selections</i>	51
• <i>Specificity verification:</i>	52
• <i>Substrate characterization:</i>	53
• <i>Figures for Section 1.3</i>	54
<i>1.4: Results of Diffuse Selection</i>	55
• <i>Assessing binding efficiency</i>	55
• <i>Surface characterization</i>	58
• <i>Figures for Section 1.4</i>	59
<i>1.5: Discussion & Recommendations for Future Work</i>	67
• <i>Figures for Section 1.5</i>	71
<i>Appendix 1.A: Germanium Substrate Preparation</i>	73

<i>Appendix 1.B: AFM Quantification of Phage Binding</i>	74
<i>Appendix 1.C: Fluorescent Quantification of Phage Binding</i>	75
• <i>Figures for Appendix 1.C</i>	77
<i>Appendix 1.D: Agar Plate Titration Quantification of Phage Binding</i>	79
<i>Appendix 1.E: Surface Characterization Techniques</i>	80
<i>1.Ref: References</i>	81
Chapter 2: Surface Patterning of Genetically Programmed Viruses	83
2.1: <i>Introduction</i>	83
2.2: <i>Surface Patterning</i>	85
• <i>Figures for section 2.2</i>	86
2.3: <i>Three approaches to virus assembly</i>	87
• <i>Hydrophobic Attachment</i>	87
• <i>Divalent Chelation (Electrostatic Attachment)</i>	88
• <i>Covalent Attachment</i>	90
• <i>Figures for Section 2.3</i>	92
2.4: <i>Materials Assembly</i>	101
• <i>Figures for Section 2.4</i>	103
2.5: <i>Discussion & Recommendations for Future Work</i>	106
<i>Appendix 2.A: Gold Substrate Preparation</i>	107
<i>Appendix 2.B: Virus Patterning Protocol</i>	109
<i>Appendix 2.C: Divalent Chelation Activation of MHA</i>	112
<i>Appendix 2.D: Covalent (Carbodiimide) Activation of MHA</i>	113
• <i>Figures for Appendix 2.D</i>	114
<i>Appendix 2.E: Gold Nanoparticle Assembly/Imaging on Patterned Phage</i>	115
• <i>Figures for Appendix 2.E</i>	117
<i>Appendix 2.F: Siloxane Microcontact Printing Protocol</i>	118
<i>2.Ref: References</i>	120
Chapter 3: A Kelvin Probe Biosensor	121
3.1: <i>Introduction</i>	121
• <i>Figures for Section 3.1</i>	126
3.2: <i>Patterning Biological Molecules</i>	128
• <i>Antibody Patterning</i>	129
• <i>Thiol-Modified DNA Patterning</i>	130
• <i>Figures for Section 3.2</i>	132
3.3: <i>Detection of bound target analyte molecules</i>	137
• <i>Protein Detection</i>	138
• <i>DNA Detection</i>	139
• <i>Figures for Section 3.3</i>	141
3.4: <i>Characterization of DNA detection</i>	148
• <i>Concentration</i>	148
• <i>Base Pair Mismatches</i>	149
• <i>Feature Size & Maximum Lateral Resolution</i>	149
• <i>Scan Height</i>	150
• <i>Scan rate</i>	151
• <i>Figures for Section 3.4</i>	153

3.5: Discussion & Recommendations for Future Work 159
Appendix 3.A: Antibody Patterning 162
Appendix 3.B: DNA Dip Pen Nanolithography 164
Appendix 3.C: Kelvin Probe Biosensing Protocol..... 166
Appendix 3.D: Scan Height Characterization of Kelvin Probe 168
Appendix 3.E: Scan Rate Characterization of Kelvin Probe 169
3.Ref: References 170
Conclusions and Closing Remarks:..... 173

Listing of Figures

Figure 1.0-1: Comparison of length scales.	Page: 15
Figure 1.2-1: A schematic depiction of the M13 bacteriophage.	27
Figure 1.2-2: Schematic depiction of a phage display library.	28
Figure 1.2-3: Examples of materials interactions derived through phage display.	29
Figure 1.2-4: The mechanism of DPN.	30
Figure 1.2-5: Some useful thiol inks.	31
Figure 1.2-6: Dip Pen Nanolithography defined patterns.	32
Figure 1.2-7: A schematic depiction of the Kelvin Probe.	33
Figure 1.A-1: A schematic depiction of phage display.	36
Figure 1.A-2: Sample exposure in this work.	37
Figure 1.1-1: Lateral epitaxial overgrowth.	43
Figure 1.2-1: Negative selection	47
Figure 1.3-1: Misfit and threading dislocations in germanium grown on silicon.	54
Figure 1.4-1: AFM comparison of phage binding.	59
Figure 1.4-2: Scheme for fluorescently tagging bound phage.	60
Figure 1.4-3: Summary of binding density from fluorescence.	61
Figure 1.4-4: Binding assessment using titration data.	62
Figure 1.4-5: XPS comparison of germanium wafer and germanium-on-silicon.	63
Figure 1.4-6: Surface roughness comparison measured using AFM.	64
Figure 1.4-7: XRD data indicating a strong (100) preference for both substrates.	65
Figure 1.4-8: EPD comparison of the two substrates.	66
Figure 1.5-1: Comparison of sequence and structure of defect binding polypeptides.	71
Figure 1.5-2: The effect of oxidation on fluorescence signal.	72
Figure 1.C-1: Germanium substrate exposure to phage.	77
Figure 1.C-2: Unadjusted fluorescence data	78
Figure 2.2-1: Process for patterning viruses.	86
Figure 2.3-1: The three generalizable approaches to phage patterning.	92
Figure 2.3-2: Hydrophobic phage attachment.	93
Figure 2.3-3: Surface potential measurement of Zn ²⁺ adsorption.	94
Figure 2.3-4: Previous examples of divalent virus patterning.	95
Figure 2.3-5: Carboxylates on the phage pVIII protein.	96
Figure 2.3-6: M13 bacteriophage patterned using divalent chelation.	97

Figure 2.3-7: Previous examples of covalently patterning viruses.	Page: 98
Figure 2.3-8: Carbodiimide chemistry for activating carboxylates for reaction with primary amines.	99
Figure 2.3-9: Covalently patterned M13 bacteriophage.	100
Figure 2.4-1: Gold nanoparticle binding to p8#9 phage.	103
Figure 2.4-2: Cobalt randomly deposited on a patterned substrate.	104
Figure 2.4-3: Microcontact printing of amine terminated siloxane.	105
Figure 2.D-1: Carbodiimide activation of a carboxyl.	114
Figure 2.E-1: Tuning curves for an RTESP tip.	117
Figure 3.1-1: Correlation between measured surface potential and pKa.	126
Figure 3.1-2: A DNA Microarray.	127
Figure 3.2-1: Schematic protocol for patterning antibodies.	132
Figure 3.2-2: Amine-functionalized biotin molecule.	133
Figure 3.2-3: Thiol-functionalized DNA inks for Dip Pen	134
Figure 3.2-4: Patterning of multiple DNA inks.	135
Figure 3.2-5: Spatially addressable photolithographic chemical patterning.	136
Figure 3.3-1: An AFM tip operating in interleave scan mode.	141
Figure 3.3-2: Kelvin Probe detection of Avidin.	142
Figure 3.3-3: Kelvin Probe measurement of a neutrally charged protein.	143
Figure 3.3-4: Quantitative protein potential comparison.	144
Figure 3.3-5: Detecting an anthrax DNA sequence using Kelvin Probe.	145
Figure 3.3-6: Kelvin Probe measurement of non-complementary DNA.	146
Figure 3.3-7: A quantitative comparison of Kelvin Probe measurements.	147
Figure 3.4-1: The effect of target concentration on Kelvin Probe signal.	153
Figure 3.4-2: The effect of base pair mismatches on signal strength.	154
Figure 3.4-3: The ability of Kelvin Probe to resolve nanoscale features.	155
Figure 3.4-4: Maximum lateral resolution of the Kelvin Probe.	156
Figure 3.4-5: The effect of probe height on signal strength.	157
Figure 3.4-6: The effect of scan rate on Kelvin Probe signal strength.	158

Listing of Accronyms

AFM	Atomic Force Microscope
DPN	Dip-Pen Nanolithography
EDC	1-Ethyl-3-[3-dimethylaminopropyl]carbodiimide Hydrochloride
EML	Experimental Materials Laboratory
EPD	Edge Pit Density
FWHM	Full Width Half Maximum
GFP	Green Fluorescent Protein
HEPES	4-(2-hydroxyethyl)-1-piperazineethanesulfonic acid
ICL	Integrated Circuits Laboratory
MHA	Mercapto Hexadecanoic Acid
MTL	Microsystems Technology Laboratories
ODT	Octadecanethiol
PBS	Phosphate Buffered Saline
SEM	Scanning Electron Microscope
S-NHS	Sulfo N-Hydroxysuccinimide
TBS	Tris Buffered Saline
TBST	Tris Buffered Saline + Tween-20
TMR	Tetramethyl Rhodamine
TRITC	tetramethylrhodamine-5-isothiocyanate
XPS	X-Ray Photoelectron Spectroscopy
XRD	X-Ray Diffraction
ssDNA	Single stranded deoxyribonucleic acid
dsDNA	Double stranded deoxyribonucleic acid

Biographical Note

- D.O.B.: April 14, 1980. Denver, CO.

- Education: George Washington High School – Graduated 5/1998 - International Baccalaureate. Salutatorian.

University of California Berkeley – Graduated 5/2002 - B.S. Materials Science and Engineering. Bechtel Achievement award (like the valedictory award for the College of Engineering).

Massachusetts Institute of Technology – Currently enrolled – PhD Candidate. Department of Materials Science and Engineering.

- Publications:
 1. Biomolecular recognition of crystal defects: A diffuse-selection approach. Sinensky, AK and Belcher, AM. ADV MAT 18 (8): 991+ APR 18 2006.
 2. Model-Based Processing of Microcantilever Sensor Arrays. Tringe, JW; Clague, DS; Candy, JV; Sinensky, AK; Lee, C; Rudd, RE; Burnham, AK. IEEE – J MEMS 15 (5)1379-1391 OCT 6 2006
 3. A Kelvin Probe Biosensor: Label-free and High Resolution Scanning Probe Approach to Protein/DNA Nanoarray Analysis. Sinensky, AK and Belcher, AM. Submitted.

- Patents (Filings):
 1. United States Patent 6573150: Integration of CVD tantalum oxide with titanium nitride and tantalum nitride to form MIM capacitors. US Patent Issued on June 3, 2003.
 2. United States Patent 6677254: Processes for making a barrier between a dielectric and a conductor and products produced therefrom. US Patent Issued on Jan 13, 2004.
 3. United States Patent Filing 60/620,386: Biomolecular Recognition of Crystal Defects. Filed Oct 19, 2004

- Work Experience:
 1. As part of my DHS fellowship I worked at Lawrence Livermore National Laboratory (5/2004-8/2004) developing a biosensor based on a microcantilever array approach. For this work I used a custom multicantilever system developed by Veeco. This work resulted in a publication in the *IEEE Journal of MEMS*.

 2. My research project at Sandia (5/2001-8/2001; Internship) was developing a micro fuel injector nozzle as part of a MEMS group specializing in LIGA. The nozzle was eventually

constructed using a combination of electrodeposition and wire EDM. This work resulted in an *Employee Recognition Award*.

3. At Applied Materials (1/2000-7/2000; Co-op experience) I worked as a research engineer developing a modular process for the construction of a high dielectric constant capacitor. I characterized the capacitor using a microprobe station to tune its properties as the application warranted. For this work, I used CVD, PVD, Microwave anneal and a microprobe station. This work resulted in several Patent Filings.
- Honors (undergrad):
 1. Chancellor Scholar (8/1998; Most prestigious undergraduate scholarship offered by the UC system)
 2. Barry M. Goldwater Scholarship (4/2001; For excellence in the sciences and engineering)
 3. Outstanding Student Citation 2000-01 from the Materials Science and Engineering Department, UC – Berkeley
 4. Sandia National Security Scholarship (5/2001; A merit based award that included a summer internship)
 5. Outstanding Bay Area Undergraduate in Electronic Materials (4/2002; Awarded at the 30th Annual Electronic Materials Symposium.)
 6. Sandia Employee Recognition Award (2003) for my participation in the Diesel Engine Combustion Simulation Team – I helped in the design of a fuel injection nozzle.
 7. The Bechtel Achievement Award (5/2002; Awarded to the top graduating senior in the UC - Berkeley College of Engineering.)
 - Honors (graduate):
 1. Presidential Fellowship (5/2002-5/2003; Department fellowships given by MIT to promising incoming graduate students).
 2. Department of Homeland Security Fellowship (9/2003-8/2006; I was part of the first class of students to receive this award. The fellowship included a summer practicum at an approved DHS facility.)
 3. National Science Foundation Fellowship (9/2006 – present)
 4. Department of Homeland Security Dissertation Grant Award (9/2006; an award designed to help students complete their dissertation research and graduate.)
 - Service:
 1. MSER Group (1998-99; A group that puts together presentations on Materials Science to gain the interests of High School students in the bay area.)
-

2. President of the Materials Science and Engineering Association (2001- 02; MSEA, the student group for Materials Science students at Berkeley.)
3. Engineering Joint Council (2001-02; EJC Representative for MSE students at UC - Berkeley)
4. EJC High School Outreach program (2001-02)
5. MIT Graduate Materials Council: Academic and Career Chair (2004-05)
6. MIT Graduate Materials Council: Representative to the DCGS (Department Committee on Graduate Students; 2005-present)

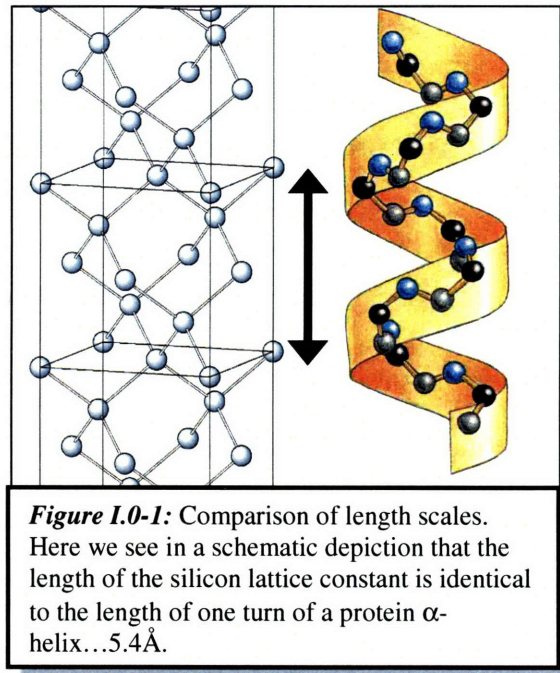
• Policy Interest:

1. Science and Technology Policy Minor – A course of study designed to complete the DMSE minor requirement. The courses taken were a Science Technology and Public Policy course at Harvard and a Defense Policy Course at MIT.
2. Science Policy Bootcamp – A science policy course created with the help of several students and Prof. William Bonvillian from the MIT Washington Office.
The purpose of the course is to teach students who are already scientifically literate about Policy Issues.
The course is taught in a rapid-fire bootcamp style with 15+ hours of lecture in one week.
The course was first taught to a group of 25 hand selected students during the 2007 IAP period and was extremely successful. A second version of the course was taught in spring 2007.
3. Congressional Visit Day – An opportunity to meet with congressional staffers to discuss issues of relevance to the scientific community.
Hosted by the Federation of Materials Society in March of 2007, a group of MSE students visited several congressional offices to lobby on behalf of the American Competitiveness Initiative.

Introduction

It has been shown time and time again that nature is remarkably adept at structuring inorganic materials at multiple length scales. From the atomic level (control of the crystalline phase in abalone⁽³⁾) to the macroscopic scale (skeletons and corals) we see biological systems that are able to

structure materials of a distinctly non-biological character. This ability of nature occurs at the interface between biological molecules and inorganic structures because at interfaces, both biological molecules and inorganic molecules are ordered at the same length scale. My favorite example of this scaling is a comparison of the lattice constant of silicon and the length of one turn



of a protein α -helix (Fig I.0-1). As it turns out, a coincidence of forces has allowed these two lengths to be identically valued at 5.4Å. This example is not meant to imply that just because two structures have the same length scale they are somehow able to control one

another, rather, it is illustrative of just how similar the length scales are between inorganic materials and biological molecules.

In general, the ability of biological materials to structure inorganic materials is referred to as biomineralization⁽⁵⁾. In nature, this process takes millions of years of evolution to be made viable. When we make attempts to mimic this behavior in a laboratory setting using new systems the better term is biotemplating. This is because the laboratory design process, while evolutionary, is more directed than in natural systems. There has been considerable success in our lab developing biological systems that are able to interact with inorganic systems in a number of ways ranging from simple binding^(1, 8) to controlled nucleation^(4, 6, 7, 9-13).

- *Structure of this Dissertation*

This document has three chapters, one on each of the projects described in this introduction. Each chapter includes a set of detailed appendices describing the protocols used in the project. The chapters are divided into sub-sections each on a particular topic related to the overall project. The figures for each sub-section occur at the end of the sub-section as opposed to in the text. References are placed at the end of each chapter.

Int.1: My Work

During my time at MIT, my work has focused on three similar but distinct projects. Each of these projects is concerned with how biological molecules interact with surfaces and how that interaction can be exploited for different applications. My first project was a phage display experiment in which I tried to identify a poly-peptide which showed a particular affinity for defects on a materials surface⁽⁸⁾. My second project was exploring the possibility of patterning genetically modified viruses on a surface such that there genetic modifications are still useful for materials biotemplating. My third project looked at the possibility of using the Kelvin Probe technique as a tool for detecting biological molecules.

Below is a brief description of each project:

- *Biomolecular Defect Recognition*

In this work we attempt to extend the capability of phage display beyond just materials recognition to the recognition of specific features on a materials surface. The surface features chosen for this project are the defects that occur when a dislocation intersects with a surface. Studying defects has several motivations: The first reason to look at defect binding is merely to see whether it is possible to extend phage display to this sort of capability. A second motivation was to see if a defect study would provide information about what role (if any) defects play in a typical selection where defects are not the target. A third motivation is based on the fact that defects are a very important

part of the properties (mechanical/electrical/other) of many material systems and the ability to identify defects in a non-destructive fashion could be very useful.

This work resulted in the discovery of a peptide sequence which shows a preferable binding affinity for surfaces with defects relative to surfaces without. The surfaces used were germanium which can produce highly defective surfaces when grown on silicon substrates. Using AFM, fluorescence, and titration the binding affinity was verified. Using surface characterization it was possible to show that the primary difference between the high defect and low defect surfaces was in fact the presence of defects. Early results indicate that the mechanism for preferential binding may be the localized oxidation that occurs near dislocations, but there is still considerable room for additional study into mechanism.

- *Surface Patterning of Genetically Programmed Viruses*

In this work the goal was to see whether viruses expressing useful proteins could be patterned on 2-dimensional surfaces and still maintain their genetically programmed function. Our lab has developed numerous viruses with a whole range of materials functionality including the ability to nucleate materials including Au, Ag, Co, CdS, ZnSe, and Ti. In order to use this ability to nucleate materials to its fullest extent (e.g. build devices) it is necessary to assemble these genetically programmed viruses into structures. In some cases it may be possible to self-assemble a device such as a battery electrode⁽¹¹⁾, but self-assembly may not always be possible.

Using Dip-Pen Nanolithography it was possible to pattern viruses onto chemically patterned features using a variety of different approaches. The approaches used range from hydrophobic adsorption to covalent attachment while still insuring that the materials-related genetic programming of the virus was not compromised. It was demonstrated that these viruses still maintain their ability to assemble materials when patterned using a gold nanoparticle binding phage.

- *Kelvin Probe Biosensor*

In this work the goal was to detect patterned biological molecules on a surface using a technique known as Kelvin Probe Microscopy. The Kelvin Probe is a tool for identifying variations in surface potential over a surface of interest. If a probe molecule is patterned on a surface, it can be used to detect the presence of a target analyte when the analyte binds to the probe. Because biological molecules tend to be charged in their native state, the Kelvin Probe is able to identify the presence of a biological molecule bound to a surface. This is demonstrated using the avidin-biotin system and more usefully using a DNA-DNA system.

The advantages of the Kelvin Probe technique are that it is a label-free detector, it can be operated at high resolution (<10nm), it can detect analytes with good sensitivity (<50nM) and it can detect at high speed (>1100µm/sec) all under ambient conditions. Additionally, this technique is shown to be able to distinguish target DNA molecules with as few as three nucleotide mismatches. Using features patterned with Dip Pen Nanolithography it was possible to use Kelvin Probe to detect target biomolecules on

features as small as 250nm. At these dimensions, it would be possible to analyze a DNA microarray with areal densities over 1000 times greater than the state of the art of current fluorescent DNA microarrays.

Int.2: Experimental Techniques

In these projects, many experimental techniques were used, but three in particular are worthy of an introduction. The first of these techniques is phage display on inorganic substrates. This is in many ways the founding technique of our research group and represents the basic approach we take to finding useful biomolecules. The second technique is Dip Pen Nanolithography which is a tool for chemically patterning a receptive substrate. This tool is capable of producing patterns with features as small as 10's of nanometers although typical features are closer to 100nm. Because these features are chemically distinct from the rest of the surface on which they are patterned, they make useful handles for a wide array of surface chemistries. The last technique is Kelvin Probe Microscopy which is a tool for measuring variations in surface potential across a surface. By combining a Kelvin Probe with an AFM it is possible to measure variations in surface potential at the nanoscale, allowing us to identify biological molecules on a surface of interest.

These techniques are presented in more detail below:

- *Phage Display*

The technique we use to find biological molecules that may have useful interactions with a material of interest is referred to as *Phage Display*. The phage display technique has been around for many years and has served many purposes⁽¹⁴⁻²⁰⁾. The term *phage* comes from the use of a virus called the M13 bacteriophage which is part of a

larger family of filamentous fd-bacteriophage. This virus has a long and thin body which contains the virus genome (Fig I.2-1). The body of the virus is just under a micron long and is less than 8nm wide and is composed primarily of a single protein referred to as pVIII. pVIII occurs 2700 times on the virus coat and is accompanied by a handful of proteins that occur in groups of five at each end of the virus body (pIII, pVI, pVII & pIX). Although pVIII is by far the most common protein, the most important protein for phage display is the pIII protein. Phage display works by adding a short, random peptide fusion to the end of the pIII protein. By combining a large population of these randomly modified viruses into one collection it is possible to create what is referred to as a *Random Library*. The random libraries we use are supplied by New England Biolabs and have peptide fusions that are seven to eleven residues in length. Such a library represents potentially billions of distinct viruses which are almost genetically identical except for the small peptide fusion on pIII.

When this random library is exposed to a material of interest, the interactions of the individual phage with the material will only be distinguished by their random peptide fusions. If this interaction results in the individual phage binding to the material, these viruses can be collected by rinsing away the non-binding viruses. The binding phage represent a new library which has less genetic diversity than the original random library. Because the M13 virus is a non-lytic bacteriophage, it can be easily amplified by exposure to its bacterial host, *E. coli*. The amplified library can then be used to perform a second round of exposure with the material of interest. Each round of exposure results in an increasingly monodispersed virus population (Fig I.2-2). Ideally the resulting virus population will represent just one of the initial peptide fusions and the other billions of

peptide fusions will have been removed through selection pressure. In practice, the virus population will reach a maximum in its genetic monodispersity after around five rounds of selection. At this point, the phage population will generally be expressing a family of structurally similar peptide fusions rather than just one. Beyond five rounds of selection, wild-type bacteriophage may start to infiltrate the phage population due to an advantage in bacterial infectivity compared to the genetically modified phage.

This technique has shown great success with a variety of inorganic materials. In addition to simply binding materials, another interesting quality has emerged from the various peptide fusions identified through phage display. It turns out that frequently when phage display identifies a protein that binds to a material, it can also be used to induce the nucleation of that same material. This protein driven materials nucleation is extremely useful if the peptide fusion identified through phage display is fused onto the pVIII protein which makes up the virus coat. Through this genetic programming it is possible to create a virus which will spontaneously form a semiconducting or metal nanowire under the right aqueous conditions. This has been shown with compound semiconductors as well as metals and is an example of biotemplating (Fig I.2-3).

A step-by-step phage display protocol for inorganic materials can be found in Appendix I.A.

- *Dip Pen Nanolithography*

Dip Pen Nanolithography (DPN) is a technique that was developed in 1999⁽²⁾ at Northwestern University. The tool is designed to allow a surface to be chemically

patterned at the nanoscale with almost any chemical functionality. DPN is a scanning probe technique in which the tip of an Atomic Force Microscope (AFM) is coated in a chemical “ink”. The choice of ink is important and is largely dependant on the choice of substrate. The most common ink-substrate system used is the thiol-gold system. It turns out that thiol groups will form spontaneous covalent bonds with clean gold substrate. As a result, if an AFM tip is coated in thiol containing molecule it will leave behind a trail of covalent thiol-gold bonds when dragged across a gold substrate (Fig I.2-4). The mechanism is based on diffusion of the ink through a water meniscus which forms between the AFM tip and the gold substrate. Once the ink molecule reaches the gold surface, there is a competition between surface diffusion and reaction kinetics which determines the size of the features that are generated.

The power of DPN is that it is an easy and quick way to pattern a surface at the nanoscale with features that are chemically distinct from the background substrate. The choice of ink goes a long way in determining what sort of functionality the patterns will exhibit. The prototypical molecule used for writing is mercaptohexadecanoic acid (MHA) (Fig I.2-5). MHA has a thiol group at one end of a 15 carbon chain and a carboxylate at the other end. Writing on gold with this molecule results in the creation of a pattern that is terminated in carboxylic acids. These functional groups can be used as a handle to perform a variety of chemistries. Other inks can be used to perform other chemistries or to modify the surface properties of a substrate of interest. Once the ink and substrate have been chosen, it is quite easy to write almost any pattern (Fig I.2-6).

In the gold substrate system, it is useful to ‘backfill’ the portions of the substrate that have not been written on in order to make them even more chemically distinct from

the pattern. This is especially true when dealing with biological molecules which have a natural non-selective attraction to gold substrates. Octadecanethiol (ODT) and methoxy PEG thiol are good choices as backfilling molecules depending on the biological molecules that need to be repelled. This backfilling can be accomplished by simply soaking the dip-pen patterned substrate in a solution containing the desired background molecule. This will produce a disordered self-assembled monolayer on the unpatterned gold within an hour or two.

- *Kelvin Probe Microscopy*

The Kelvin Probe Microscope (also known as the Surface Potential Force Microscope or the Capacitive Probe) is a tool designed to detect regional variations in surface potential across a substrate of interest. The tool works by measuring the difference in work function between a fixed substrate and a movable probe. The probe is brought close to the substrate and if there is any difference in surface potential (or work function) between the probe and the substrate they exert a mutual force on one another (Fig I.2-7). By modulating the applied potential on the probe until this force is extinguished, it is possible to determine the local potential of a surface.

The concept of measuring the difference in work function between two materials was originally proposed by Lord Kelvin⁽²¹⁾ hence the name 'Kelvin Probe'. The modern Kelvin Probe is actually a variation on Lord Kelvin's proposal known as a 'vibrating capacitor' developed by Zisman in 1932⁽²²⁾. In the vibrating capacitor model, the voltage applied to the probe is a DC voltage overlaid with an AC voltage. The reason for

overlaying the two voltages is to increase the sensitivity of the probe. By choosing an AC voltage with a frequency close to the resonant frequency of the movable probe, the resulting deflections experienced by the probe will be much larger than if they were merely the result of an applied force.

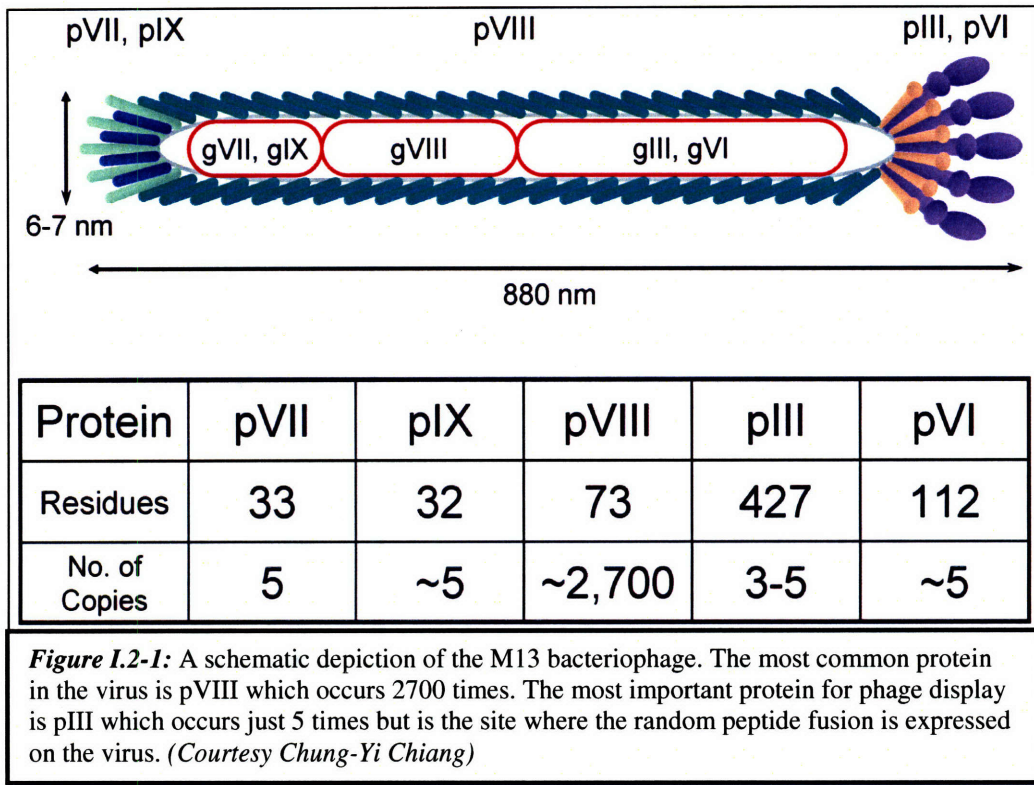
The vibrating capacitor model can be approached with a simple mathematical treatment (see Appendix I.B), the result of which is:

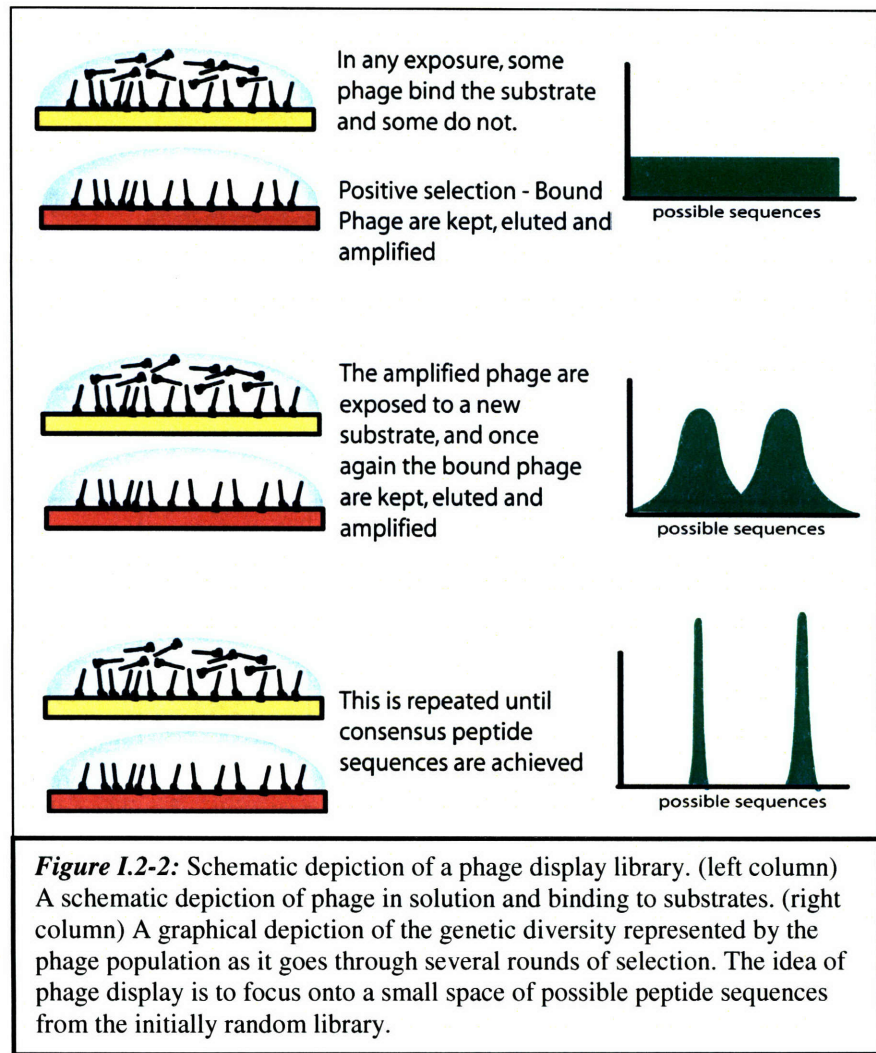
$$F_d \sim F(\omega_d) \sim 2\Delta V_{DC}\Delta V_{AC}\cos(\omega_d t)$$

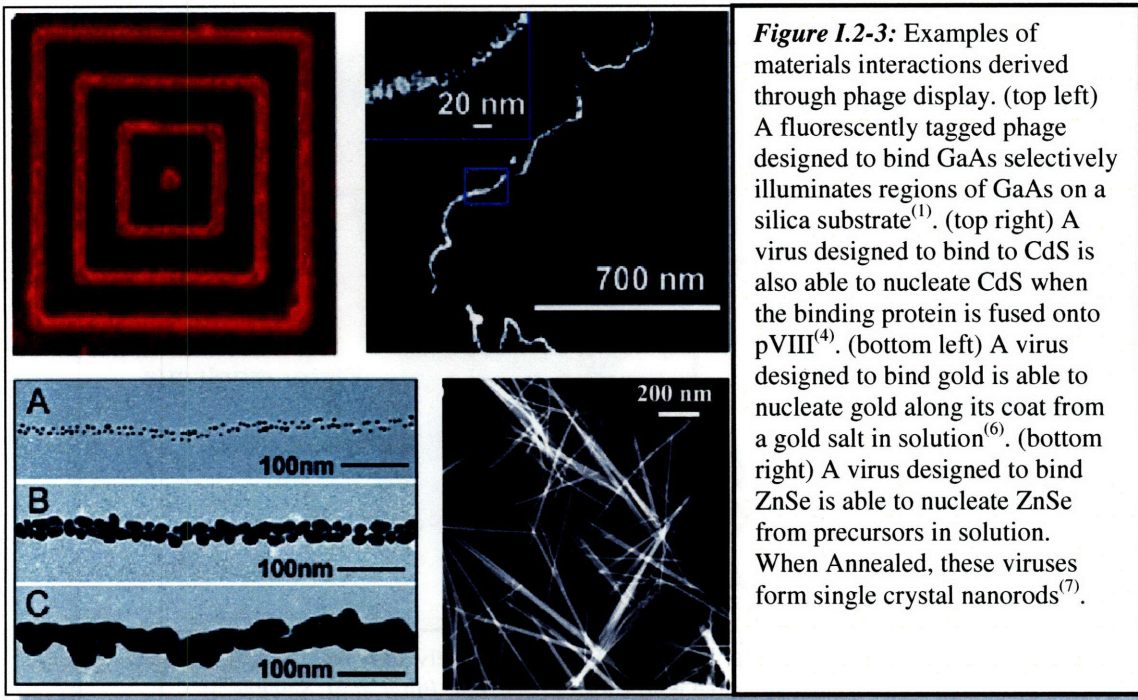
where F_d is the force felt by the Kelvin Probe, ω_d is the drive frequency of the AC voltage (which should be close to the resonant frequency of the capacitor), ΔV_{DC} is the difference in DC voltage between the capacitor plates and ΔV_{AC} is the difference in AC voltage between the capacitor plates. The important thing to note is that as the difference in DC voltage goes to zero, the force on the capacitor plates goes to zero as well. This means that by measuring the force on the capacitor plates as a function of applied DC voltage allows a user to determine the voltage where the force is minimized. Determining this force-minimizing voltage is the goal of a Kelvin Probe measurement. Additionally, the force felt by the capacitor plates is proportional to the AC voltage which means that the AC voltage can be used as a lever to increase the device sensitivity.

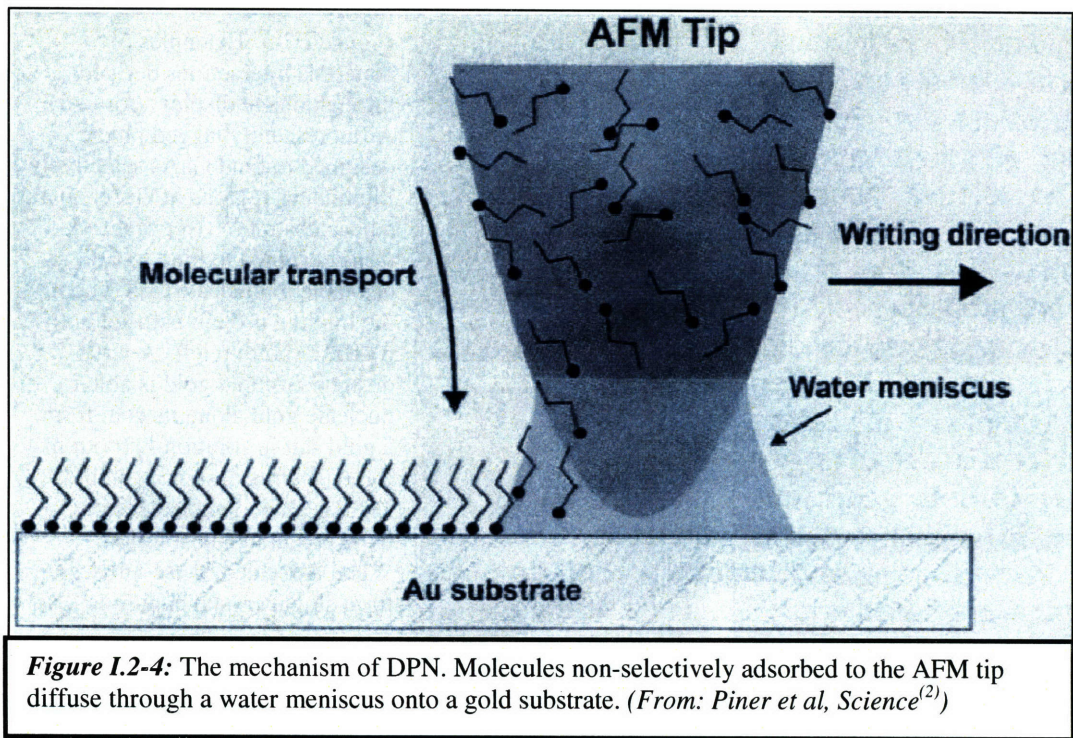
The Kelvin Probe can be used to measure the potential of any surface; conducting or insulating. In this work, the tool is used to measure surfaces that have been functionalized with biological molecules.

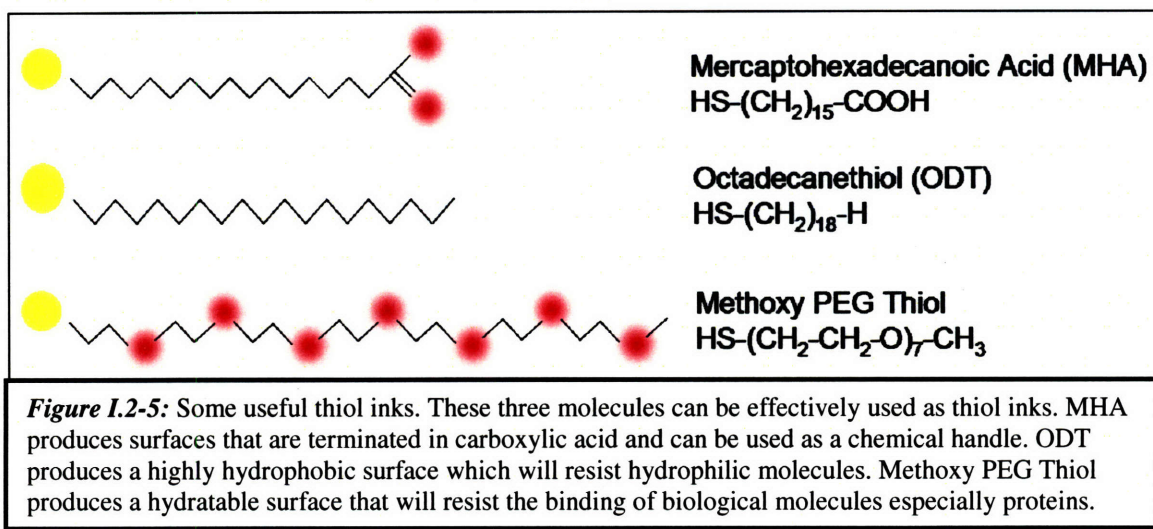
- *Figures for Section Int.2*

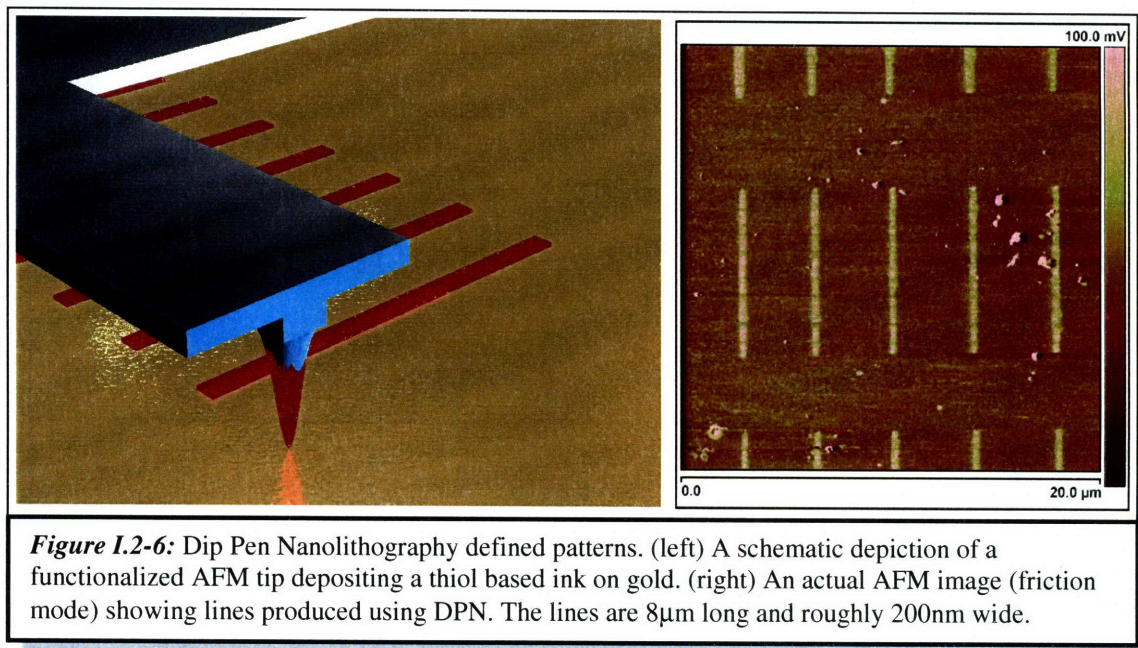












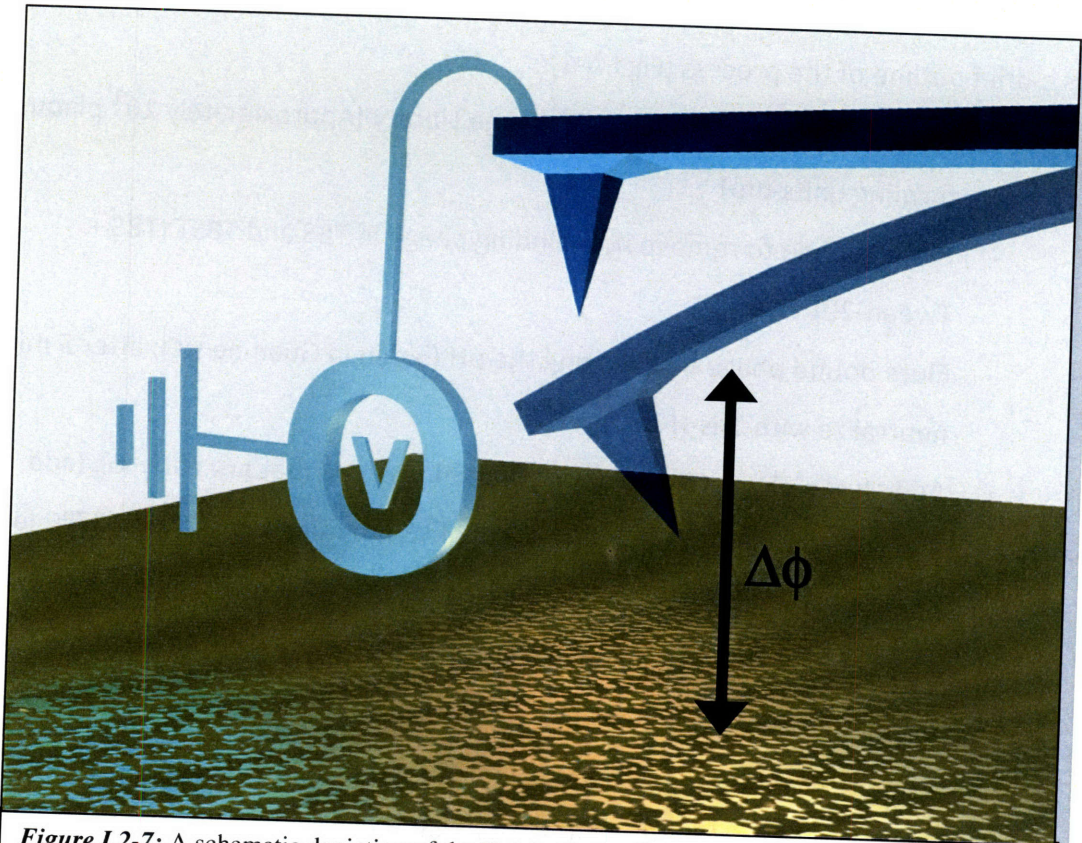


Figure 1.2-7: A schematic depiction of the Kelvin Probe. Because the Probe and the substrate are different materials, there is a difference in work function between them ($\Delta\phi$). The work function difference creates a potential drop across the air gap which results in a force felt by the probe tip. If a potential is applied to the probe, this force can be reduced to zero. The voltage required to minimize this force is exactly equal to the difference in work function. By finding this voltage, the Kelvin Probe also measures the relative surface potential of the surface.

Appendix I.A: Phage Display Protocol

The phage display protocol used is essentially identical to the one described in New England Biolabs literature for the PhD C7C Phage Display Kit⁽²³⁾. This manual describes preparation of media as well as day-by-day instructions.

Here is a brief outline of the process (Fig I.A-1):

- Expose Sample to Random C7C Phage Library (Approximately 10^9 plaque forming units-pfu)
- Rinse Sample to remove non-binding phage in TBS and TBST (TBS + Tween-20)
- Elute bound phage by changing the pH (5 min in Guanine HCl; after 5 min neutralize with Tris-HCl)
- Add eluted phage to a solution containing *e. coli* that are early log (add one colony of ER2378 *e. coli* to 20ml of LB medium and shake at 37°C for about 2 hours). Shake this solution for roughly 4.5 hours.
- At this point, the phage and *e. coli* need to be separated. This is done using selective precipitation (*e. coli* is not soluble in water, phage is soluble in water, phage is not soluble in PEG-NaCl). First spin down the amplified phage/*e. coli* solution to pellet bacteria. Remove supernatant (contains phage) and expose this to PEG-NaCl. Phage will precipitate. Spin down again to pellet phage. Remove supernatant (contains PEG-NaCl but no phage). Reconstitute phage in TBS. This is the new less random phage library.
- After each round of amplification, the concentration of phage that results can be assessed either by using titration or spectroscopic techniques. The titration protocol is also described in the NEB Phage Display manual.
- Repeat this exposure-amplification process until the phage solution has reached its maximum monodispersity. Monodispersity is determined by

sampling the phage DNA to see that only a few of the originally random peptide fusions are present.

- **The DNA sequencing is also described in the NEB phage display manual.**

The primary point of deviation from the standard protocol, and the protocol used in this work arises due to the nature of the sample exposure. Typically the sample exposure is done by gluing a substrate to the inside of a microfuge tube, adding phage solution and rocking for one hour. In this work, the samples were exposed by suspending a drop of solution directly on the germanium substrate of interest (Fig 1.A-2).

This insures that only the surface of interest is being exposed to the phage solution which is important when defects might be present on the sides of the germanium substrates where they have been cut by the die saw.

- *Figures for Appendix I.A*

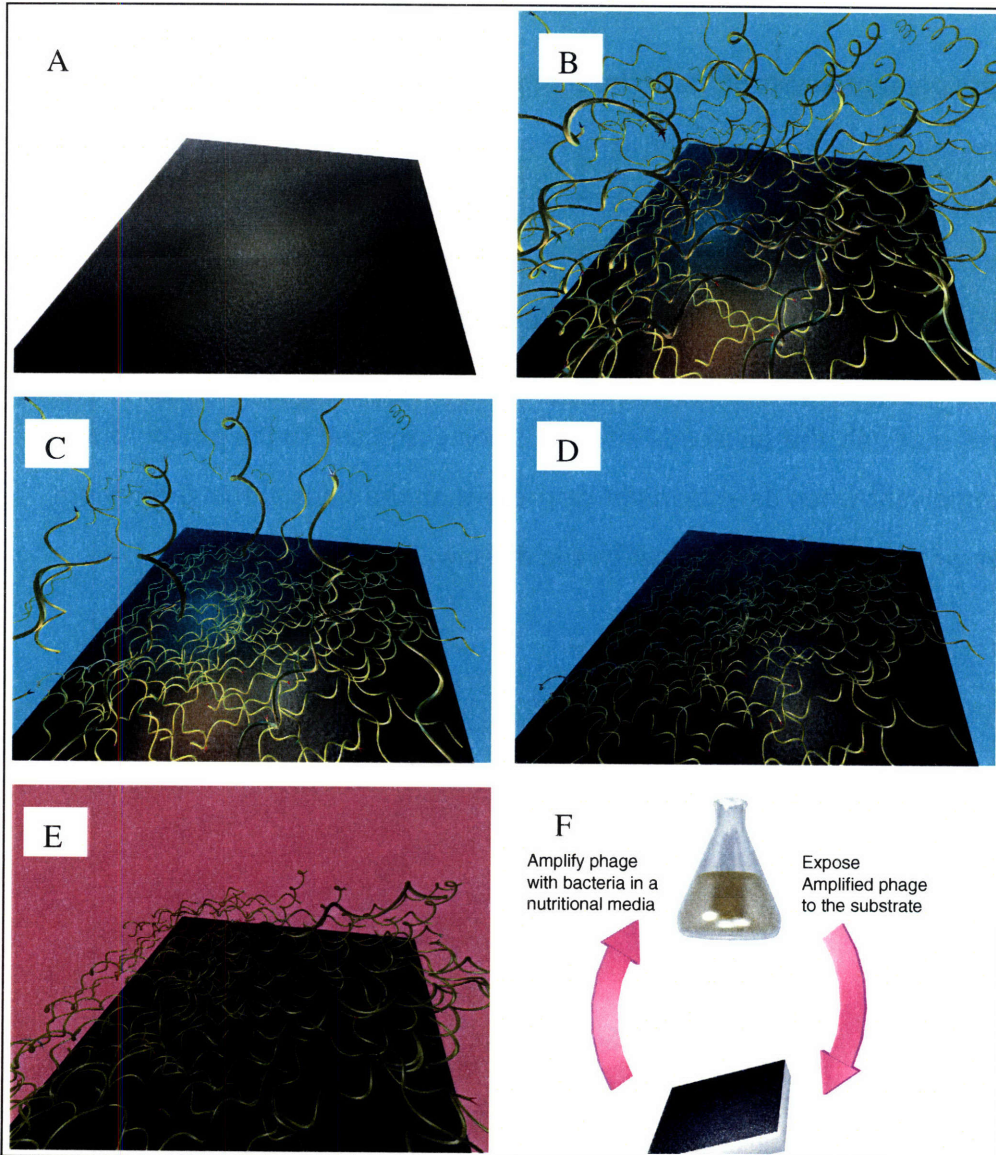
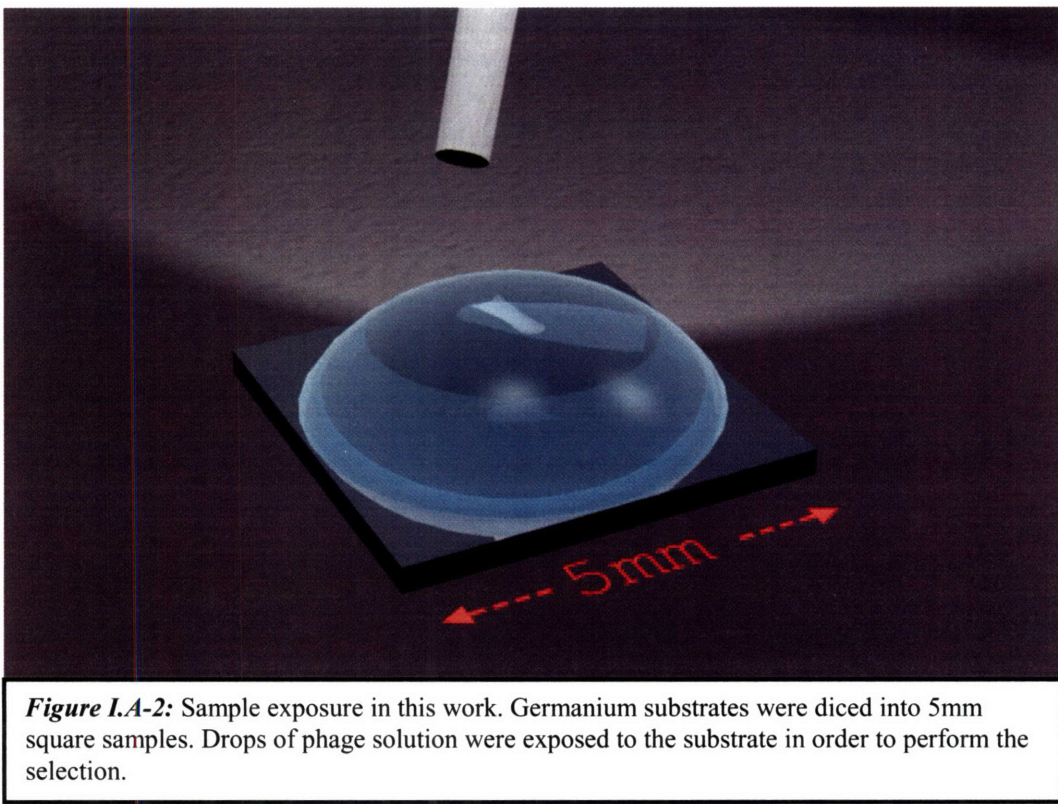


Figure I.A-1: A schematic depiction of phage display. (A) Start with an appropriately prepared substrate. (B) Expose the substrate to a solution containing phage. (C) After a short exposure, some of the phage will preferentially bind to the substrate and some will stay in solution. (D) Rinse the phage that did not bind the substrate during the exposure. (E) Elute the bound phage by changing the pH. (F) Amplify the phage and repeat in a series of exposure rounds until the phage population has achieved maximum genetic monodispersity.



Appendix I.B: Mathematical Treatment of Vibrating Capacitor

Consider a capacitor that has one fixed plate and one 'probe' plate that is being used as a Kelvin Probe. The energy (U_{cap}) of such a capacitor goes as:

$$U_{cap} = \frac{1}{2} C(\Delta V)^2$$

where C is the capacitance and ΔV is the potential difference between the capacitor plates. By taking the derivative with respect to separation, we get the force that the capacitor plates are exerting on one another.

$$\frac{dU_{cap}}{dZ} = F_{cap} = -\frac{1}{2} \frac{dC}{dZ} (\Delta V)^2$$

If we examine the ΔV term, we see that it has a DC and an AC component.

$$(\Delta V) = \Delta V_{DC} + \Delta V_{AC} \sin(\omega_{KP}t) \quad \text{where : } \Delta V_{DC} = \Delta V_{DC,app} - \Delta\phi$$

By expanding the $(\Delta V)^2$ term, we see that it breaks down into three distinct parts each with a different dependence on the AC frequency.

$$(\Delta V)^2 = \left(\Delta V_{DC}^2 + \frac{\Delta V_{AC}^2}{2} \right) - \frac{1}{2} \Delta V_{AC}^2 \cos(2\omega_{KP}t) + 2\Delta V_{DC} \Delta V_{AC} \sin(\omega_{KP}t)$$

DC term
2 ω_{KP} term
 ω_{KP} term

If the frequency (ω_{KP}) is chosen such that it is the resonant frequency of the probe plate, the ω_{KP} term will dominate the force response of the capacitor. The probe plate will experience an oscillating deflection associated with this sinusoidal force.

$$F_{cap} \approx F_{cap}(\omega_{KP}) = -\frac{dC}{dZ} \Delta V_{DC} \Delta V_{AC} \sin(\omega_{KP}t)$$

$$\therefore \text{ as } \underline{\Delta V_{DC,0}} \Rightarrow \underline{F_{cap,0}} \quad \& \quad \Delta V_{app} \approx \Delta\phi$$

Int.Ref: References

1. **Whaley, S. R., D. S. English, E. L. Hu, P. F. Barbara, and A. M. Belcher.** 2000. Selection of peptides with semiconductor binding specificity for directed nanocrystal assembly. *Nature* **405**:665-668.
2. **Piner, R. D., J. Zhu, F. Xu, S. H. Hong, and C. A. Mirkin.** 1999. "Dip-pen" nanolithography. *Science* **283**:661-663.
3. **Belcher, A. M., X. H. Wu, R. J. Christensen, P. K. Hansma, G. D. Stucky, and D. E. Morse.** 1996. Control of crystal phase switching and orientation by soluble mollusc-shell proteins. *Nature* **381**:56-58.
4. **Mao, C. B., C. E. Flynn, A. Hayhurst, R. Sweeney, J. F. Qi, G. Georgiou, B. Iverson, and A. M. Belcher.** 2003. Viral assembly of oriented quantum dot nanowires. *Proceedings of the National Academy of Sciences of the United States of America* **100**:6946-6951.
5. **Mann, S.** 2002. *Biom mineralization: Principles and Concepts in Bioinorganic Materials Chemistry.* Oxford Univeristy Press.
6. **Huang, Y., C. Y. Chiang, S. K. Lee, Y. Gao, E. L. Hu, J. De Yoreo, and A. M. Belcher.** 2005. Programmable assembly of nanoarchitectures using genetically engineered viruses. *Nano Letters* **5**:1429-1434.
7. **Mao, C. B., D. J. Solis, B. D. Reiss, S. T. Kottmann, R. Y. Sweeney, A. Hayhurst, G. Georgiou, B. Iverson, and A. M. Belcher.** 2004. Virus-based toolkit for the directed synthesis of magnetic and semiconducting nanowires. *Science* **303**:213-217.
8. **Sinensky, A. K., and A. M. Belcher.** 2006. Biomolecular recognition of crystal defects: A diffuse-selection approach. *Advanced Materials* **18**:991-+.
9. **Flynn, C. E., C. Mao, A. Hayhurst, J. L. Williams, G. Georgiou, B. Iverson, and A. M. Belcher.** 2003. Synthesis and organization of nanoscale II-VI semiconductor materials using evolved peptide specificity and viral capsid assembly. *J.Mater.Chem.* **13**:2414-2421.
10. **Qi, J., C. Mao, J. M. White, and A. M. Belcher.** 2003. Optical anisotropy in individual CdS quantum dot ensembles. *Phys.Rev.B* **68**:125319.
11. **Nam, K. T., D. W. Kim, P. J. Yoo, C. Y. Chiang, N. Meethong, P. T. Hammond, Y. M. Chiang, and A. M. Belcher.** 2006. Virus enabled synthesis and assembly of nanowires for Lithium ion battery electrode. *Abstracts of Papers of the American Chemical Society* **231**:-
12. **Reiss, S., and A. Belcher.** 2005. Guiding the Evolution of Things from engineered viruses, novel material. *Technology Review* **108**:24-24.
13. **Seeman, N. C., and A. M. Belcher.** 2002. Emulating biology: Building nanostructures from the bottom up. *PNAS* **99**:6451-6455.
14. **Azzazy, H. M. E., and W. E. Highsmith.** 2002. Phage display technology: clinical applications and recent innovations. *Clinical Biochemistry* **35**:425-445.
15. **Binetruy-Tournaire, R., C. Demangel, B. Malavaud, R. Vassy, S. Rouyre, M. Kraemer, J. Plouet, C. Derbin, G. Perret, and J. C. Mazie.** 2000. Identification of a peptide blocking vascular endothelial growth factor (VEGF)-mediated angiogenesis. *Embo Journal* **19**:1525-1533.

16. **Koolpe, M., R. Burgess, M. Dail, and E. B. Pasquale.** 2005. EphB receptor-binding peptides identified by phage display enable design of an antagonist with ephrin-like affinity. *Journal of Biological Chemistry* **280**:17301-17311.
17. **Kragler, F., J. Monzer, B. Xoconostle-Cazares, and W. J. Lucas.** 2000. Peptide antagonists of the plasmodesmal macromolecular trafficking pathway. *Embo Journal* **19**:2856-2868.
18. **Rodi, D. J., and L. Makowski.** 1999. Phage-display technology - finding a needle in a vast molecular haystack. *Current Opinion in Biotechnology* **10**:87-93.
19. **Rodi, D. J., R. W. Janes, H. J. Sanganee, R. A. Holton, B. A. Wallace, and L. Makowski.** 1999. Screening of a library of phage-displayed peptides identifies human Bcl-2 as a taxol binding protein. *Journal of Molecular Biology* **285**:197-203.
20. **Rozinov, M. N., and G. P. Nolan.** 1998. Evolution of peptides that modulate the spectral qualities of bound, small-molecule fluorophores. *Chemistry & Biology* **5**:713-728.
21. **Kelvin, L.** 1898. The Contact Electrification of Metals. *Philosophy Magazine* **46**:82-120.
22. **Zisman, W. A.** 1932. A New Method of Measuring Contact Potential Differences in Metals. *Review of Scientific Instruments* **3**:367-368.
23. The C7C Manual can be found at:
<http://www.neb.com/nebecomm/products/productE8120.asp>

Chapter 1: **Biomolecular Recognition of Crystal Defects:** **A Diffuse Selection Approach[†]**

1.1: Introduction

Specificity is a hallmark of biological interactions. In natural systems, biomolecules are able to differentiate individual target molecules from thousands of competitors. Mimicking this specificity represents a challenge in some inorganic systems where the target is diffuse and inseparable from a large, competing background. In this project, an approach was developed for ‘diffuse selection’ on inorganic substrates using biomolecular recognition of surface defects as an example. Specifically, phage display is used to find a polypeptide which shows binding specificity for surface defects. The system explored is based on threading dislocations in (100) germanium grown heteroepitaxially on silicon. Using a diffuse selection approach, a consensus peptide sequence was found and tested using atomic force microscopy (AFM) fluorescence microscopy and titration. The data indicates binding specificity for highly defective crystal surfaces versus non-defective crystal surfaces.

In the past decade considerable progress has been made in the understanding of how biological molecules interact with inorganic materials. Biomolecules have been used

[†] Portions reproduced with permission from Advanced Materials

to influence the phase⁽¹⁾, growth^(1, 3, 4) and organization⁽⁵⁻⁸⁾ of inorganic materials in ways that may provide a glimpse into the future of self-assembly. In the case of semiconducting materials, phage display using the filamentous M13 bacteriophage has played a crucial role in identifying peptides which have binding affinity and specificity⁽⁹⁾ for a chosen substrate. However, there is a class of problems in which challenges arise because the target of selection is diffuse and inseparable from a large competing background. This inseparability complicates a selection process in which it is normally desirable to isolate the selection target.

Two examples of such inseparable/diffuse targets are surface defects (dislocations, step edges, grain boundaries) and impurities (intentional or otherwise). In both cases, it is impossible to separate the target from the background because without the background, the target itself is meaningless. The example examined herein is the utilization of phage display to identify a peptide which shows binding affinity for surface defects in a crystalline substrate. Defect binding is an interesting example because in systems where defect distribution can be controlled (e.g. epitaxial lateral overgrowth),⁽²⁾ defect binding can be used to direct templated assembly (Fig 1.1-1). In addition, in any system where defect density influences functionality (e.g. leakage current,⁽¹⁰⁾ strain hardening) it is useful to be able to locate defects in a non-destructive manner. Unfortunately, it is impossible to isolate surface defect from the background substrate during the selection. An approach is needed that will force the selection to target the inseparable features. In this work, we present an approach titled “diffuse selection” for selecting targets of this nature.

- *Figures for Section 1.1*

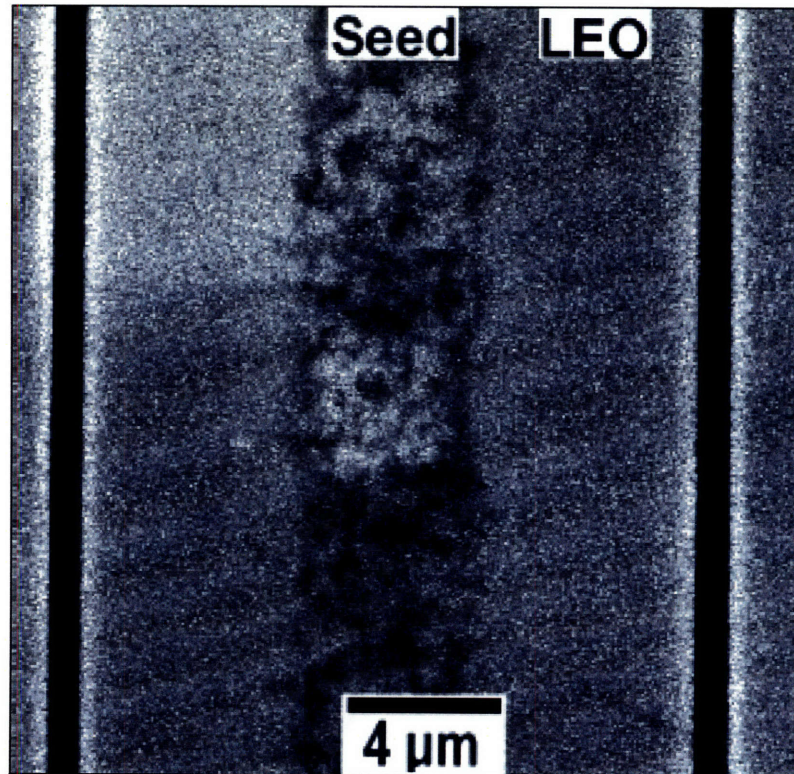


Figure 1.1-1: Lateral epitaxial overgrowth. LEO is a technique that allows for the growth of defect free material on a lattice mismatched substrate. It does this by opening 'windows' in which defects congregate, while defect-free material grows laterally as can be seen in this cathodoluminescence image. This is an example of a circumstance in which defects can be localized. In this situation, a defect-binding protein could be used as a handle for patterning. (Reproduced with permission: Rosner et al. *App Phys Lett*)⁽²⁾

1.2: The First Iteration

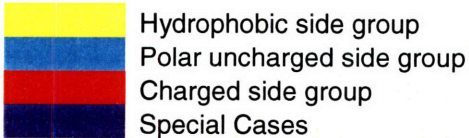
This portion of the project represents the first experiment attempted in the course of this PhD research, and as such it was primarily an opportunity to learn lessons that would guide future research. The goal is to use phage display to find a defect binding poly-peptide. The basic protocol for the selection is the same described in Appendix I.A. The first step in any selection is the appropriate choice of a selection target for the phage display biopanning. The question that occurs when selecting for defects is how the selection is going to be able to distinguish defects from the rest of a surface. It is not possible to merely select for a surface with lots of defects as it will not be possible to distinguish viruses that show an affinity for defects from those that bind the surface in between defects. As a result of this observation, a simple conceptual model was developed:

When a selection is performed on a defect rich surface, two general populations of viruses emerge. One population binds defects and the other one binds other aspects of the surface.

The goal is to somehow separate these two populations. The technique that was used to accomplish this separation is termed 'negative' selection (Fig 1.2-1). In a negative selection, the viruses are exposed to a surface but, instead of keeping the viruses that bound the surface, the non-binders are kept. The negatively-selected surface acts as a filter for the virus populations.

In this first experimental iteration, the high defect surface was merely the backside of a germanium wafer. The backside of a wafer is roughened to help getter impurities and defects and so was presumed to be defect rich. The surface used for the

negative selection was the front side of the germanium wafer which should have no defects present. The substrates were prepared as described in Appendix 1.A. The positive selections followed the protocol laid out in the New England Biolabs PhD-C7C phage display manual. The selection followed a simple progression of two positive selections against the wafer backside followed by a negative selection. The negative selection consists of two exposures to the wafer frontside followed by a positive exposure to the wafer backside (Fig 1.2-1). Sequences were taken after the second positive selection and after the first negative selection and are presented in the table below.

Table 1.2-1: Sequencing result for initial defect selection									
Sequences found after second positive selection – no consensus is observed									
C	K	L	G	T	P	P	Y	C	
C	Y	S	P	D	P	R	S	C	
C	Y	K	N	L	T	S	A	C	
C	P	R	N	N	L	A	P	C	
C	H	P	N	V	S	Y	R	C	
C	H	P	N	V	S	Y	R	C	
C	N	P	L	M	K	T	L	C	
C	S	P	T	T	G	N	S	C	
C	S	T	Q	N	S	I	Q	C	
Sequences found after first negative selection – two consensus sequences are observed									
C	Y	K	H	G	T	P	K	C	
C	Y	K	H	G	T	P	K	C	
	D	K	H	G	T	P	K	C	
C	E	I	S	H	H	H	M	C	
S	E	I	S	H	H	H	M		
C	E	I	S	H	H	H	M	C	
C	E	I	S	H	H	H	M	C	
									

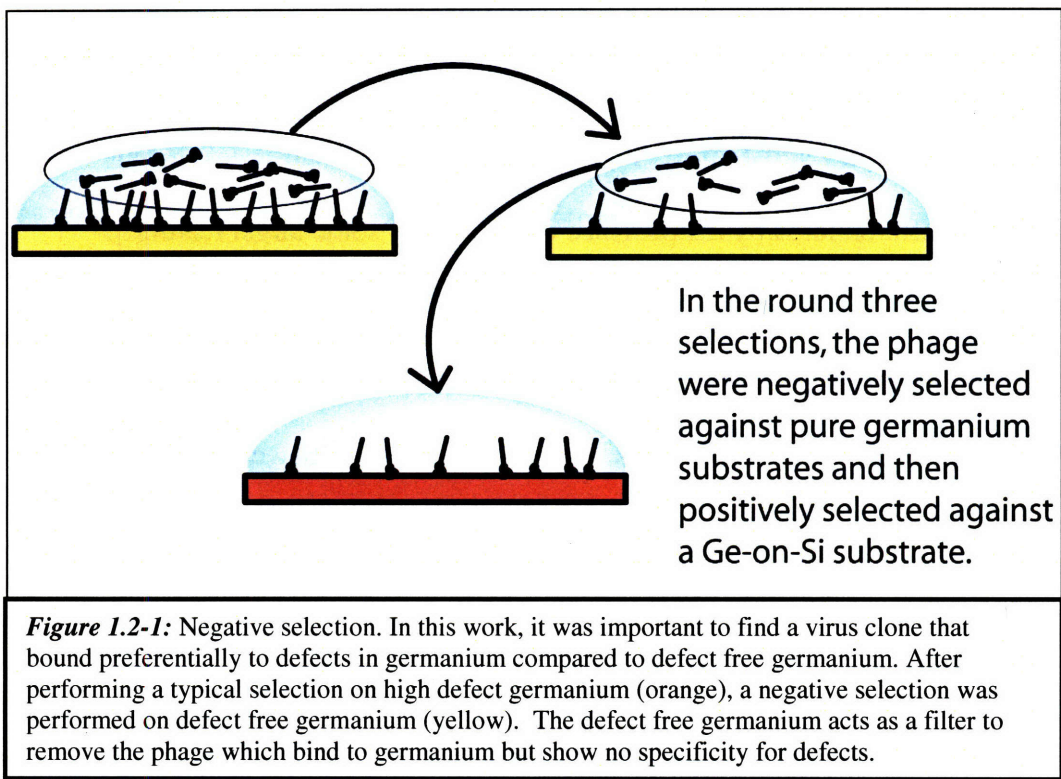
From this table it is clear that polar and charged groups are dominating the binding behavior. The presence of three consecutive histidines found in the consensus sequence from the negative selection is quite notable as histidine is frequently found as part of the functional portion of an enzyme.

The next step after identifying the sequences is determining whether or not they are defect binders and potentially to characterize how good they actually are at binding defects. The method first used to assess binding efficiency was based on fluorescent tagging of the virus clone expressing the 3-histidine sequence. The hope was that virus binding could be assessed, and then Edge Pit Density (EPD) could be used to spatially correlate the fluorescent signal with the etch pits. The viruses were tagged with biotinylated anti-fd (an M13 antibody) and streptavidin conjugated phycoerythrin (this approach is described in more detail in section 1.4 - see Figure 1.4-2). This approach yielded no useful results as it was too difficult to correlate the location of fluorescence with the location of defects.

At this point, it was realized that the selection employed would not distinguish surface defects from a generally rough surface. Despite the achievement of interesting consensus sequences, this observation necessitated repeating the selection on better substrates. This initial iteration provides several useful lessons learned:

1. Negative selection is an effective way to arrive at consensus sequences.
2. The choice of substrates is critical because it is the difference between the selection substrates that drives the selection.
3. Fluorescent tools were developed for evaluating binding behavior, but using defect-fluorescence correlation will not be effective.

- *Figures for Section 1.2*



1.3: Diffuse Selection

Based on the observations delineated at the end of the previous section, the 'Diffuse Selection' approach was proposed. In order to perform a selection on diffuse surface features, a typical phage display approach will not be effective. Diffuse selection is a methodological approach for selecting surface features while limiting selection of the general surface. Following is a listing of the basic principles that make diffuse selection on inorganic materials possible.

Complementary substrates: Two otherwise identical substrates that are differentiated by the presence or absence of some target feature.

Combinatorial selection: A selection approach in which many randomly generated possibilities can be simultaneously tested.

Positive and negative selections: Positive and negative selections provide discrimination between the two substrates.

Specificity verification: Once the selection is complete, it is necessary to verify that indeed the target feature has been selected.

Substrate characterization: It is also necessary to verify that the target feature is indeed the differentiating feature between the complementary substrate.

An elaboration of these principles by way of example is below.

- *Complementary substrates*

The system explored during the second iteration of this project was based on threading dislocations in (100) Germanium. There are two advantages to the use of

germanium for this selection: Firstly, germanium oxidizes slowly⁽¹¹⁾ and germanium oxide has considerable miscibility in water so a clean surface can be created and maintained in a lab setting. Secondly, growing heteroepitaxial germanium thin films on silicon (Ge-on-Si) is an effective way to create single crystal, albeit highly defective, germanium substrates. Defects in the Ge-on-Si system have been well studied in the hopes of integrating optical devices with silicon logic.^(12, 13) The defects created in the deposition of germanium thin films on silicon are threading dislocations whose density can be partially controlled through processing.⁽¹⁴⁾ Threading dislocations form near the germanium/silicon interface and exit the germanium through the exposed (100) surface (Fig 1.3-1). The point where a dislocation exits a crystal surface is a localized surface defect with a geometry, reactivity and electronic structure that differs from the rest of the crystal surface. The primary dislocation system in germanium has a burgers vector with length and direction $(a/2)\langle 011 \rangle$ ^(15, 16) (a length of $\sim 4\text{\AA}$). A detailed description of the germanium substrate preparation is in Appendix 1.A.

The correct choice of complementary substrates is crucial to a successful selection. In the first iteration of this work, the substrates chosen were merely the polished and unpolished faces of a germanium wafer. The idea was that the unpolished face was loaded with defects as a result of being roughened for gettering purposes. However, it is important to consider what is actually being selected for. The major distinction between those two substrates was that one was rough and one was smooth. The selection process did results in consensus sequences, but the sequences were only shown to be able to distinguish clean surfaces from dirty surfaces, likely due to the difference in roughness.

Germanium grown on silicon represents one half of the complementary substrates (unannealed, high defect density); the other half is a Ge wafer (negligible defect density). The Ge-on-Si substrate is composed of an epitaxially grown thin film of germanium that is approximately one micron thick grown on a silicon wafer. The surface defect density is roughly $10^9/\text{cm}^2$.⁽¹⁴⁾ While this high density would render any solid state device ineffective, it actually impacts only a small percentage of the crystal surface. The distance over which a dislocation significantly affects the geometry of a crystal is on the order of the burgers vector. For germanium with a dislocation density of $10^9/\text{cm}^2$, a burgers vector of 4\AA implies that roughly 0.0001% of the surface is geometrically influenced by the defects. It is because of this tiny influence that dislocations are described as “diffuse”. However, it should be noted that the space charge region associated with the dislocation is on the order of the Debye length ($\sim 50\text{nm}$ in undoped Ge) which can be considerably larger than the burgers vector.

- *Combinatorial selection*

Combinatorial approaches allow for the simultaneous testing of many possible answers to a specific question. In the case of this work, the combinatorial approach used is phage display which allows for the simultaneous testing of approximately one billion different peptide fusions. In the course of a phage display experiment, it is expected that these billions of initially random peptide fusions will eventually be reduced to just a few (or one) peptide fusions that have the desired quality.

The phage display library used in this work is based on the M13 bacteriophage expressing a modification on one of the minor coat proteins known as pIII. M13 is a

filamentous phage (~880nm long and 6nm in diameter) with a capsid composed of roughly 2700 copies of the major coat protein (pVIII). The modified pIII protein is expressed at one end of the viral assembly and has five copies. At the N-terminus of each one of these pIII copies is the random peptide fusion that is the target of identification through selection. Depending on the library used, the peptide fusion can have different lengths and functionalities. The phage display library employed in this work utilizes a 7-amino acid constrained library (New England Biolabs PhDC7C). 'Constrained' refers to the fact that the random peptide sequence is always flanked by a pair of cysteine residues. These cysteines form a disulfide linkage which forces the peptide fusion into a ring-like structure. This is beneficial because it limits the space of conformational freedom available to the peptide, thus insuring a more specific fit to the substrate. Linear (unconstrained) libraries can also be used, but they tend to be less specific due to the fact that the peptide fusion can adopt a wide space of possible conformations.

- *Positive and negative selections*

In diffuse selection, the goal is to target a particular feature of a material surface. Positive selections necessarily sample the whole surface with no built-in discrimination for certain surface features. In order to alleviate this problem, after a round of positive selection is complete, a round of negative selection is performed on a complimentary substrate, in this case a germanium wafer (Fig 1.2-1). The idea is that after a positive selection, that are two populations of viruses, those that bind dislocations preferentially and those that bind the rest of the germanium surface preferentially. By keeping the

phage that *do not* bind the germanium wafer (i.e. negative selection), the wafer is essentially being used as a filter for sequences which are just general binders of germanium but not defects in germanium.

In this experiment we performed two rounds of positive selection, followed by two rounds of negative selection followed by a final positive selection. This resulted in only two sequences being represented by the initially random collection of peptide fusions. These sequences can be considered consensus peptide sequences, and have been named 1v (CSYHRMATC) and 3v (CTSPHTRAC).

- *Specificity verification:*

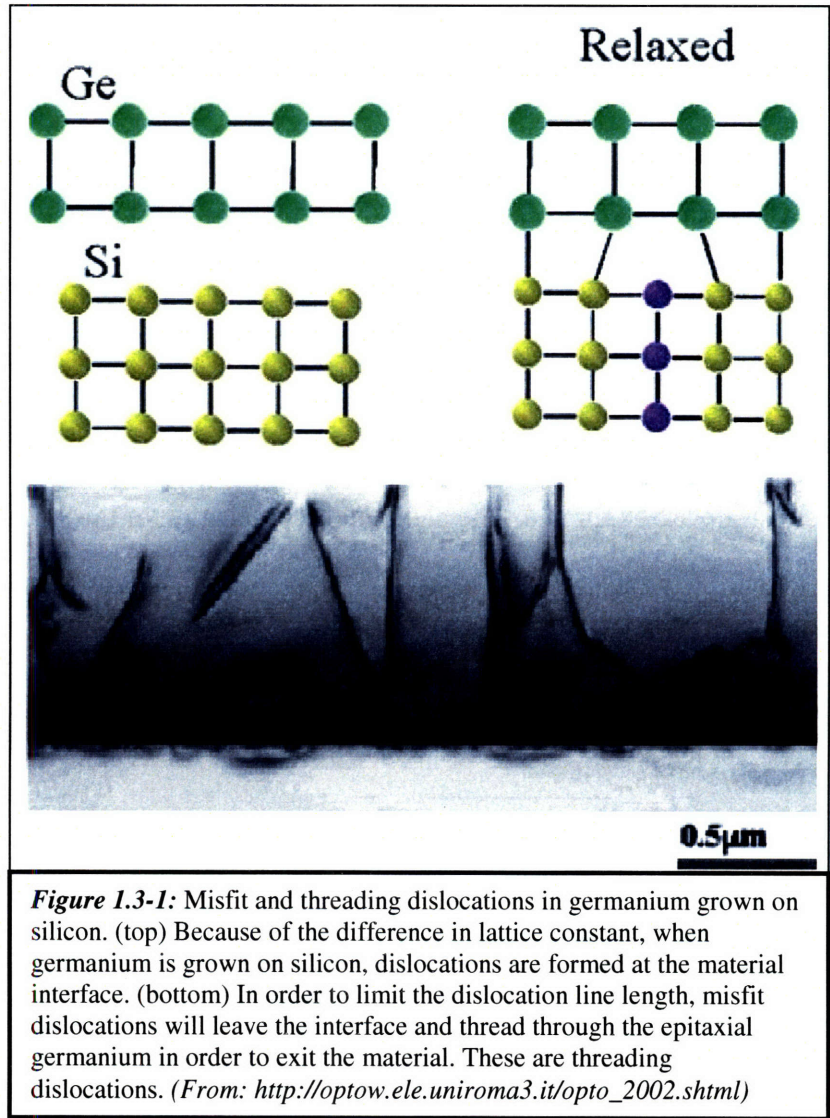
The author is not aware of any technique to directly image an 880nm phage particle bound to an atomic scale defect, so indirect techniques were employed to verify binding. The first technique used was atomic force microscopy which is likely the most direct technique possible. AFM allows the direct observation of phage on the substrate but can not simultaneously give the atomic resolution necessary to detect defects as well. Additionally, an AFM can only measure a field roughly 10 μ m square at a time, meaning large variations in phage binding density over a surface are difficult to detect. The second technique involves fluorescently tagging the phage that are bound to the substrates and then measuring the fluorescence as an indirect measure of phage concentration. This is a more indirect technique than AFM but is capable of measuring a field roughly 1mm square in a single measurement providing better ability to detect variations in binding density. The last technique is titration which is the most indirect but also samples the

entire surface in one measurement. In titration the bound phage are eluted and then plated in order to quantify the number that are bound. In all three cases comparisons are made between phage binding on the two complementary substrates to infer the effect of defects, because defects can not be imaged simultaneously with viruses.

- *Substrate characterization:*

In diffuse selection, the goal is to find a polypeptide with affinity to a specific, albeit rare, target on our material surface. However, the technique will tend to find whatever differences there are between the two substrates used. To ensure that the most significant difference is the one that is being initially targeted, several properties of the complementary substrate are examined. The elemental composition of the surface was examined using X-Ray Photoelectron Spectroscopy (XPS); the surface roughness was examined using Atomic Force Microscopy (AFM); the crystal orientation was examined using X-Ray Diffraction (XRD); and defect density was examined using Edge Pit Density (EPD).

- *Figures for Section 1.3*



1.4: Results of Diffuse Selection

After the fifth round of selection it was observed that the 3v peptide sequence occurred in 60% of clones and the 1v peptide sequenced occurred in 30% of clones. Because the 3v peptide sequence occurred with the highest frequency efforts were focused on that peptide. The ability of the 3v peptide to bind was assessed using three techniques: atomic force microscopy, fluorescence microscopy and titration. After assessing this binding efficiency it becomes necessary to perform surface characterization of the complementary substrates.

- *Assessing binding efficiency*

Assessing the binding efficiency was accomplished using several techniques the first of which is atomic force microscopy. Tapping mode AFM is an excellent tool for imaging phage on a surface in a small field. Equal concentrations of M13 bacteriophage expressing the 3v sequence (M13-3v) were exposed to Ge-on-Si substrates and germanium wafers to determine the difference in binding efficiency for the two substrates. AFM measurements show that M13-3v has a clear preference for the Ge-on-Si substrate compared to the germanium wafer. Overall, the measured preference is roughly 3:1 with AFM measurements (Fig 1.4-1). A detailed accounting of this technique can be found in Appendix 1.B.

Fluorescent measurements were performed using two distinct phage populations. One population was a monodispersed collection of viral clones all expressing the 3v

peptide on pIII (M13-3v). The second population was made up of 'wild-type' phage known as M13KE which are identical to M13-3v, except they have no peptide fusion on pIII, thus providing a good control for the effect of non-selective background binding. The phage were fluorescently tagged using an antibody for the phage (biotinylated anti-fd) which is linked to a fluorescent dye (streptavidin conjugated tetramethylrhodamine - TMR) via the biotin-streptavidin linkage (Fig 1.4-2). The choice of fluorescent dye is important for yielding useful results and several dyes were examined in the course of process optimization (Table 1.4-1). The dye found to work the best was TMR due to its superior resistance to bleaching.

Table 1.4-1: Comparison of streptavidin-conjugated dyes for fluorescent quantification of phage binding.

Dye	Absorption/Emission	Filter Used (Excitation/Emission)	Comments
Phycoerythrin	546nm / 575nm	PI (546±6nm/585±20nm)	Bleaches very easily
Oregon Green 488	496nm / 524nm	GFP (470±20nm/525±25nm)	Filter is not optimized for this dye
Tetramethyl-rhodamine (TMR)	555nm / 580nm	TRITC (535±25nm/610±38nm)	Good resistance to bleaching and good filter optimization

Fluorescence, while powerful, has considerable ability to be swayed by an undesirable background signal. Overall, there are four potential contributions to background fluorescent signal: 1) any noise experienced by the CCD during exposure, 2) any non-selective antibody/dye binding to the substrate, 3) any non-selective binding of the large viral assembly, and 4) any germanium affinity that the selected peptide may

have. The first two contributions were small and simply subtracted from the measured fluorescence. After careful process optimization, the resulting M13-3v fluorescence measurements showed a roughly 2:1 preference for the Ge-on-Si substrate compared to the Ge substrate (Fig 1.4-3). The fluorescence signal resulting from M13KE binding showed no selectivity for either substrate and was slightly smaller than the signal due to M13-3v on Ge. When the M13KE binding is treated as background to the M13-3v binding, the Ge-on-Si to Ge preference grows to 10:1. The most important parameters to optimize in this procedure are the concentrations of phage, anti-fd and fluorescent dye. The careful balance of these three constituents will maximize signal while minimize background noise. It was found that quite small phage concentrations (20ul of 10^6 pfu/ul solution) were required to achieve good signal to noise. A detailed accounting of this treatment can be found in Appendix 1.C.

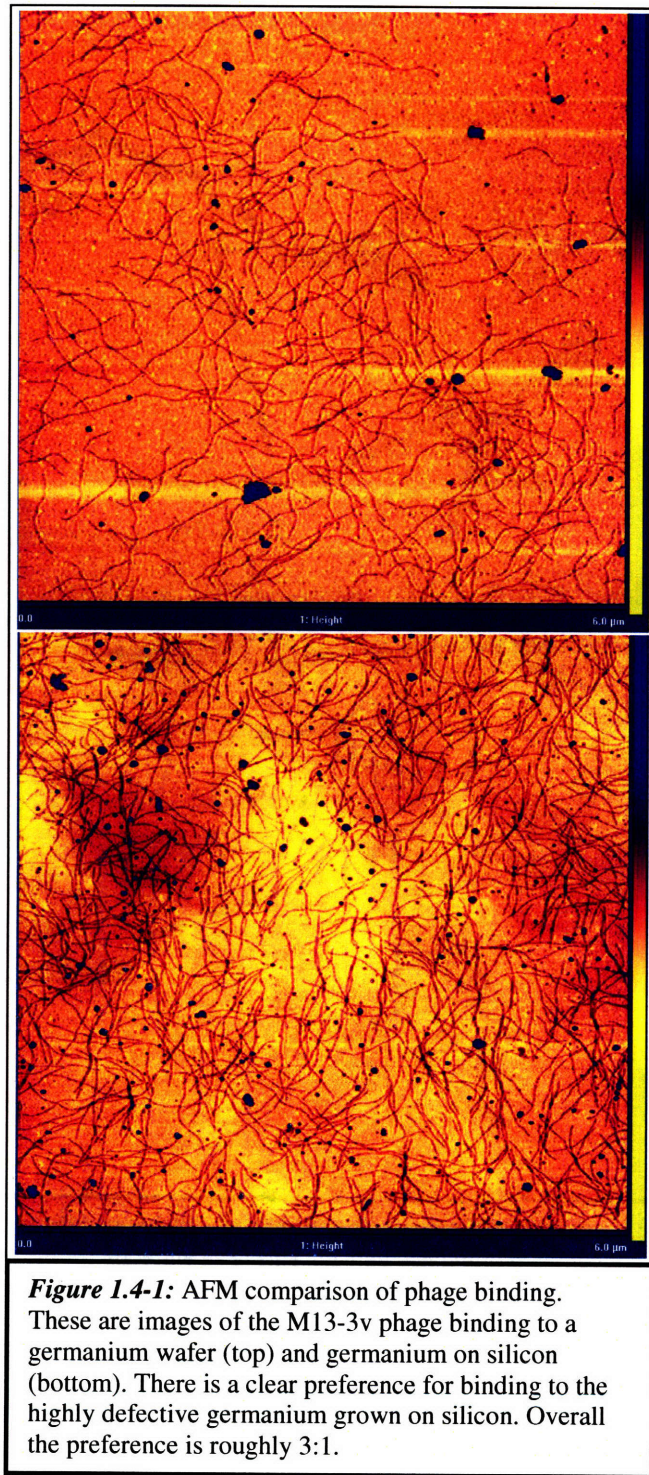
Titration is a quantitative technique for measuring the number of phage that bind a substrate. After substrate exposure and before amplification, a fraction of the eluted phage population is exposed to a bacterial lawn that has been grown on culture plates. At each point where the bacterial lawn becomes infected, a viral plaque forms. The phage are modified with a *lacZ* gene causing the viral plaque to turn blue. If the phage are sufficiently diluted, each plaque corresponds to only one infection event. By counting the number of plaques on a given plate at a given dilution, it is possible to determine the number of phage that bound the original substrate. Titration measurements were made using the monodispersed M13-3v phage population (these results were not compared to the wild type M13KE because wild type phage show a higher rate of infectivity). No antibody or fluorescent dye was needed for titration. The resulting plates indicated a 3:1

preference for the Ge-on-Si substrate compared to the Ge substrate (Fig 1.4-4), which is identical to the preference seen using AFM and similar to the 2:1 preference seen in fluorescence. A detailed accounting of the titration technique can be found in Appendix 1.D.

- *Surface characterization*

Between AFM, fluorescence and titration, we are confident that M13-3v shows a preference for Ge-on-Si. Next it is necessary to demonstrate that the surfaces are identical except for the presence of dislocations. The surfaces were examined using XPS, surface roughness (AFM), XRD and finally EPD. The XPS data show that the substrates have the same elemental composition (Fig 1.4-5). The AFM measurements show that the substrates are very smooth with very similar surface roughness; Ge-on-Si: $R_{\text{rms}} = 0.235 \pm 0.098 \text{nm}$ and Ge wafer: $R_{\text{rms}} = 0.201 \pm 0.034 \text{nm}$ (Fig 1.4-6). The XRD measurements show that the substrates both have a strong (100) orientation (Fig 1.4-7). Finally, the EPD testing shows that there are numerous defects in the Ge-on-Si substrate and none in the Ge wafer (Fig 1.4-8). A detailed accounting of these characterization techniques can be found in Appendix 1.E.

- *Figures for Section 1.4*



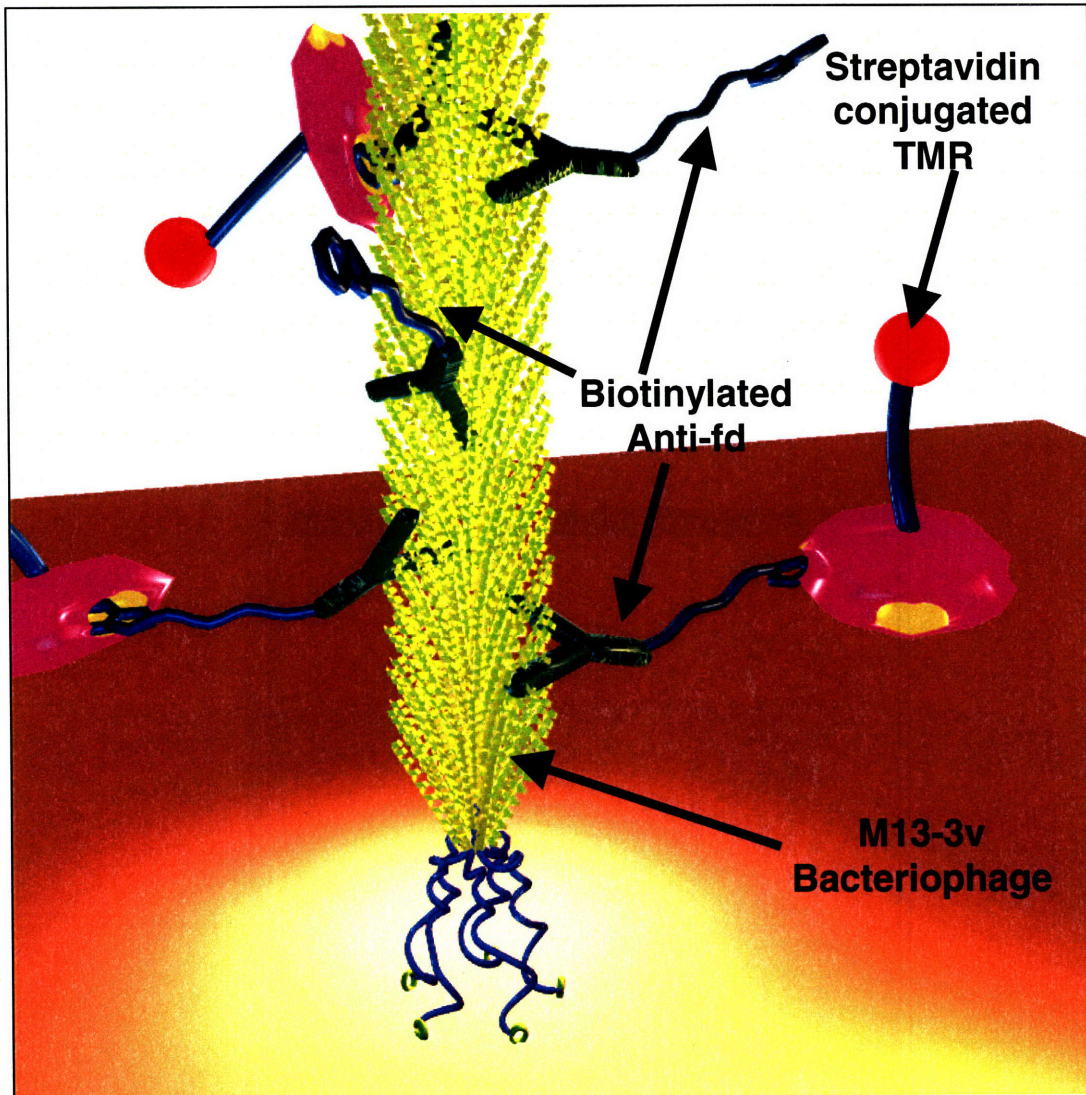
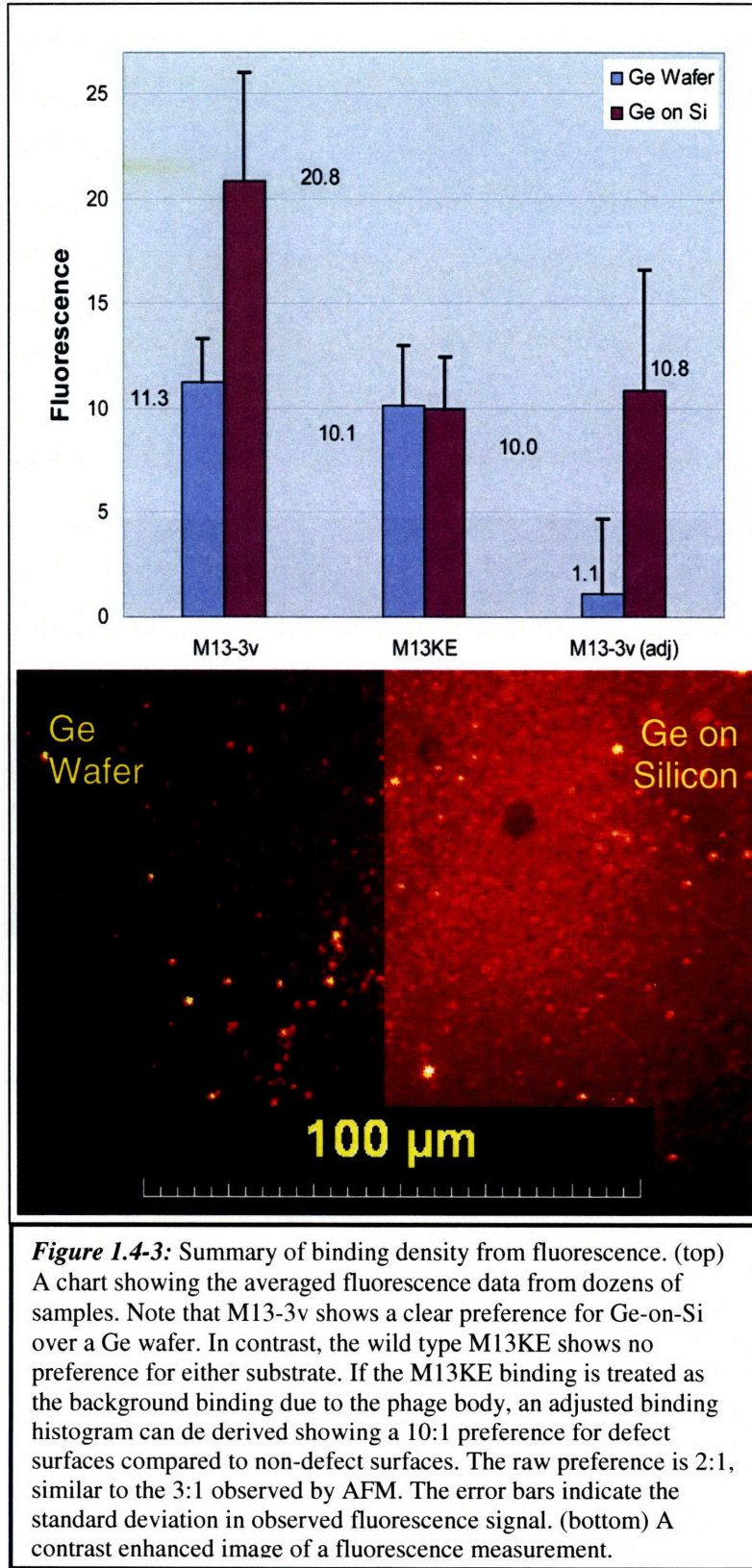
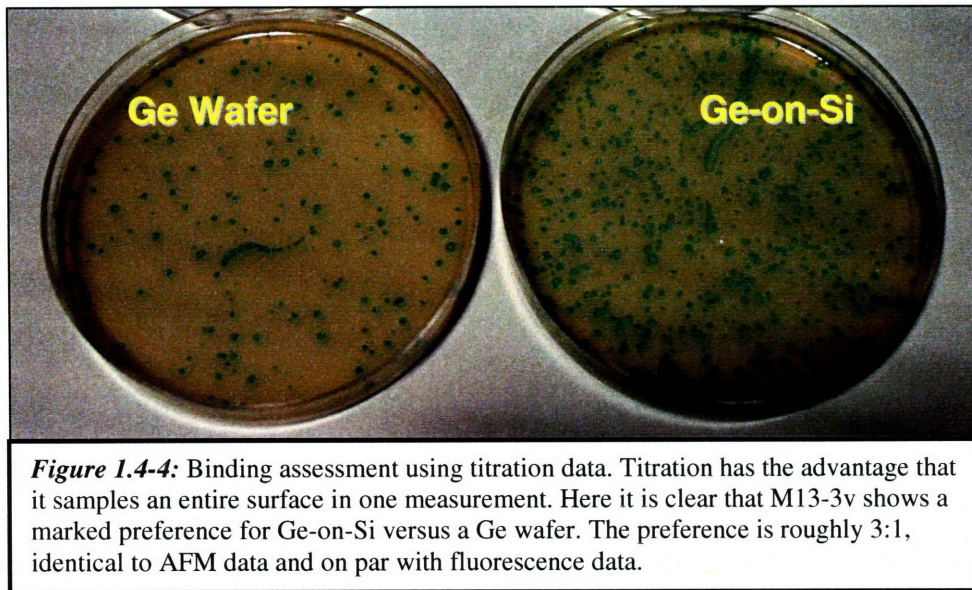


Figure 1.4-2: Scheme for fluorescently tagging bound phage. Once bound the phage are exposed to a solution containing biotinylated anti-fd. This is an antibody for the phage coat that has a biotin linker attached. This is then rinsed and subsequently exposed to streptavidin conjugated tetramethyl rhodamine (TMR). TMR is a red fluorescent dye with good resistance to photobleaching. This procedure makes it possible to identify the presence of phage on a surface using fluorescence.





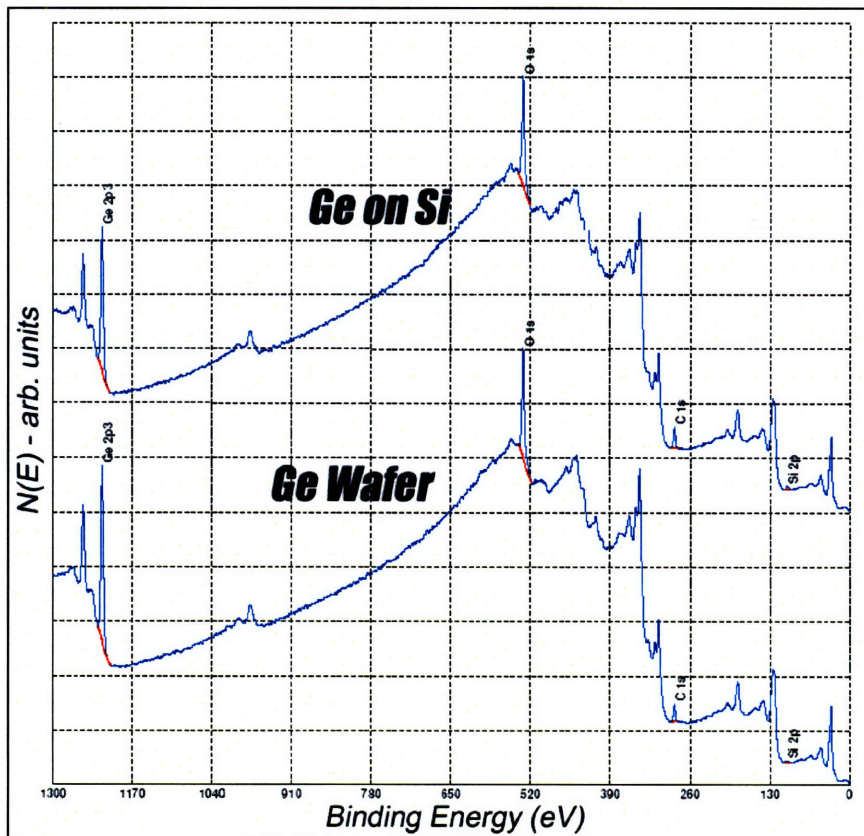


Figure 1.4-5: XPS comparison of germanium wafer and germanium-on-silicon. The identical curves reveal that the elemental composition of the two substrates is the same. This indicates that elemental difference are not responsible for the difference in phage affinity.

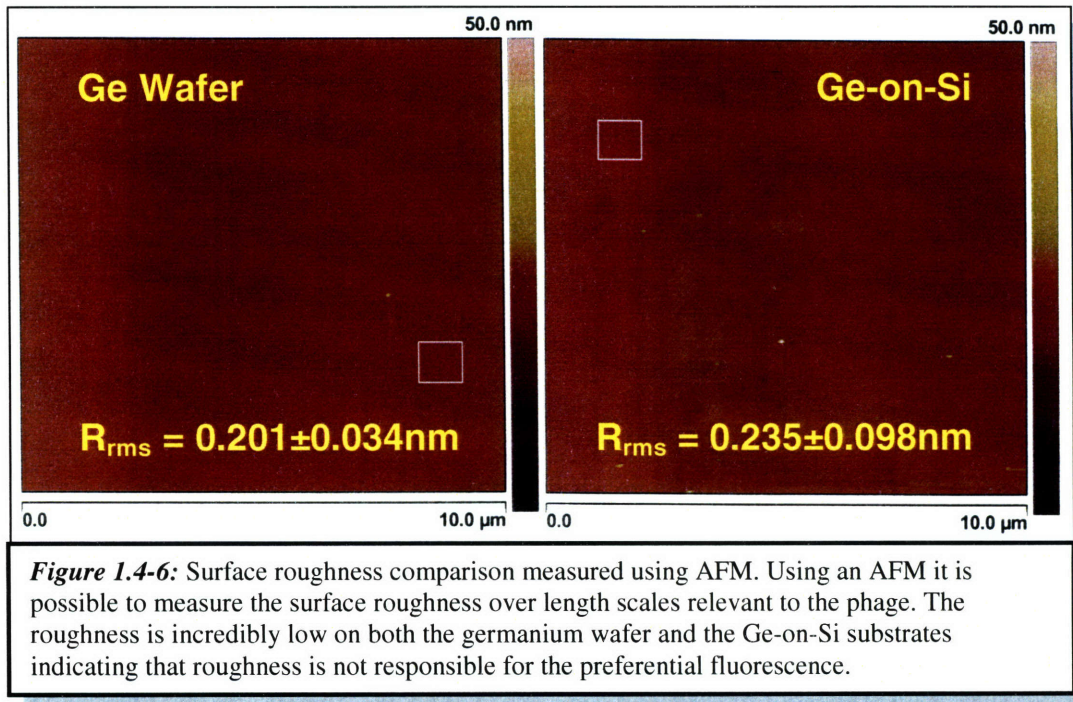
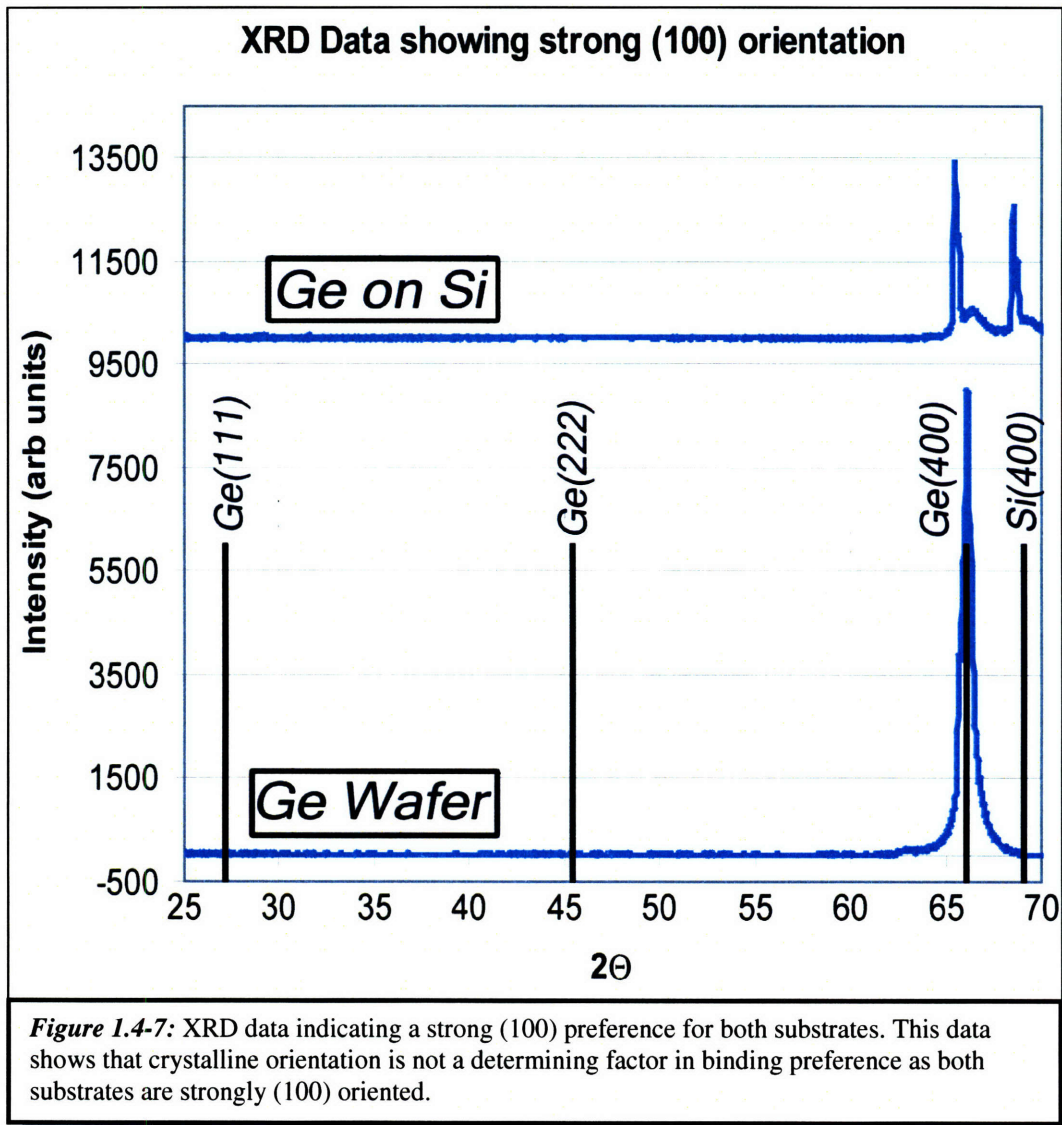
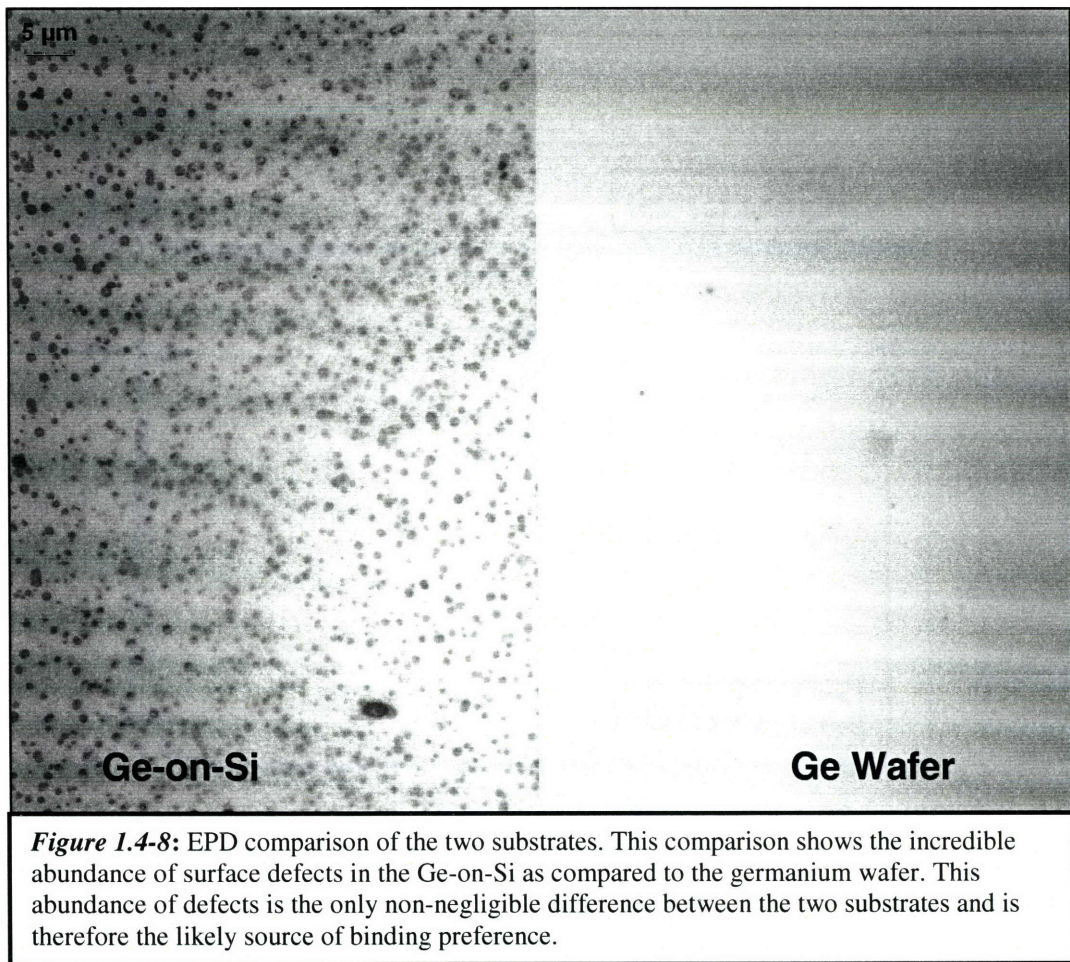


Figure 1.4-6: Surface roughness comparison measured using AFM. Using an AFM it is possible to measure the surface roughness over length scales relevant to the phage. The roughness is incredibly low on both the germanium wafer and the Ge-on-Si substrates indicating that roughness is not responsible for the preferential fluorescence.





1.5: Discussion & Recommendations for Future Work

The two peptide sequences derived from the phage display experiment are quite similar: 1v (CSYHRMATC) and 3v (CTSPHTRAC) (Fig 1.5-1). The odds of this level of similarity occurring by chance are roughly 0.02%. This probability is determined by first imagining that a sequence is taken at random from a pool of all possible 7-residue constrained sequences. Then a second sequence is pulled at random from the same pool and compared to the original sequence. There are 7-choose-4 ways to select 4 residues at random for comparison between the two sequences. Assuming all amino acids are independent and equally likely, the odds that the 4 residues are the same is $(1/20)^4$. There is then an additional 7-fold degeneracy because the looped structures can be superimposed on one another in seven different ways. As a result, the odds of two random sequences demonstrating the degree of overlap seen in our sequences is:

$$\binom{7}{4} \cdot \left(\frac{1}{20}\right)^4 \cdot 7 = 0.0015$$

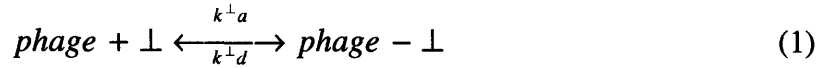
This is extremely encouraging as the sequences were essentially arrived at independently. This level of overlap gives confidence that we were able to focus on the proper space of possible binding sequences. This assertion is born out by the AFM, fluorescence and titration data.

In an effort to quantify the phage binding, a basic model was developed. The phage-surface interactions were treated as simple bimolecular interactions ($A + B \leftrightarrow A-B$). This approximation assumes that the phage do not interact on the sample surface and that each phage interacts with only one surface site at a time (and vice versa). The result

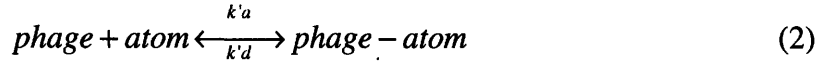
of this analysis predict a 100,000 fold improvement in binding constant for the M13-3v phage with defects compared to non-defect binding sites. This analysis is shown below:

(In this treatment *phage* refers specifically to M13-3v phage, \perp refers to a dislocation and *atom* refers to a non-defect binding site.)

For the phage-dislocation interaction, we have:



For the phage-background interaction, we have:



At equilibrium we have:

$$K_D^\perp = \frac{k_d}{k_a} = \frac{[phage][\perp]}{[phage - \perp]} \quad (3)$$

$$K'_D = \frac{k'_d}{k'_a} = \frac{[phage][atom]}{[phage - atom]} \quad (4)$$

where K_D are equilibrium dissociation constants. Because the whole sample surface is exposed to the phage solution, $[phage]$ is the same for defects and non-defect binding sites. Additionally, because the complimentary substrates were exposed to the same phage solution simultaneously, $[phage]$ is the same for both substrates. Solving for $[phage]$ and rearranging:

$$\frac{K'_D [phage - atom]}{[atom]} = \frac{K_D^\perp [phage - \perp]}{[\perp]} \quad (5)$$

We assume that the level of fluorescence is proportional to the concentration of bound phage. If the Ge-on-Si fluorescence ($[phage - atom] + [phage - \perp]$) is twice

the Ge wafer fluorescence ($[phage-atom]$), then (assuming $[phage-atom]$ is the same on either substrate):

$$[phage-atom] = [phage-\perp] \quad (6)$$

Substituting and canceling:

$$K_D' / [atom] = K_D^\perp / [\perp] \quad (7)$$

Note that the atomic surface density is roughly $10^{14}/\text{cm}^2$ while the dislocation density is $10^9/\text{cm}^2$.

$$\begin{aligned} \rightarrow [atom] / [\perp] &= 10^5 \\ \therefore K_D^\perp / K_D' &= 10^{-5} \end{aligned} \quad (8)$$

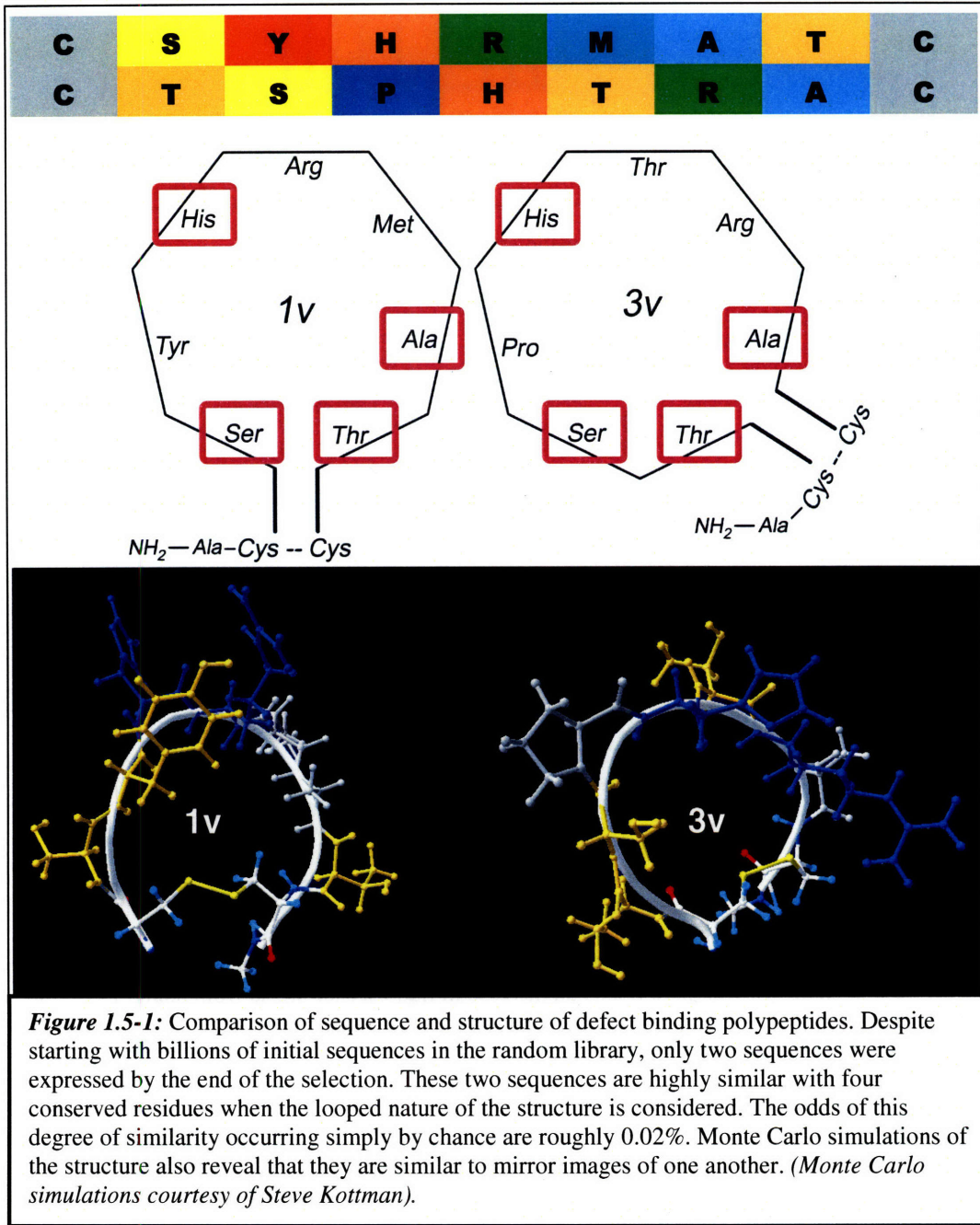
So there is effectively a 100,000 fold improvement in selectivity.

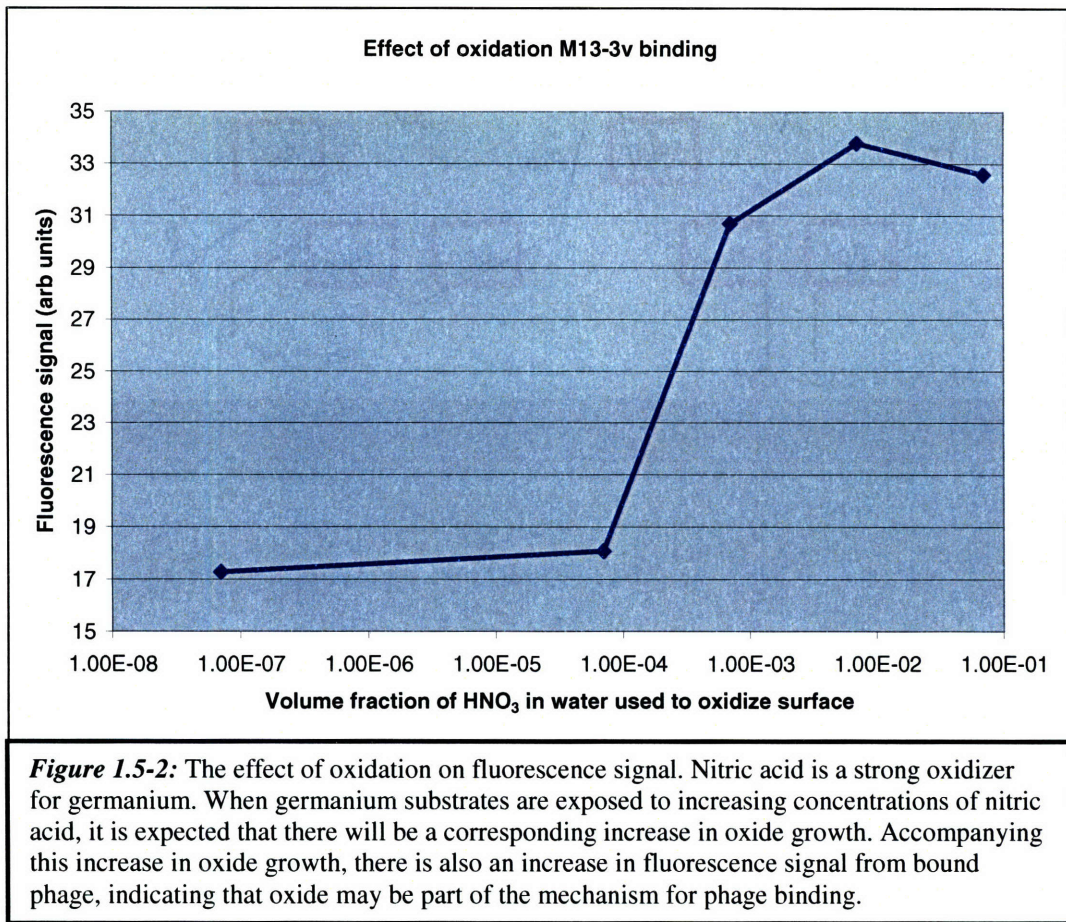
The mechanism for binding is not entirely clear at this stage and is one area that calls for future examination. There is likely a space charge region associated with the surface defects. This could be the source of a primarily electrostatic interaction. However, the germanium film is nominally undoped (lightly p-type, $N_A \sim 10^{16}/\text{cm}^3$)⁽¹⁷⁾. At a junction in a semiconductor, the magnitude of the electric field is generally proportional to the doping density and the width of the space charge region is proportional to the reciprocal square root of the doping density. As a result, for the light doping present in this case, the expectation is that the space charge region will be broad and shallow. It is also possible that the binding mechanism may be due to the local chemistry of the defect. We expect that the sight of a dislocation will oxidize preferentially as this is the mechanism for selective edge pit etching. It has been shown that hydroxyl containing

amino acids will bind to metal oxides⁽¹⁸⁾ so oxide binding is also a potential mechanism in this case. Additionally, it has been demonstrated that serine-histidine structures play a role in silica formation in natural systems⁽¹⁹⁾. Early experimentation using nitric acid as a strong oxidizer for germanium has revealed that the fluorescence signal observed increases when the substrate is exposed to higher acid concentrations (Fig 1.5-2). At higher acid concentrations, we expect higher rates of oxidation which would then correlate with fluorescence signal. Future work should include additional exploration of binding mechanism including amino acid substitution to determine how different parts of the binding motif function.

These results are a verification of the diffuse selection approach for diffuse/inseparable targets in inorganic materials. Although we have not shown direct defect binding, we have demonstrated a biomolecular affinity for highly defective surfaces that is clearly driven by a selected peptide sequence. There are many similar problems that will all have unique materials challenges especially when it comes to surface preparation. Examples of similar problems that may draw technological interest would be the selection of a semiconductor given a desired doping profile, the selection of a step edge in a crystal that has been cut along a vicinal plane or perhaps even micro-cracks that exhibit consistent morphology. It could also be applied to an analogous system such as defect binding in heteroepitaxially grown GaN on sapphire.⁽²⁰⁾ Diffuse selection should provide a good outline for approaching these problems.

- *Figures for Section 1.5*





Appendix 1.A: Germanium Substrate Preparation

Two types of germanium samples were used for this experiment; germanium wafers and germanium-on-silicon

The germanium wafers are undoped CZ grown 4 inch <100> wafers supplied by Wafer World (<http://www.waferworld.com/>).

The germanium-on-silicon wafers were prepared Jifeng Liu of the Kimerling Group here at MIT. The samples were prepared using CVD epitaxy to produce germanium films one micron thick. At this thickness, the wafers are fully relaxed.

Samples were prepared by cutting the samples into 5mm x 5mm squares using the die saw in the ICL.

Before any exposure, the samples were stripped of any oxide using a concentrated HF dip (10sec x 3) with DI water rinse and a brief (10sec) 0.07% v/v HNO₃ soak followed by a final water rinse.

Appendix 1.B: AFM Quantification of Phage Binding

AFM quantification was achieved using a Nanoscope IV with a multimode AFM operating in Tapping Mode with an RTESP tip.

The germanium substrates were prepared in the fashion described in Appendix 1.A.

After substrate preparation, the samples were exposed to a solution containing 20 μ l/sample of phage solution (10^6 phage/ μ l; determined by titration and spectrometric analysis).⁽²¹⁾

After an hour of phage exposure the phage were rinsed to remove any non-selectively bound phage (1x TBST-BSA [TBS + 0.5g/L BSA + 0.5% Tween-20], 1x TBST [TBS + 0.2% Tween-20], 1x 10%TBS).

Finally, the sample was rinsed in DI water to remove salt from the surface which would interfere with surface imaging.

A germanium wafer substrate and a germanium-on-silicon substrate were both treated to this phage exposure and were subsequently imaged (Fig 1.3-1). Imaging was performed repeatedly in order to get a feeling for what constituted a representative surface site.

Once imaged, the phage pictured were counted by hand to determine their relative binding affinity.

Appendix 1.C: Fluorescent Quantification of Phage Binding

The fluorescence measurements were made using a TRITC filter on an Olympus IX51 fluorescence microscope. Images were taken of the samples using an Olympus Q-Color 3 CCD and their average luminescence was determined using a standard software suite (Adobe Photoshop 6.0: Histogram function). Fluorescence was collected for numerous samples as the process was optimized to yield the maximum differential signal between the two substrates.

The samples were tagged using streptavidin conjugated Tetramethylrhodamine (TMR) which was bound to the major coat protein of the phage using a biotinylated antibody (Fig 1.3-2).

The samples were prepared by first cutting the substrates into 5mm x 5mm squares. All the samples were dipped in 48% HF three times for 10sec each with a water rinse in between. The samples were then dipped in 0.07% HNO₃ for 10sec and rinsed again. The samples then received 2x rinse in acetone, 2x rinse in ethanol and a final rinse in acetone.

The samples were then arranged in a 2x2 array, 2 germanium wafers and two germanium-on-silicon substrates (Fig 1.C-1), and exposed to 20μl/sample of phage solution (10⁶ phage/μl; determined by titration and spectrometric analysis).⁽²¹⁾

After half an hour, the samples received an intermediate wash (1x TBST-BSA [TBS + 0.5g/L BSA + 0.5% Tween-20], 1x TBST [TBS + 0.2% Tween-20], 1x 10%TBS).

Next the samples were exposed to 20μl/sample of biotinylated anti-fd (1:50 dilution of stock solution, Sigma) for half an hour. A second intermediate wash was done and the

samples were finally exposed to 20ul/sample of streptavidin conjugated Tetramethylrhodamine (1:100 dilution of stock solution, Molecular Probes).

The sample then received a final wash (4x TBST-BSA [TBS + 0.5g/L BSA + 0.5% Tween-20], 4x TBST [TBS + 0.2% Tween-20], 1x 10%TBS, 1x H₂O). The samples were then mounted and measured.

Because the anti-fd shows some non-selective attachment to the germanium substrates, the anti-fd signal had to be subtracted from the virus based signal (Fig 1.C-2). Error bars are the standard deviations of the average fluorescence signal from different samples.

- *Figures for Appendix 1.C*

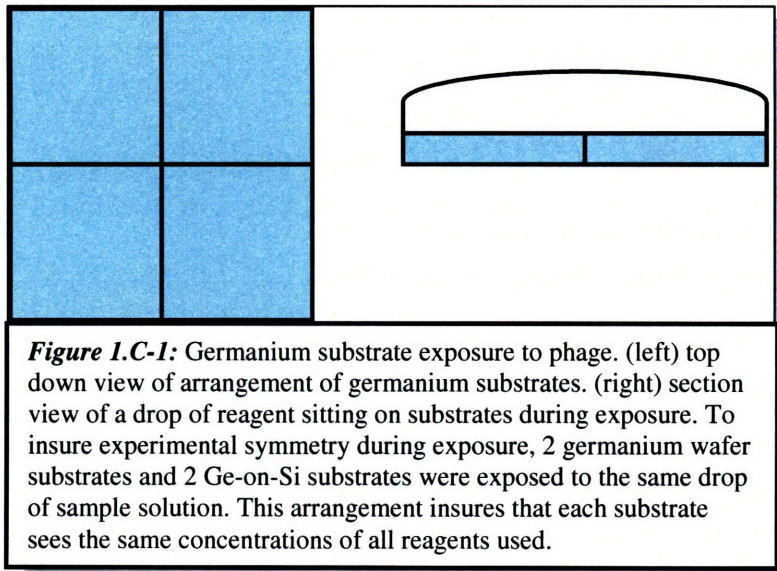
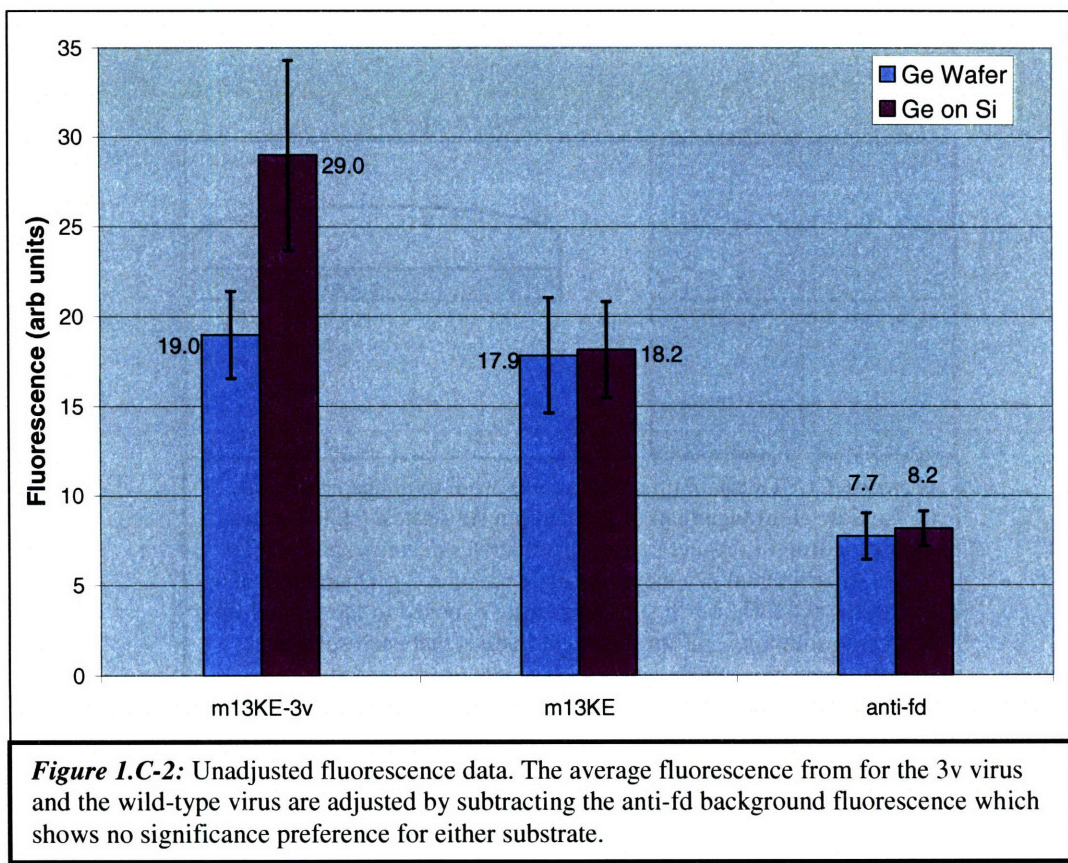


Figure 1.C-1: Germanium substrate exposure to phage. (left) top down view of arrangement of germanium substrates. (right) section view of a drop of reagent sitting on substrates during exposure. To insure experimental symmetry during exposure, 2 germanium wafer substrates and 2 Ge-on-Si substrates were exposed to the same drop of sample solution. This arrangement insures that each substrate sees the same concentrations of all reagents used.



Appendix 1.D: Agar Plate Titration Quantification of Phage Binding

The samples were prepared using the same steps as in the fluorescence measurement (Appendix 1.C) except after the phage exposure, the samples received the final wash in lieu of the anti-fd and TMR exposure. The phage were then eluted and titered as described in the NEB phage display kit.

Elution is a process of serial dilutions to find a concentration where plates will not be totally covered by plaques. The viral population is diluted before plating so that the number of plaques on a given plate can be counted by hand.

The results of the titration are plates with blue viral plaques. The number of plaques corresponds to the number of phage which bound the substrate.

Appendix 1.E: Surface Characterization Techniques

XPS Measurements:

XPS was done using a small spot ESCA with an Al source and a pass energy of 187.85 eV. The binding energy was swept from 0 to 1300 eV.

AFM Measurements:

AFM was done using a Digital Instruments Nanoscope 4 with a multimode AFM operating in tapping mode with an RTESP tip from VEECO. Spot sizes of approximately 1 micron in size were used with a built in roughness measurement protocol.

XRD Measurements:

XRD was done using a Cu K α source in the CMSE XRD facility. The 2 Θ angle was swept from 25 $^{\circ}$ to 70 $^{\circ}$.

EPD Measurement:

The etchant used is 67ml CH₃COOH, 20ml HNO₃, 10ml HF, 30mg I₂. The samples were dipped for 10sec and then imaged using an Olympus optical microscope.

1.Ref: References

1. **Belcher, A. M., X. H. Wu, R. J. Christensen, P. K. Hansma, G. D. Stucky, and D. E. Morse.** 1996. Control of crystal phase switching and orientation by soluble mollusc-shell proteins. *Nature* **381**:56-58.
2. **Rosner, S. J., G. Girolami, H. Marchand, P. T. Fini, J. P. Ibbetson, L. Zhao, S. Keller, U. K. Mishra, S. P. DenBaars, and J. S. Speck.** 1999. Cathodoluminescence mapping of epitaxial lateral overgrowth in gallium nitride. *Applied Physics Letters* **74**:2035-2037.
3. **Flynn, C. E., C. Mao, A. Hayhurst, J. L. Williams, G. Georgiou, B. Iverson, and A. M. Belcher.** 2003. Synthesis and organization of nanoscale II-VI semiconductor materials using evolved peptide specificity and viral capsid assembly. *J.Mater.Chem.* **13**:2414-2421.
4. **Mao, C. B., D. J. Solis, B. D. Reiss, S. T. Kottmann, R. Y. Sweeney, A. Hayhurst, G. Georgiou, B. Iverson, and A. M. Belcher.** 2004. Virus-based toolkit for the directed synthesis of magnetic and semiconducting nanowires. *Science* **303**:213-217.
5. **Lee, S.-W., C. Mao, C. E. Flynn, and A. M. Belcher.** 2002. Ordering of quantum dots using genetically engineered viruses. *Science* **296**.
6. **Seeman, N. C., and A. M. Belcher.** 2002. Emulating biology: Building nanostructures from the bottom up. *PNAS* **99**:6451-6455.
7. **Alivisatos, A. P., K. P. Johnsson, X. G. Peng, T. E. Wilson, C. J. Loweth, M. P. Bruchez, and P. G. Schultz.** 1996. Organization of 'nanocrystal molecules' using DNA. *Nature* **382**:609-611.
8. **Mirkin, C. A., R. L. Letsinger, R. C. Mucic, and J. J. Storhoff.** 1996. A DNA-based method for rationally assembling nanoparticles into macroscopic materials. *Nature* **382**:607-609.
9. **Whaley, S. R., D. S. English, E. L. Hu, P. F. Barbara, and A. M. Belcher.** 2000. Selection of peptides with semiconductor binding specificity for directed nanocrystal assembly. *Nature* **405**:665-668.
10. **Giovane, L. M., H. C. Luan, A. M. Agarwal, and L. C. Kimerling.** 2001. Correlation between leakage current density and threading dislocation density in SiGe p-i-n diodes grown on relaxed graded buffer layers. *Applied Physics Letters* **78**:541-543.
11. **Deegan, T., and G. Hughes.** 1998. An X-ray photoelectron spectroscopy study of the HF etching of native oxides on Ge(111) and Ge(100) surfaces. *Applied Surface Science* **123**:66-70.
12. **Colace, L., G. Masini, G. Assanto, H. C. Luan, K. Wada, and L. C. Kimerling.** 2000. Efficient high-speed near-infrared Ge photodetectors integrated on Si substrates. *Applied Physics Letters* **76**:1231-1233.
13. **Colace, L., G. Masini, F. Galluzzi, G. Assanto, G. Capellini, L. Di Gaspare, E. Palange, and F. Evangelisti.** 1998. Metal-semiconductor-metal near-infrared light detector based on epitaxial Ge/Si. *Applied Physics Letters* **72**:3175-3177.

14. **Luan, H. C., D. R. Lim, K. K. Lee, K. M. Chen, J. G. Sandland, K. Wada, and L. C. Kimerling.** 1999. High-quality Ge epilayers on Si with low threading-dislocation densities. *Applied Physics Letters* **75**:2909-2911.
15. **Gan, S., L. Li, and R. F. Hicks.** 1998. Characterization of dislocations in germanium substrates induced by mechanical stress. *Applied Physics Letters* **73**:1068-1070.
16. **Kruml, T., D. Caillard, C. Dupas, and J. L. Martin.** 2002. A transmission electron microscopy in situ study of dislocation mobility in Ge. *Journal of Physics-Condensed Matter* **14**:12897-12902.
17. Personal correspondence with David Danielson of the Kimerling Group at MI. Feb. 25, 2005.
18. **Sarikaya, M., C. Tamerler, A. K. Y. Jen, K. Schulten, and F. Baneyx.** 2003. Molecular biomimetics: nanotechnology through biology. *Nature Materials* **2**:577-585.
19. **Cha, J. N., K. Shimizu, Y. Zhou, S. C. Christiansen, B. F. Chmelka, G. D. Stucky, and D. E. Morse.** 1999. Silicatein filaments and subunits from a marine sponge direct the polymerization of silica and silicones in vitro. *Proceedings of the National Academy of Sciences of the United States of America* **96**:361-365.
20. **Wu, X. H., L. M. Brown, D. Kapolnek, S. Keller, B. Keller, S. P. DenBaars, and J. S. Speck.** 1996. Defect structure of metal-organic chemical vapor deposition-grown epitaxial (0001) GaN/Al₂O₃. *Journal of Applied Physics* **80**:3228-3237.
21. **Barbas, C. F., D. R. Burton, J. K. Scott, and G. J. Silverman.** 2001. Spectrometric Phage Quantification, p. 15.17-15.18, *Phage Display: A Laboratory Manual*, 1st ed. Cold Spring Harbor Laboratory Press.

Chapter 2: Surface Patterning of Genetically Programmed Viruses

2.1: Introduction

It has been found that it is possible to use the M13 bacteriophage as a platform on which to bind and/or nucleate an expansive array of materials. These materials include compound semiconductors (GaAs⁽¹⁾, ZnSe⁽²⁾, CdS⁽³⁾), metals (Au⁽⁴⁾, Ag), and metal oxides (Co₃O₄⁽⁵⁾, IrO₂, TiO₂). Finding viruses capable of this feat is usually accomplished using phage display. In a typical M13 phage display experiment, the goal is to determine what modification to pIII will result in the best virus binding. Once this peptide fusion is identified, it can be moved via genetic modification to any other protein in the virus (or anywhere for that matter). Interestingly, it often turns out that when this binding protein is moved to the M13 pVIII protein, it will frequently act as a site where material nucleation and growth can occur.

The question that arises is how this material nucleation can be used to build useful devices. In certain cases it may be possible to spontaneously assemble viruses into useful structures⁽⁶⁾, but in general it is expected that to build a useful structure it will be necessary to direct the assembly of the viruses. In this project, viruses were assembled on surfaces that had been chemically patterned using Dip Pen Nanolithography (DPN).

Because the viruses are being assembled for the express purpose of nucleating a specific material, it is important that the viruses are patterned in such a way that their ability to nucleate materials is not hindered by the method used to assemble them. As such, all the techniques presented here are designed to be generalizable regardless of the genetic modification made to the viral coat.

This work presents three generalizable approaches to patterning M13 bacteriophage that have short pVIII modifications. The approaches presented are hydrophobic, electrostatic and covalent respectively, but only the covalent approach would really be effective for materials nucleation. However, all three techniques are demonstrated to be viable approaches to pattern the M13 bacteriophage.

2.2: Surface Patterning

As described previously, all the virus patterning presented here is mediated by Dip Pen Nanolithography. The molecule used for patterning is mercaptohexadecanoic acid (MHA: HS-(CH₂)₁₅-COOH) which results in features terminated in carboxylic acids when applied to gold substrates. The gold substrates are prepared by electron beam evaporation of gold onto clean silicon substrates. A complete accounting of the gold substrate preparation can be found in Appendix 2.A. Because gold will provide an amenable substrate for non-selective virus adsorption, it is necessary to cover any unpatterned background gold once the MHA has been patterned. In this work, the unpatterned background gold was backfilled with a methoxy PEG thiol which creates a poly ethylene glycol (PEG) terminated surface. PEG is a highly hydratable polymer which resists non-selective protein adsorption and thus serves to resist the undesirable binding of viruses on the unpatterned gold.

The surface patterning process is a multi-step protocol (Fig 2.2-1). The first step is the preparation of a gold substrate. Next, MHA lines are patterned on the substrate using DPN. After the MHA patterning is complete, the rest of the surface is backfilled using methoxy PEG thiol. Finally, the MHA lines are chemically activated to drive viruses to bind to the lines. A detailed accounting of this process is presented in Appendix 2.B.

- *Figures for section 2.2*

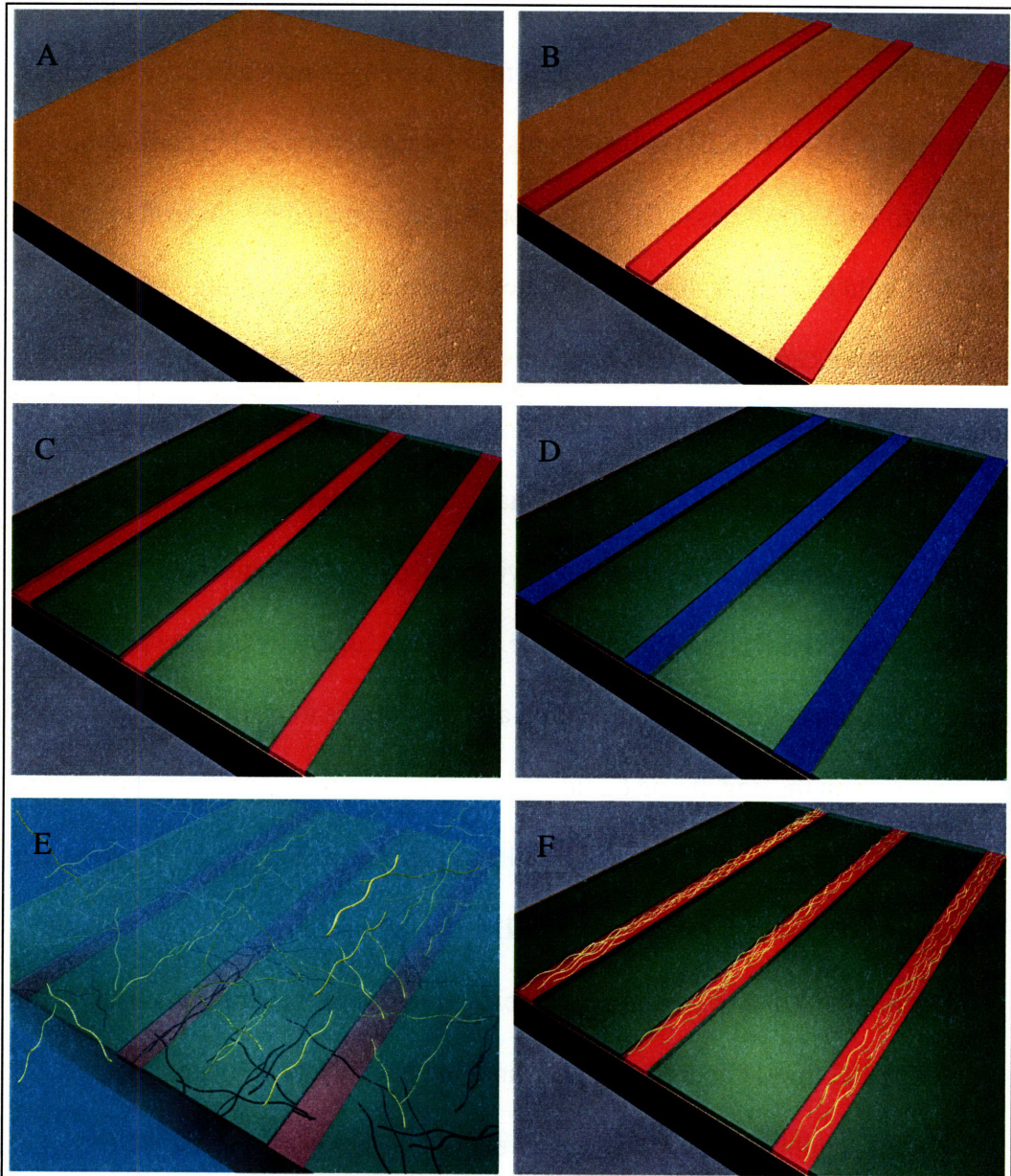


Figure 2.2-1: Process for patterning viruses. (A) Start with a gold substrate. (B) Using DPN deposit MHA features. (C) Using methoxy PEG thiol backfill the remaining gold surface. (D) Activate the MHA to encourage virus binding. (E) Expose the activated MHA lines to a solution containing viruses. (F) Rinse the remaining solution leaving behind only the bound phage.

2.3: Three approaches to virus assembly

Once the MHA template is patterned, the next step is to assemble the genetically modified M13 bacteriophage on the MHA features. The approach used to assemble the viruses must be carefully chosen. Typically, it would be possible to genetically modify the viruses to direct virus assembly through some form of activation chemistry. However, in this case it is important that the choice of activation chemistry does not interfere with the genetic modification of the virus. As a result it is not allowable to make a modification to the virus that would facilitate binding as this could interfere with the genetically programmed materials functionality. Using the carboxylate-terminated MHA surface it is possible to perform a variety of chemistries to encourage virus binding that won't interfere with the viruses ability to nucleate a desired material. In this work, the approaches used are hydrophobic attachment, divalent chelation (electrostatic attachment) and covalent attachment (Fig 2.3-1). A more thorough accounting of these techniques follows below.

- *Hydrophobic Attachment*

The first and simplest virus assembly approach is to simply use the relative hydrophobicities of the surface features to drive virus assembly. The carboxylate-terminated MHA is very hydrophilic while the methyl-terminated methoxy PEG thiol is relatively hydrophobic. As a result, when a hydrophilic phage interacts with the patterned substrate, it preferentially adsorbs to the MHA patterns (Fig 2.3-2). This effect is quite

non-specific and will be effective as long as the virus is water soluble. If features are patterned closely, phage can bridge features by forming clumps of virus. This bridging may actually prove useful in certain scenarios assuming it can be controlled through careful attention to feature spacing.

Hydrophobic attachment is a conceptually elegant patterning technique; however it is not useful when trying to assemble materials on the patterned viruses because the patterning is extremely sensitive to pH and ionic strength. If nucleating a material requires any sort of reduction chemistry or high concentration of precursor salt, then hydrophobic attachment will not be effective. However, hydrophobic attachment could prove useful as a route to patterning viruses before covalently cross-linking them with the substrate.

- *Divalent Chelation (Electrostatic Attachment)*

The concept of divalent chelation is that certain metal ions carrying a 2+ charge will form ligand complexes with nearby carboxylates. These divalent cations can act as a bridge between two (or more) carboxylates. Zinc and copper are good examples of such metal ions. Once MHA lines are patterned and the gold substrate is backfilled, the MHA lines can be incubated with a zinc nitrate solution. The result of this incubation is that the carboxylates should start to become decorated with Zn^{2+} cations. Using Kelvin Probe it is possible to assess the degree to which the MHA is being decorated with Zn^{2+} ions (Fig 2.3-3). Initially the MHA should have a considerable negative potential due to the

carboxylates. As the concentration of Zn^{2+} in solution rises, there is a clear rise in the local surface potential corresponding to an increase in local net charge as expected.

Divalent chelation is an electrostatic technique that has proven to be useful in previous efforts to assemble nanoparticles⁽⁷⁾ and viruses⁽⁸⁾ (Fig 2.3-4) on patterned substrates. In this technique, the fact that many viruses naturally tend to have carboxylates on their major coat proteins is exploited for patterning. The presence of carboxylates on a virus makes sense because most viruses exist in an aqueous environment where carboxylates will aid in virus solubility. The M13 bacteriophage is no exception. It has four carboxylates on each copy of its coat proteins that can all be used as sites for divalent chelation (Fig 2.3-5).

Once the MHA features are exposed to zinc nitrate and decorated with divalent ions, they can be exposed to phage. Because of the carboxylates decorating the phage coat, the viruses will spontaneously assemble onto the MHA features using the Zn^{2+} cations as a bridge (Fig 2.3-6). In this case, because the features are thin lines and the phage have a high aspect ratio, the viruses will naturally tend to align themselves with the lines in order to maximize the interaction. A detailed accounting of the divalent chelation protocol can be found in Appendix 2.C.

Once again, similar to hydrophobic attachment this is a conceptually elegant technique. It is going to be generalizable to most any phage modification as the M13 bacteriophage naturally has carboxylates along its body. However, divalent chelation also has the problem that it is sensitive to pH and ionic strength, albeit less so than hydrophobic attachment. Again, as a result, any attempts to perform any oxidation-reduction chemistry, or any chemistry that requires a high concentration of precursor salt

will disrupt the phage binding. The only answer is to move to a covalent binding approach.

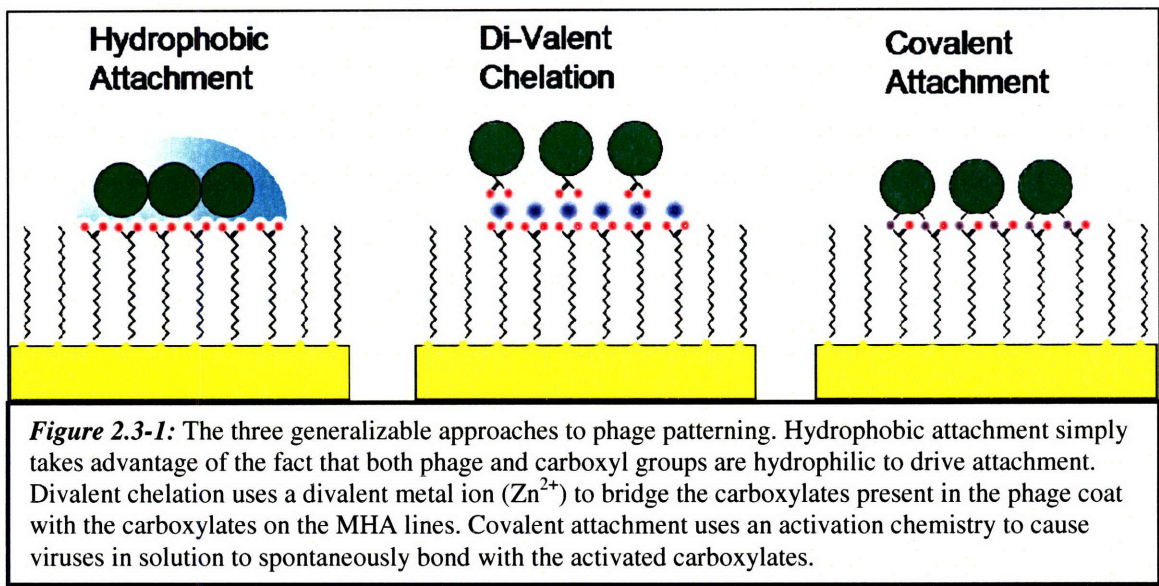
- *Covalent Attachment*

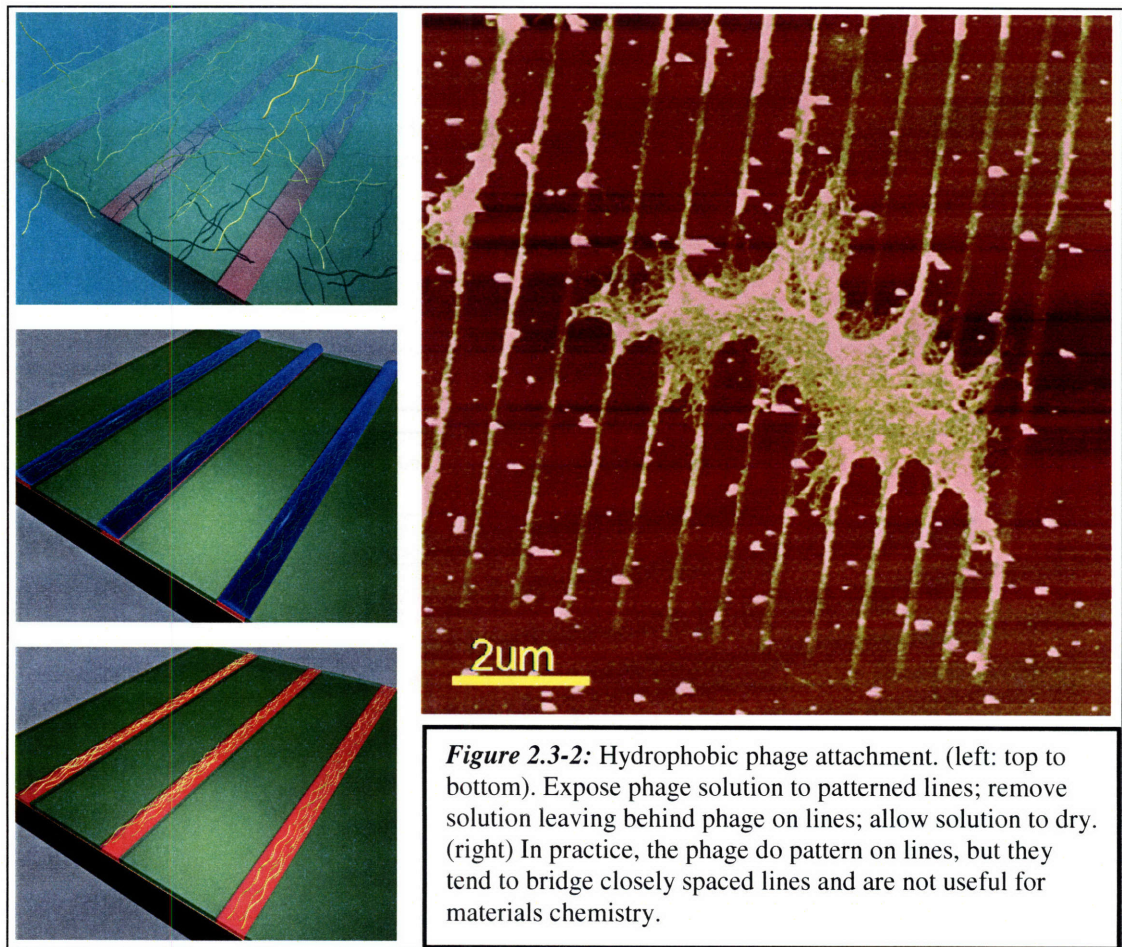
Hydrophobic and electrostatic approaches are both good ways to assemble viruses, however they are not amenable to materials assembly; as a result, the only remaining option is to use covalent attachment. Covalent patterning of viruses has been performed before⁽⁹⁻¹¹⁾ (Fig 2.3-7), however, it has always been dependant on the use of specific genetic modification of the virus to drive the assembly. In the case presented here, the genetic modification of the virus is meant to drive materials assembly, not virus patterning. A covalent attachment method is needed that will be generalizable to any genetic modification.

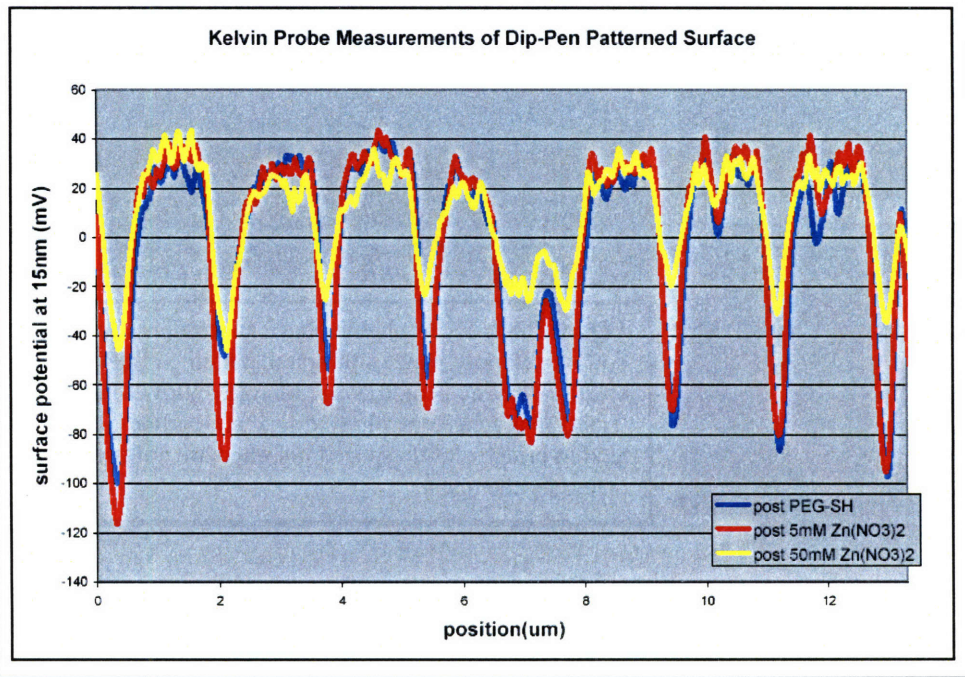
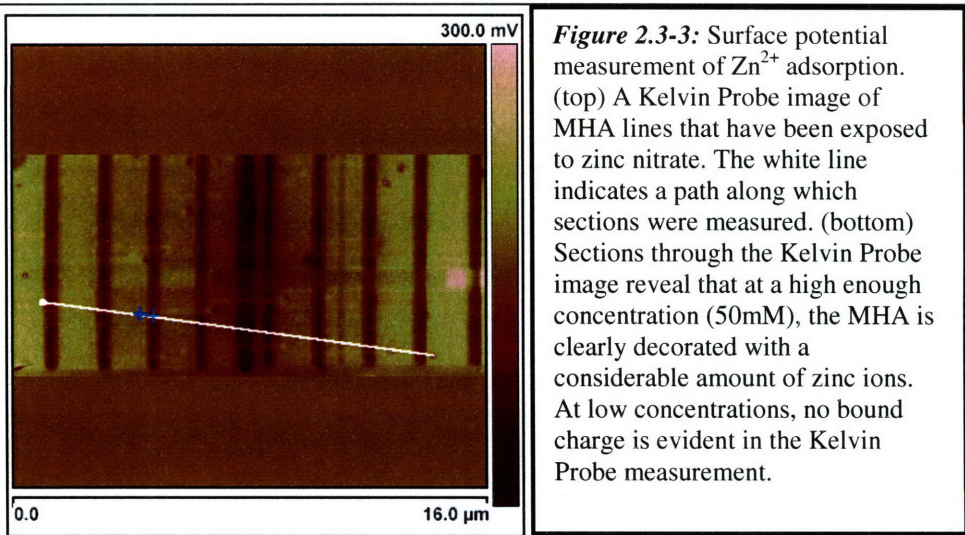
Fortunately, a generalizable approach does exist for covalently patterning the M13 bacteriophage. As it turns out the pVIII protein which makes up the phage coat is oriented such that the amino-terminus of the protein is pointing away from the virus. This creates a huge number of potential attachment points for virus patterning that will be present regardless of the pVIII genetic modification (i.e. there will always be an N-terminus expressed on the virus coat). Using a carbodiimide chemistry, it is possible to activate the carboxylates in the MHA patterns such that they will spontaneously form covalent bonds with any primary amines in solution (Fig 2.3-8). This chemistry can be performed in a two-step fashion which will ensure that none of the carboxylates on the virus are activated.

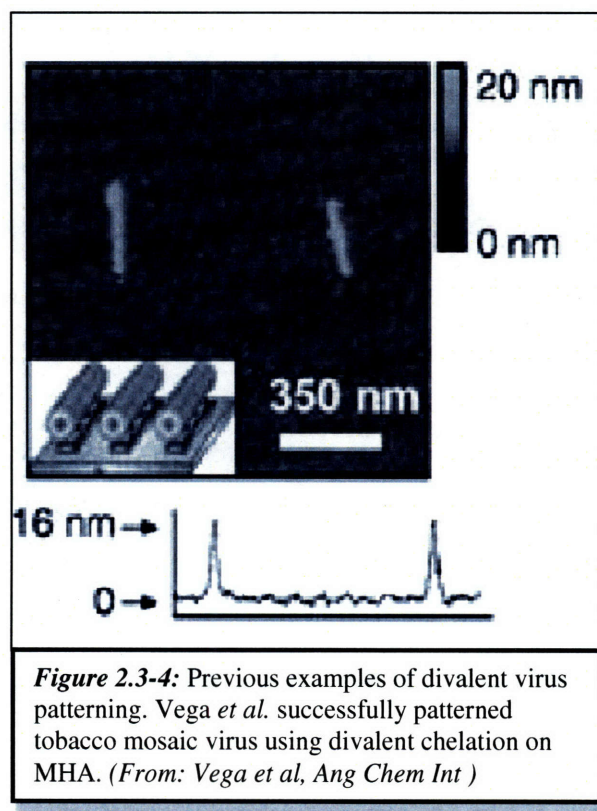
This covalent approach results in very nicely assembled viruses (Fig 2.3-9). The approach is generalizable and was demonstrated for two different viruses, E4 and p8#9. The E4 virus has four glutamic acids fused to the N-terminus of pVIII. This virus is useful for nucleating many metals (and metal oxides). It is also probably the most difficult virus to pattern using this covalent approach because all the carboxylates near the binding site will cause an electrostatic repulsion between the MHA and virus. Nevertheless, it patterned quite well. The p8#9 virus has a sequence which has been selected for binding to gold. This virus can nucleate gold from gold salt in solution (with a reducing agent) or assemble gold nanoparticles on its pVIII protein. The #9 sequence is val-ser-gly-ser-ser-pro-asp-ser⁽⁴⁾. The p8#9 viruses also assemble quite nicely onto activated MHA patterns (Fig 2.3-9). A detailed accounting of the covalent patterning protocol can be found in Appendix 2.D.

- *Figures for Section 2.3*









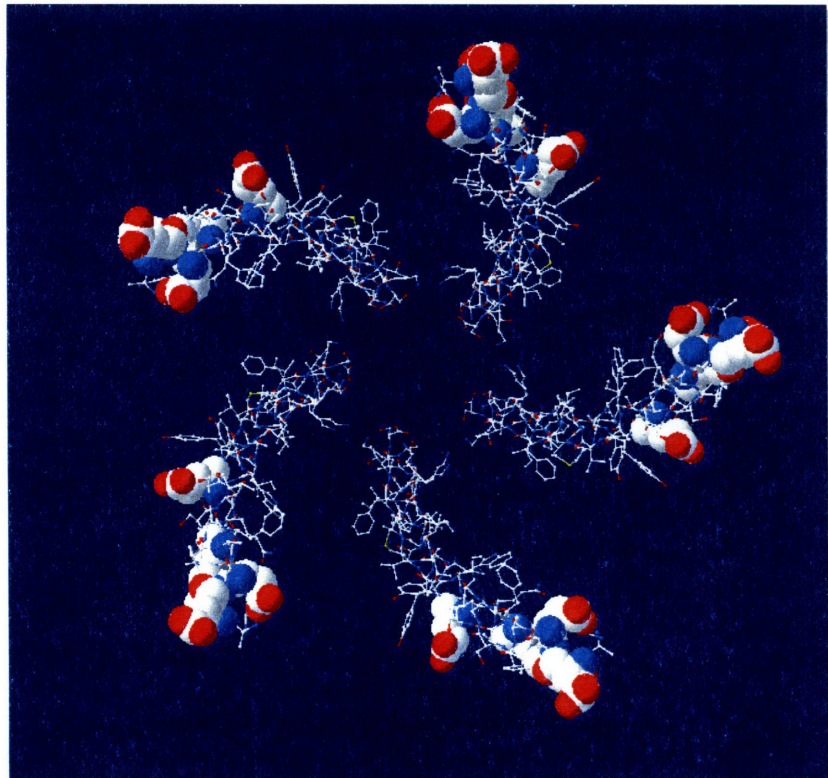
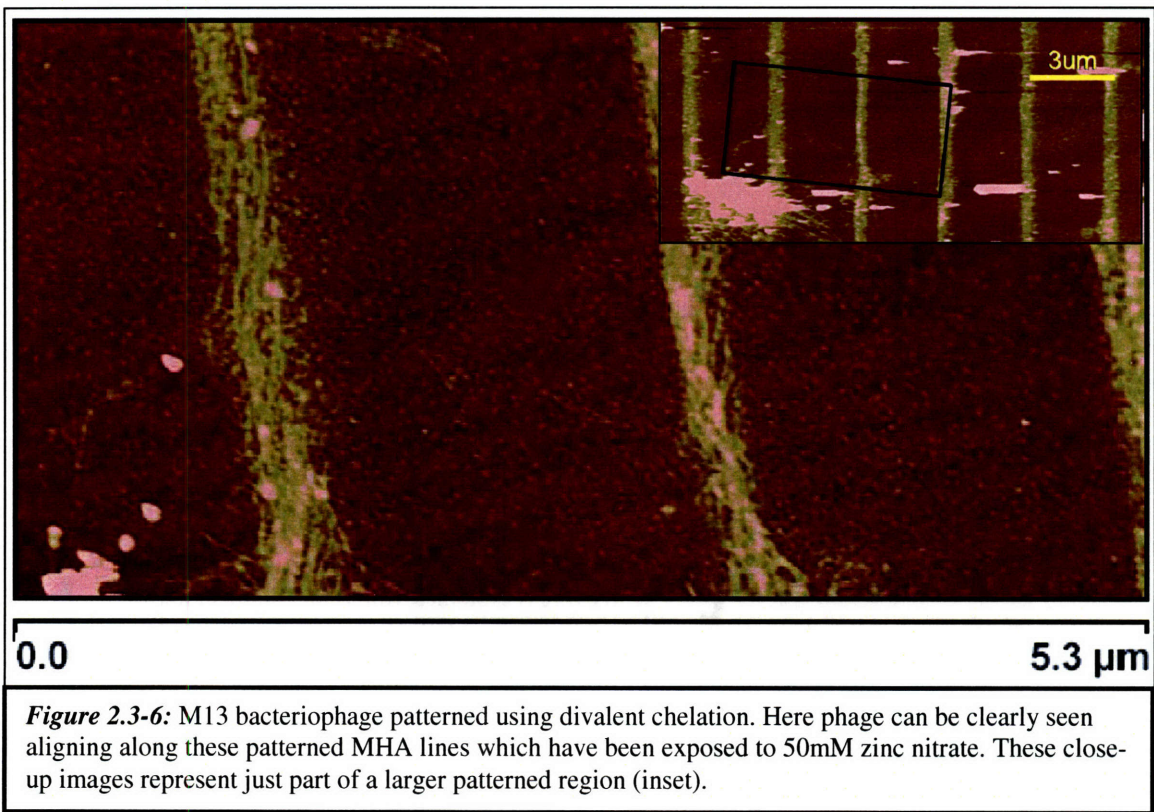


Figure 2.3-5: Carboxylates on the phage pVIII protein. Looking down the axis of the virus, the pVIII proteins have a 5-fold symmetry. Looking at just 5 of these proteins we see that there are 4 carboxylates per pVIII that are present on the surface of the phage. These carboxylates can be used to create one part of the bridge in a divalent chelation between MHA and phage.



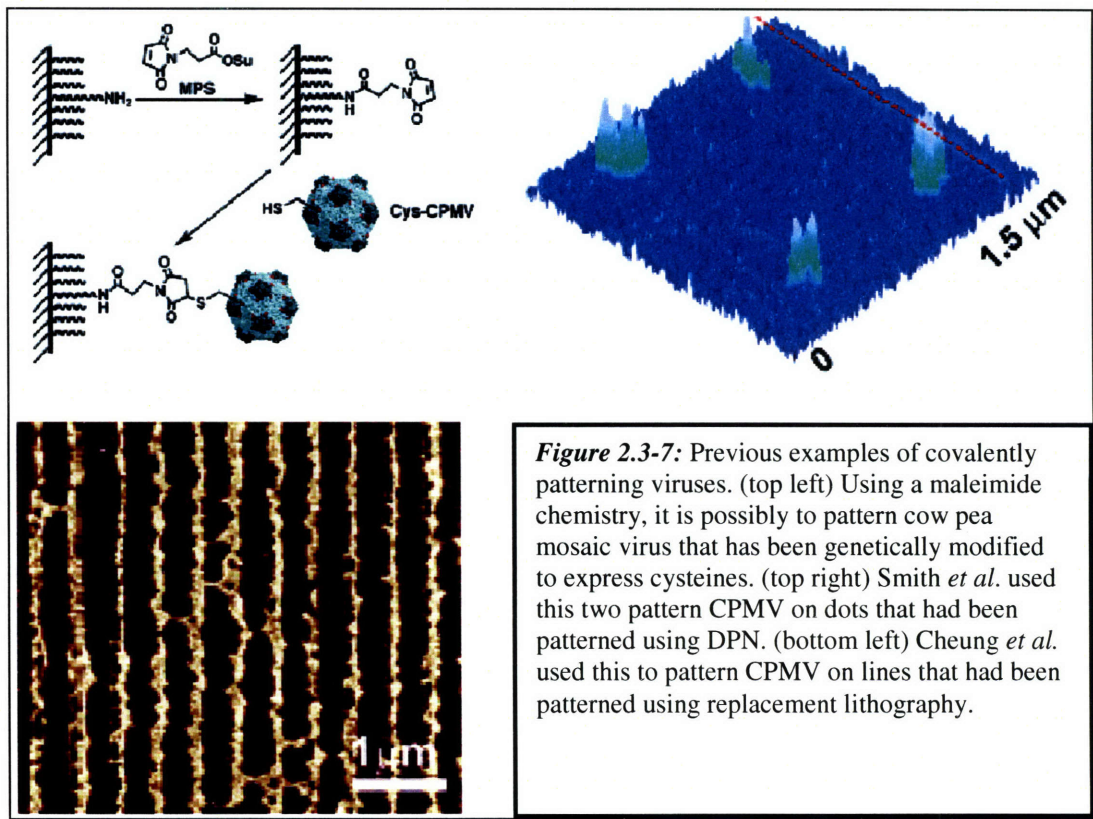
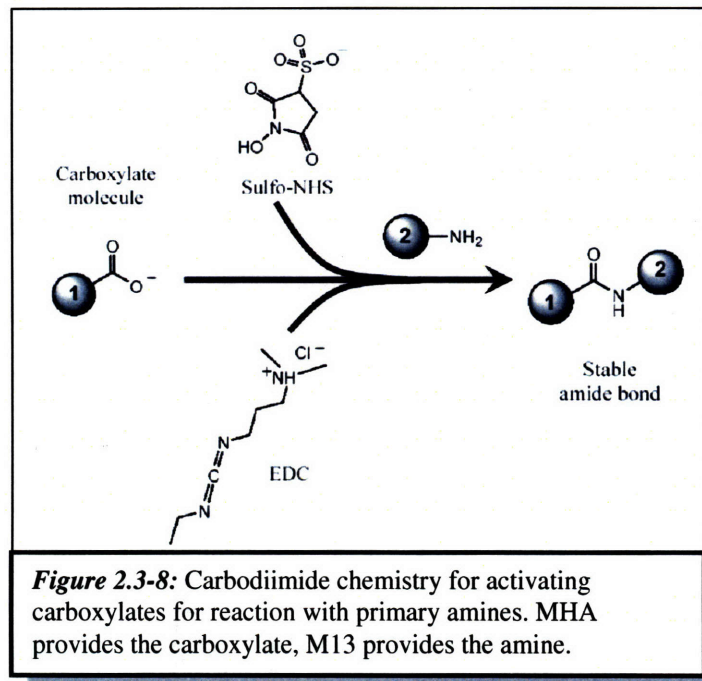


Figure 2.3-7: Previous examples of covalently patterning viruses. (top left) Using a maleimide chemistry, it is possible to pattern cow pea mosaic virus that has been genetically modified to express cysteines. (top right) Smith *et al.* used this two pattern CPMV on dots that had been patterned using DPN. (bottom left) Cheung *et al.* used this to pattern CPMV on lines that had been patterned using replacement lithography.



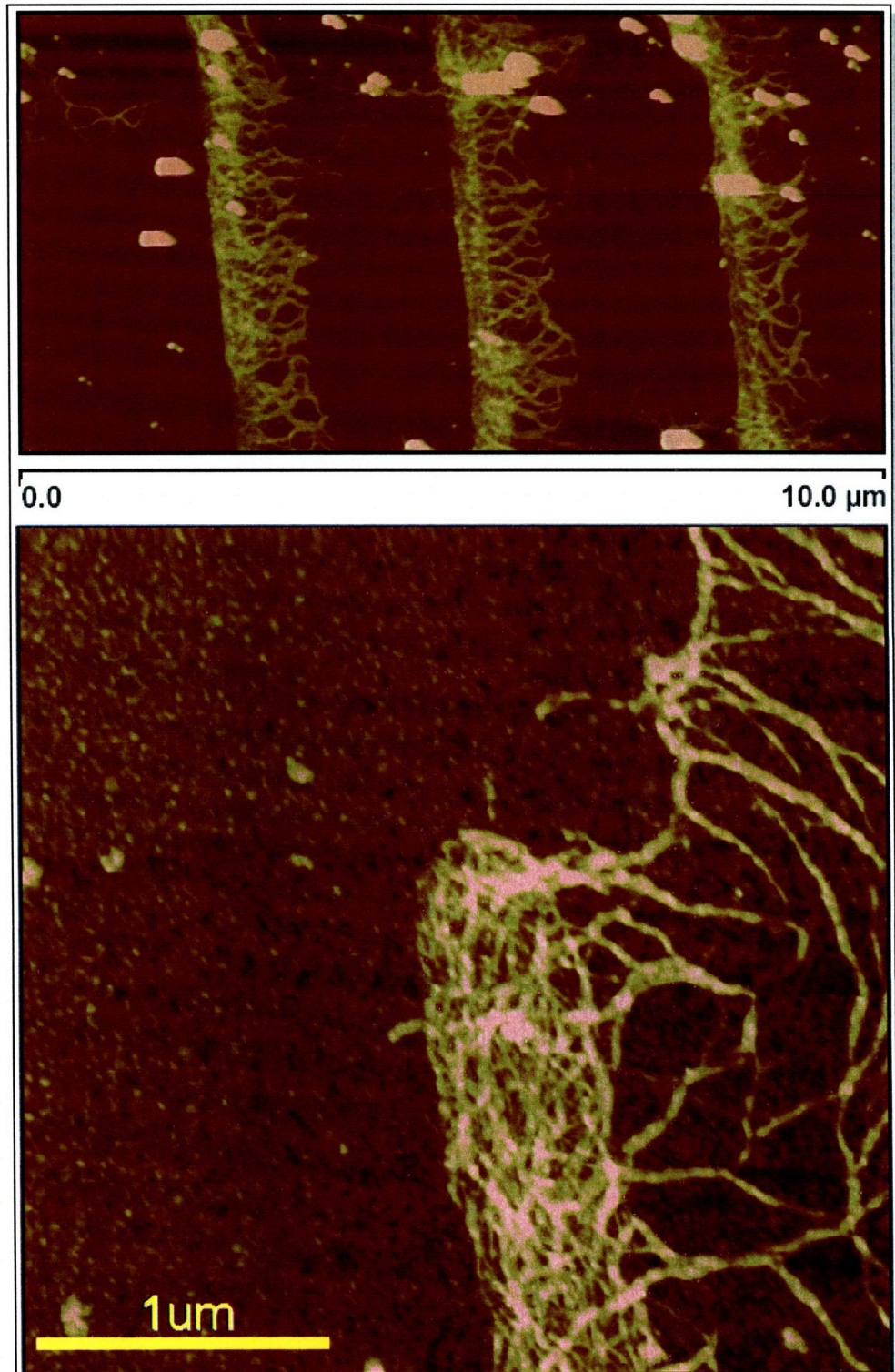


Figure 2.3-9: Covalently patterned M13 bacteriophage. (top) Using the E4 phage it is clear that the phage have been patterned on carbodiimide activated MHA lines. (bottom) Using the p8#9 phage it is again clear that the phage easily patterned on the carbodiimide activated MHA. In each case there is no particular phage alignment to the patterning in contrast to the divalent chelation. It is important to note that both phage clones were patterned using the same protocol indicating this is a generalizable technique regardless of phage modification.

2.4: Materials Assembly

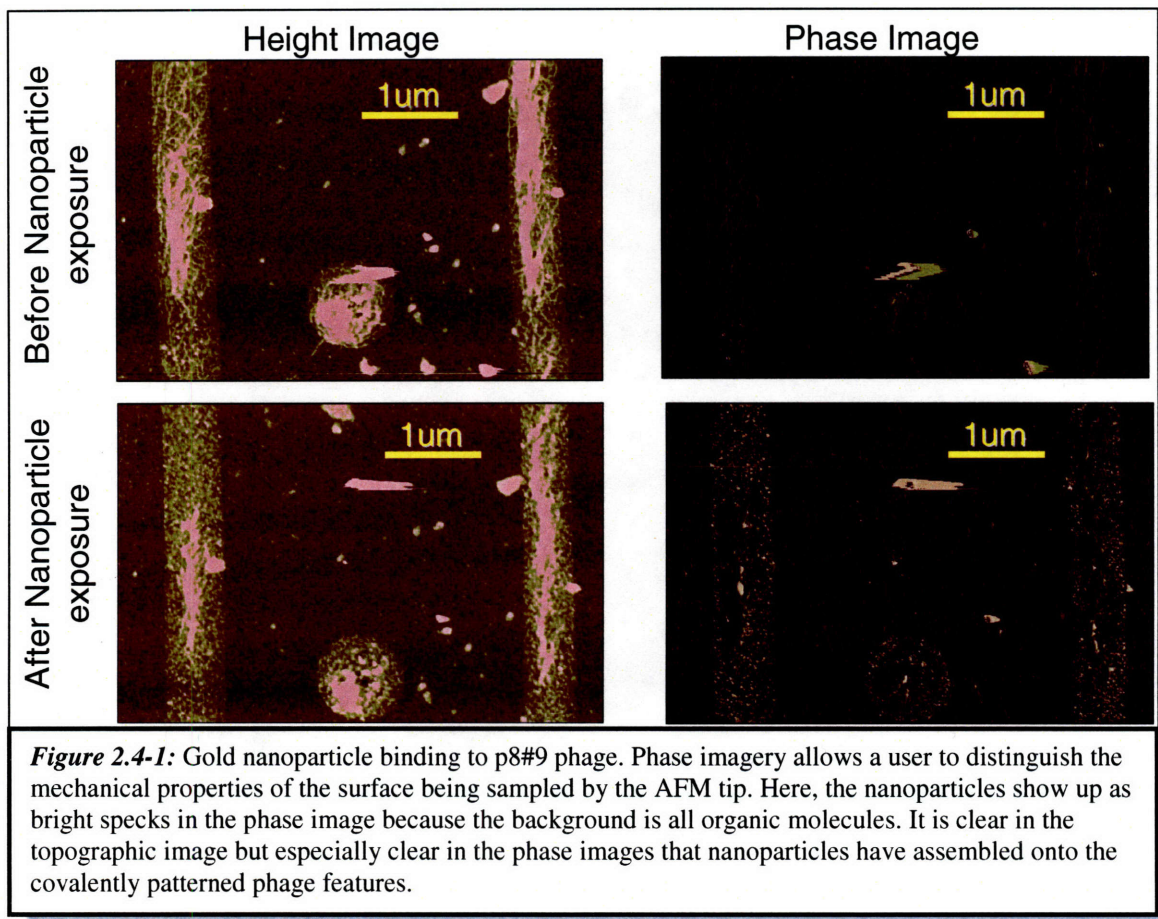
Once virus patterning is complete, it is necessary to show that the viruses can actually assemble materials. This can be accomplished by either trying to nucleate materials from a solution precursor, or by using the virus as a scaffold to assemble prefabricated nanoparticles. It is quite simple to test that the p8#9 viruses have maintained their genetic programming by exposing them to a solution with gold nanoparticles. If the programming has been maintained, the patterned viruses should spontaneously decorate themselves with a coating of nanoparticles during the exposure.

To test this, patterned p8#9 viruses were exposed to a solution of 5nm gold nanoparticles. It was found using AFM techniques that the patterned viruses do indeed assemble gold nanoparticles onto their coats (Fig 2.4-1). Atomic force microscopy proved to be the best tool to assess the binding of nanoparticles. Using simple AFM topographic imaging, it appears that gold nanoparticles are assembled on the virus body because the viruses, which initially appear quite clear, appear 'grainy' after exposure to the nanoparticles. Using another AFM technique (termed "phase imaging") provides better evidence of gold nanoparticle binding. Phase imaging distinguishes surface features based mainly on their mechanical properties. Because gold nanoparticles are considerably harder than the surrounding viruses, they appear as bright specs in the phase image. The nanoparticles also appear bright compared to the background because it has been functionalized with methoxy PEG thiol which provides a soft PEG surface for imaging. A detailed accounting of this gold nanoparticle assembly protocol and phase imaging is found in Appendix 2.E.

The next step would obviously be to try and assemble a material from a precursor salt. Unfortunately, because of the presence of the gold substrate, it is not possible to perform reduction chemistries. The large conducting substrate short circuits any electron transfer and reduced material is seen all over the surface (Fig 2.4-2) . It will be necessary to move to a new ink-substrate system (such as silane-silicon) in order to get around this hurdle.

Work has already been started on the microcontact printing of 3-aminopropyl trimethoxysilane ($\text{H}_2\text{N}-(\text{CH}_2)_3-\text{Si}(\text{OCH}_3)_3$) (Fig 2.4-3). A full description of this microcontact procedure can be found in Appendix 2.F. This molecule will spontaneously bind to clean silicon or silica substrates resulting in an amine terminated substrate. Using a hetero-bifunctional cross-linker like glutaraldehyde will allow us to attach the virus terminal amines to the surface terminal amines providing a covalent attachment.

- *Figures for Section 2.4*



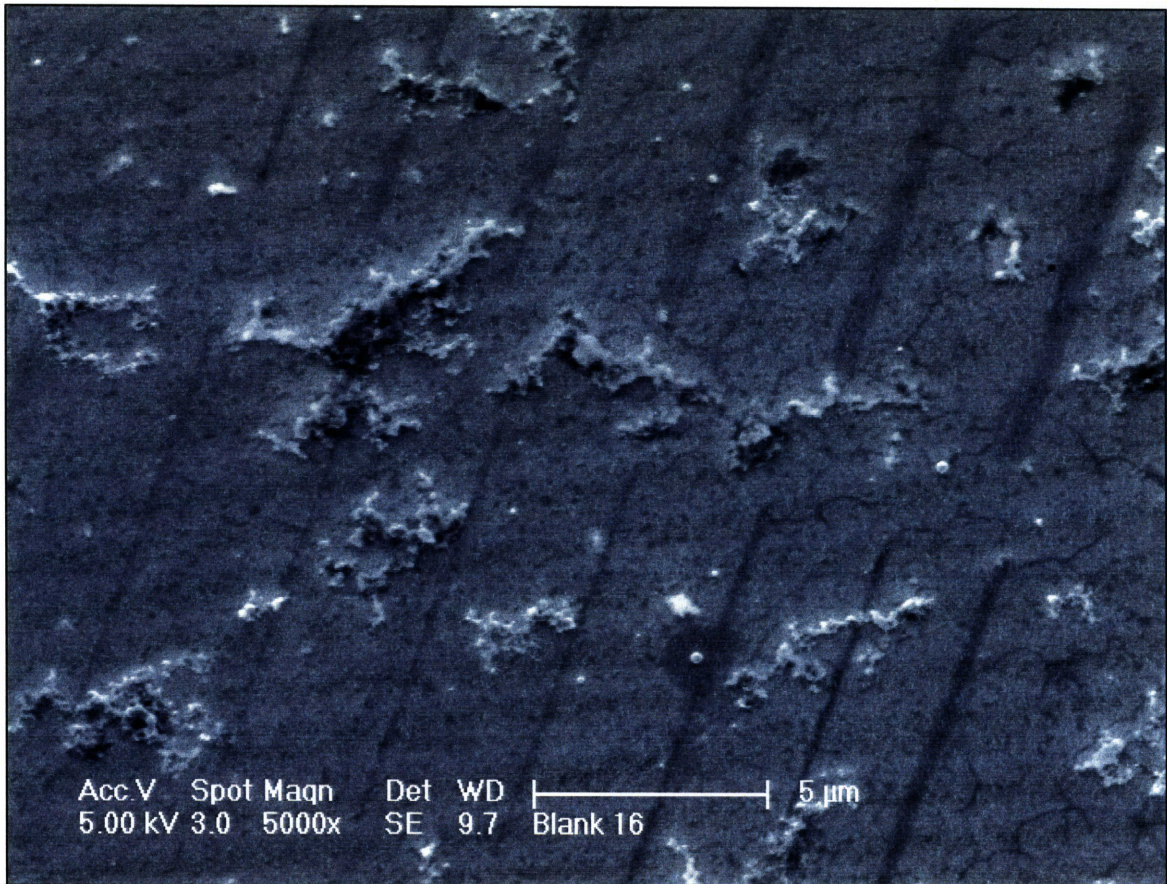
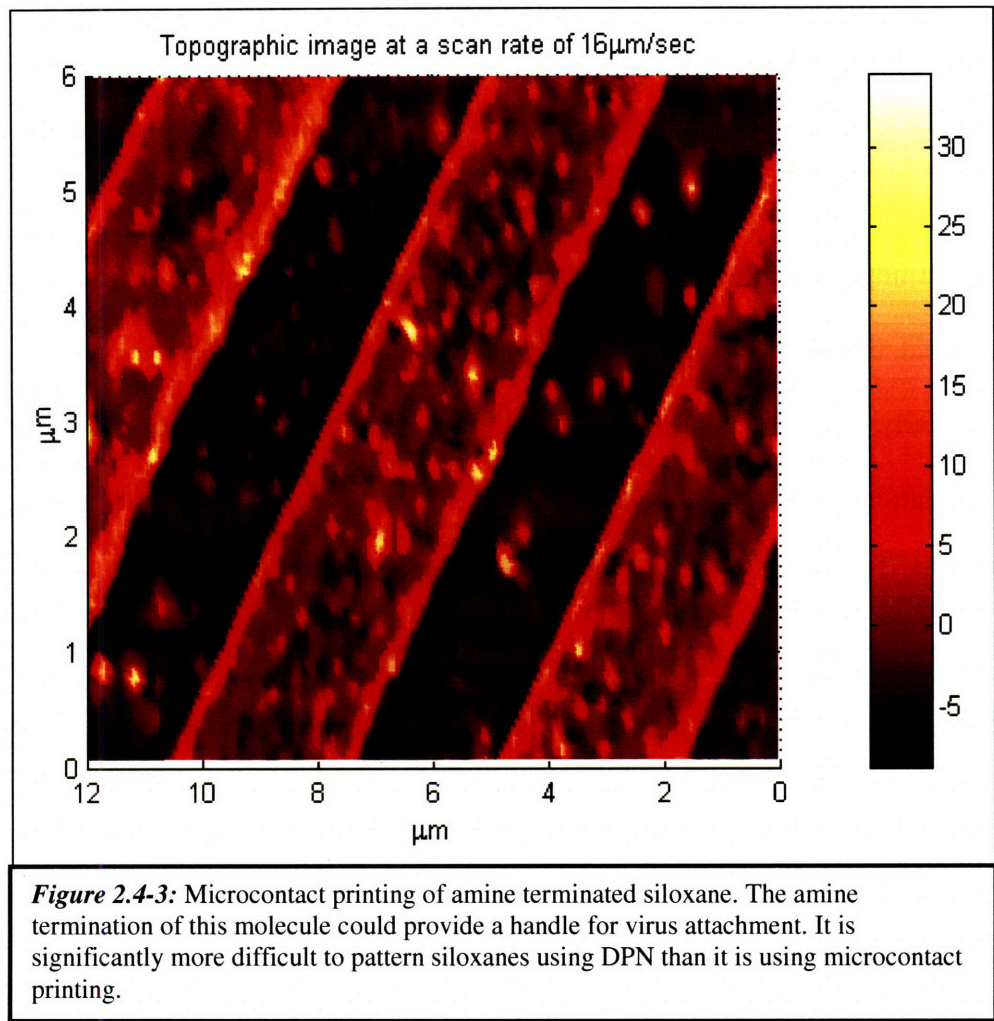


Figure 2.4-2: Cobalt randomly deposited on a patterned substrate. Here is an SEM of a substrate on which MHA lines have been patterned with phage and the background has been backfilled with methoxy PEG thiol. Cobalt chloride was introduced and reduced with sodium borohydrate. The cobalt formation showed no preference for the phage and instead deposits randomly on the conductive gold substrate. In order to perform redox chemistry with patterned phage, it will be necessary to move to a less conducting substrate such as silicon or silica.



2.5: Discussion & Recommendations for Future Work

There are numerous examples of M13 bacteriophage that have been genetically modified to effectively nucleate inorganic materials on their body. In order to really take advantage of this ability, it would be extremely useful to develop techniques for patterning these genetically modified viruses in order to build useful structures and potentially useful devices. This work has clearly and successfully demonstrated three different techniques that can be used for assembling viruses on a surface.

Patterning these viruses is only half the challenge. It is also important to show that, once patterned, these viruses can effectively nucleate the materials for which they have been genetically programmed. Because of the drawbacks of hydrophobic attachment and divalent chelation (electrostatic attachment), the only really viable approach for materials assembly is the covalent binding approach. This work has demonstrated that viruses assembled on MHA using a carbodiimide chemistry with at least two disparate genetic modifications and that, at least in the case of p8#9, this genetic programming has still maintained its initially intended function.

Of course, to really move this technology to where it is useful, it will be necessary to pattern viruses on a different substrate; preferably one that will not act as a short circuit for any oxidation-reduction chemistry. Silicon and silica are obvious choices, but other metal oxides might also be effective. Alternatively, viruses could be made to nucleate material in solution and then be stamped onto a substrate in order to build structures.

Appendix 2.A: Gold Substrate Preparation

Dip pen nanolithography requires the production of gold substrates which are highly clean and as smooth as possible. In order to do this, gold films were evaporated onto clean silicon substrates using an electron beam evaporator. The films were deposited slowly to insure small crystal size and even coverage.

The silicon substrates were obtained from 6 inch <100> silicon wafers. The wafers were diced into 5mm x 5mm pieces using the die saw in the Integrated Circuits Laboratory (ICL).

In preparation for gold deposition, the silicon samples were cleaned in a 10% HF, 90% Ethanol solution for 30 seconds, rinsed in DI water for 10 sec and then dried with acetone. Stripping the oxide in this way insures a smooth silicon surface for gold deposition.

Gold films were deposited using the electron beam evaporator in the Experimental Materials Laboratory (EML). A thin chromium adhesion layer was used to avoid gold delamination.

Chromium was deposited using a beam current of ~.01 Amps which provides a deposition rate of ~.5angstroms/second. The low beam current is possible because chromium sublimates rather than melts and evaporates. The baseline chamber pressure is $\sim 3.0 \times 10^{-6}$ torr and the deposition pressure is $\sim 1.0 \times 10^{-5}$ torr. The chromium is deposited to a thickness of just 5nm.

After the chromium is deposited, the gold is deposited without removing the substrates from the vacuum chamber. The gold is deposited at a beam current of ~.14 Amps. The higher beam current is required because the gold must melt before evaporating. This

results in a deposition rate of ~ 0.5 angstroms/second. The deposition pressure is also $\sim 1.0 \times 10^{-5}$ torr for the gold deposition. The gold is deposited to a thickness of 25nm.

After deposition, the gold is removed from the vacuum chamber and stored in glass vials. The glass vials are kept in a laboratory vacuum desiccator to keep them clean as long as possible. Under these conditions, the gold samples are useable for dip pen nanolithography for as long as a month after the deposition.

Appendix 2.B: Virus Patterning Protocol

Virus patterning is a multi-step procedure.

Dip Pen Nanolithography:

The procedure starts by performing Dip Pen Nanolithography of Mercapto Hexadecanoic Acid (MHA) on clean gold substrates (Appendix 2.A). In order to deposit MHA via DPN, it is first necessary to make the MHA ink. This is done by adding 7mg of MHA to 4ml of acetonitrile. The MHA will not be fully soluble at this concentration so the solution must be sonicated into a suspension.

Once the MHA slurry has been created, it must be coated onto a contact mode AFM tip. The tips used for this work are silicon nitride NP tips from VEECO. The tip is immersed in the MHA ink for ten seconds and then allowed to dry.

Once dry, the tip is mounted into an AFM multimode chuck. The system is toggled to operate in contact mode (AFM & LFM). The laser is zeroed in vertical and horizontal and then the vertical signal is offset to $\sim -2V$.

In the AFM software, the system is set to contact mode and the set point is set to $\sim -1.5V$. The set point setting should be less than the vertical signal offset.

The two image screens are set to Height and Friction respectively. It is much easier to image recently created DPN patterns using friction than it is using height.

The ink coated tip can be used both to image the surface and to write patterns. Imaging is done by moving the tip at high speed ($\sim 30+ \mu\text{m}/\text{sec}$) where little material will be deposited. Writing is done by moving the tip at low speed, or by moving the tip repeatedly over the same piece of the surface (can be done by setting the slow scan axis

to disabled). It is also possible to write using a C++ library installed on our system which can be used to make most any pattern

Backfilling:

Once the surface has been patterned, the next step is to backfill the unpatterned surface. For virus patterning, the best molecule to use for this is Methoxy PEG Thiol. A 5mM solution of this is made in ethanol (it is fully soluble) and the substrate is soaked for 2 hours.

This soak is enough to create a generally disordered monolayer that will be resistant to non-selective protein adsorption.

After the two hour soak, the sample is soaked in ethanol for 5 min and then rinsed with DI water.

Activation:

Once backfilled, it is necessary to activate the MHA in order to drive virus binding.

In this work activation was accomplished in three different ways: hydrophobic, divalent (Appendix 2.C) and covalent (Appendix 2.D). Hydrophobic is the simplest involving no particular activation.

Phage Exposure:

Once activated, the phage can be exposed to the patterned substrate. This exposure is done using freshly amplified phage that have been diluted to 10% in TBS or PBS or HEPES. PBS and HEPES are used with covalent activation because they will not interfere with the carbodiimide chemistry.

The phage exposure is done by placing a 30 μ l drop of the phage solution on the activated sample and letting it sit for one hour.

After an hour has passed, the sample is rinsed 3X with TBS to remove any non-selectively bound phage and to quench any unreacted succinimidyl esters. At this point, the sample can either be imaged or given a longer soak. With hydrophobic and divalent binding, it is best to image almost immediately because soaking will cause some of the patterned phage to dissociate. With covalent attachment, an hour long soak is best as none of the patterned phage will disappear.

Materials Deposition:

At this point, the patterned phage can be used for the genetically programmed function.

Appendix 2.C: Divalent Chelation Activation of MHA

Divalent Chelation uses metal ions as bridges between two carboxylates.

In this work, the metal ion used was Zn^{2+} from zinc nitrate.

After patterning and backfilling, the substrates are exposed to a 50mM solution of zinc nitrate in DI water for 45 minutes.

Kelvin Probe was used to verify that the MHA was indeed being functionalized with zinc ions (Fig 2.3-3).

After this exposure, the samples are rinsed briefly in water and exposed to the 10% phage solution. Exposure can be as short as 1-2 hours and as long as 24 hours. 18 hour samples were used in the results depicted in this work (Fig 2.3-6). After the exposure, the samples are briefly rinsed in DI water to remove excess salt.

\

Appendix 2.D: Covalent (Carbodiimide) Activation of MHA

Carbodiimide chemistry is a tool used to activate carboxylates so that they will spontaneously form amide bonds with primary amines under physiological conditions.

The carbodiimide chemistry used in this work involved two reagents; EDC (1-Ethyl-3-(3-dimethylaminopropyl)carbodiimide Hydrochloride) and Sulfo-NHS (Sulfo *N*-hydroxysuccinimide).

The EDC reacts with a carboxylate to produce an *o*-acylisourea ester. This is a highly reactive leaving group. Because this ester is unstable, NHS is used to create a more stable *N*-hydroxysuccinimidyl ester. This is also a highly reactive leaving group, but it is more stable than the urea ester (Fig 2.D-1).

After the NHS exposure, the system will now form spontaneous amide bonds whenever it is exposed to a primary amine. NHS is used for this in lieu of just EDC because this stability allows for the system to be rinsed, removing any unwanted EDC and NHS without disturbing the activated carboxylates.

The rinse step is necessary, because without it, the phage would crash out of solution when exposed to EDC.

In this work the concentrations of EDC and S-NHS used are 25mM and 50mM respectively in HEPES (0.05M, titrated to pH = 7.2) buffer. The patterned substrate is exposed to this solution for 1 hour and then rinsed in HEPES.

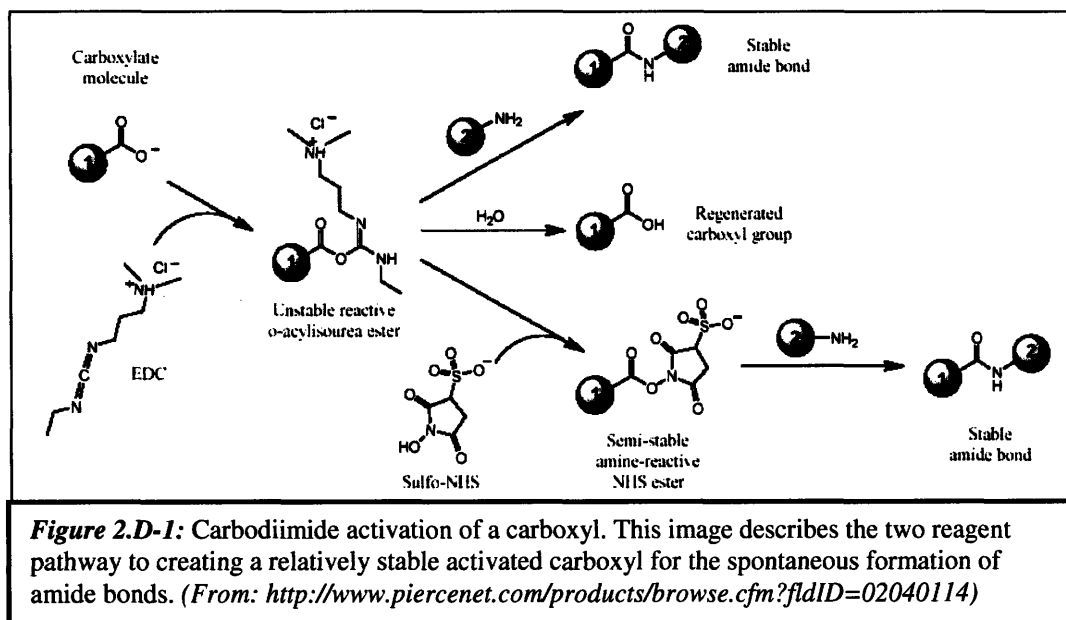
A 10% phage solution ($\sim 10^8$ pfu/ μ l) diluted in PBS is then drop coated on the activated substrate for 2 hours.

After the exposure, the sample is rinsed with TBST to remove any non-selectively bound phage from the substrate.

Finally, the substrate is soaked in TBS for two hours. This serves the dual purpose of removing any non-selectively bound phage still on the surface and quenching the activate carboxyles with the amines present on Tris.

After the two hour soak, there is a rinse with water to remove any excess salt to imopove imaging.

- *Figures for Appendix 2.D*



Appendix 2.E: Gold Nanoparticle Assembly/Imaging on Patterned Phage

Nanoparticle Assembly:

In order to test whether patterned phage have maintained their genetic programming, p8#9 phage were exposed to gold nanoparticles after covalent patterning.

The gold nanoparticles are 5nm in diameter (Sigma) and were undiluted. The exposure was done by drop coating 10 μ l of nanoparticles on the patterned viruses and letting stand for 1 hr.

After one hour, the samples were rinsed in DI water and allowed to dry for imaging.

Particle Imaging:

Imaging nanoparticles was accomplished using AFM tapping mode techniques. Simple topographic imaging is useful and depicts 'grainy' phage after the exposure (Fig 2.4-1). However, phase imaging is a better tool for imaging the nanoparticles.

Phase imaging is not a perfectly understood technique⁽¹²⁾ but it essentially images differences in the cantilever's interactions with a substrate. Phase refers to the delay that occurs between sending a voltage to the piezo and the corresponding deflection of the cantilever (Fig 2.E-1). The length of this delay can vary if the tip sticks to the surface or is otherwise deflected.

One property which phase imaging can definitively discriminate is surface hardness. Soft and hard regions on a surface will appear different in phase imaging.

The ability to discriminate hardness is why phase imaging is useful for imaging nanoparticles patterned on phage. As can be clearly seen in figure 2.4-1, the backfilled surface and the patterned phage appear almost identical under phase imaging. However,

there is a clear contrast in phase between the backfill and the assembled nanoparticles which appear as brightly colored flecks.

Phase imaging was accomplished by operating the AFM in standard tapping mode with an RTESP tip. Careful tuning of the system is important as phase imaging is notoriously finicky.

The amplitude set-point is set to one volt and the gains are made as small as small as possible. Any particulates clinging to the AFM tip will hurt imaging so clean substrates are essential.

Scan speed are generally slow (~1Hz) in order to get reliable imaging

- *Figures for Appendix 2.E*

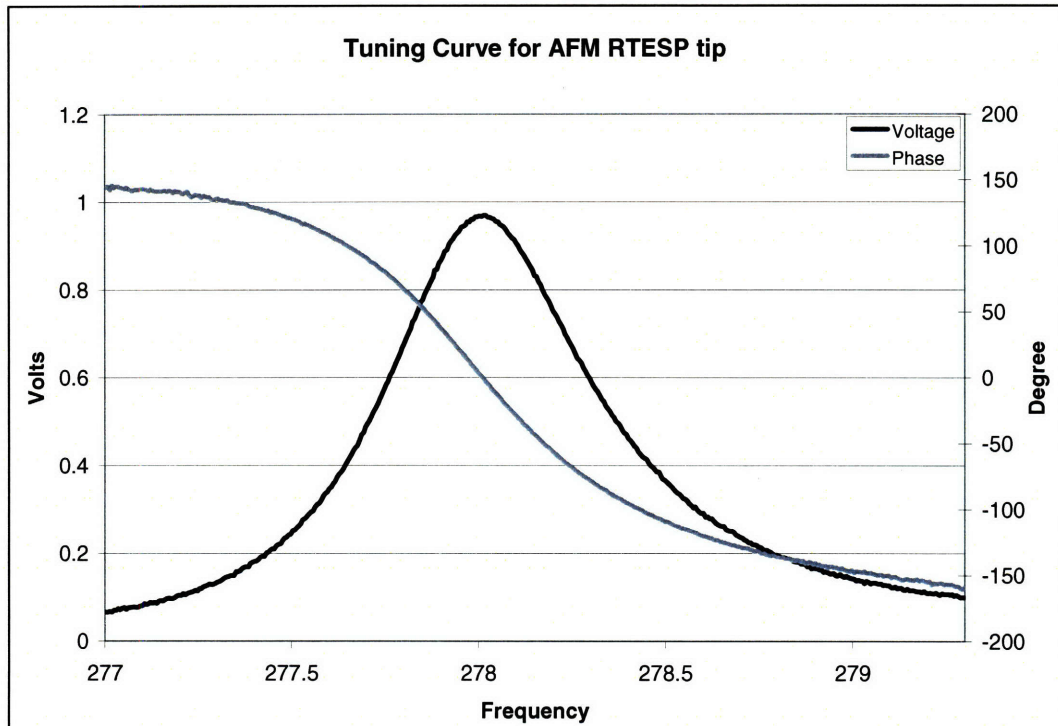


Figure 2.E-1: Tuning curves for an RTESP tip. The dark line is the standard tuning curve. This peak corresponds to the first resonance peak of the cantilever and displays the standard Lorentz shape. The voltage is actually a measure of the amplitude of the AFM tip oscillations with smaller voltage meaning smaller amplitude. The lighter colored line is the phase of the tip. The phase refers to the lag time between the cyclic piezo-actuators and the actual observed oscillations of the tip. As can be clearly seen, the phase experiences a large change in value near the resonance peak of the cantilever. This phase curve shifts up and down depending on the nature of the substrate.

Appendix 2.F: Siloxane Microcontact Printing Protocol

Microcontact printing is a route to the massively parallel application of chemical patterns on receptive substrates at the micron or even sub-micron length scale.

Typically, the process begins by fabricating a 'stamp'. The stamp is an inverted relief of the pattern that is going to be created just like a rubber stamp with ink printing. The most common material used is poly-dimethyl siloxane or PDMS which is a silicone rubber.

The stamp is coated with the chemical ink of choice and then placed into physical contact with the substrate. The ink diffuses to the substrate where it will either non-selectively adsorb or covalently attach depending on the ink and substrate chosen.

The PDMS used in this work is from Dow Corning (Sylgard® 184 Silicone Elastomer Kit) and the master is from the Langer lab. The master is fabricated in silicon and is a series of 2µm ridges with 2µm spacings.

The elastomer stamp is made by mixing the precursor reagents, degassing the mixture for 45 minutes and then pouring it over the silicon master. The mix is cured for 1hr at 50°C so the stamp can set-up.

The ink used is 3-aminopropyl trimethoxy silane which is diluted 1:100 in ethanol. This ink is applied to the elastomer stamp using a sterile cotton swab. As soon as the stamp appears dry, the stamp is pressed onto a clean silicon substrate and left for 10 min to 1 hour. This ink will leave patterns of primary amines on the sample surface.

The silicon substrates are 5mm square samples which have been cut using a die saw. Immediately prior to stamping, the substrates are cleaned using Pirhana

(3:1::H₂SO₄:H₂O₂ – Caution: extremely dangerous, use proper PPE). The samples are dried using acetone and then stamped.

2.Ref: References

1. **Whaley, S. R., D. S. English, E. L. Hu, P. F. Barbara, and A. M. Belcher.** 2000. Selection of peptides with semiconductor binding specificity for directed nanocrystal assembly. *Nature* **405**:665-668.
2. **Flynn, C. E., C. Mao, A. Hayhurst, J. L. Williams, G. Georgiou, B. Iverson, and A. M. Belcher.** 2003. Synthesis and organization of nanoscale II-VI semiconductor materials using evolved peptide specificity and viral capsid assembly. *J.Mater.Chem.* **13**:2414-2421.
3. **Qi, J., C. Mao, J. M. White, and A. M. Belcher.** 2003. Optical anisotropy in individual CdS quantum dot ensembles. *Phys.Rev.B* **68**:125319.
4. **Huang, Y., C. Y. Chiang, S. K. Lee, Y. Gao, E. L. Hu, J. De Yoreo, and A. M. Belcher.** 2005. Programmable assembly of nanoarchitectures using genetically engineered viruses. *Nano Letters* **5**:1429-1434.
5. **Nam, K. T., D. W. Kim, P. J. Yoo, C. Y. Chiang, N. Meethong, P. T. Hammond, Y. M. Chiang, and A. M. Belcher.** 2006. Virus enabled synthesis and assembly of nanowires for Lithium ion battery electrode. *Abstracts of Papers of the American Chemical Society* **231**:-.
6. **Nam, K. T., D. W. Kim, P. J. Yoo, C. Y. Chiang, N. Meethong, P. T. Hammond, Y. M. Chiang, and A. M. Belcher.** 2006. Virus-enabled synthesis and assembly of nanowires for lithium ion battery electrodes. *Science* **312**:885-888.
7. **Dr. Thierry P. Cassagneau.** 2004. Layer-By-Layer Self-Assembly of Metal Nanoparticles on Planar Substrates: Fabrication and Properties, p. 398-436. In P. F. Caruso (ed.), *Colloids and Colloid Assemblies*.
8. **Vega, R. A., D. Maspoch, K. Salaita, and C. A. Mirkin.** 2005. Nanoarrays of single virus particles. *Angewandte Chemie-International Edition* **44**:6013-6015.
9. **Smith, J. C., K. B. Lee, Q. Wang, M. G. Finn, J. E. Johnson, M. Mrksich, and C. A. Mirkin.** 2003. Nanopatterning the chemospecific immobilization of cowpea mosaic virus capsid. *Nano Letters* **3**:883-886.
10. **Cheung, C. L., S. W. Chung, A. Chatterji, T. W. Lin, J. E. Johnson, S. Hok, J. Perkins, and J. J. De Yoreo.** 2006. Physical controls on directed virus assembly at nanoscale chemical templates. *Journal of the American Chemical Society* **128**:10801-10807.
11. **Cheung, C. L., J. A. Camarero, B. W. Woods, T. W. Lin, J. E. Johnson, and J. J. De Yoreo.** 2003. Fabrication of assembled virus nanostructures on templates of chemoselective linkers formed by scanning probe nanolithography. *Journal of the American Chemical Society* **125**:6848-6849.
12. **Babcock, K. L., and C. B. Prater** 2004, posting date. Phase Imaging: Beyond Topography. Veeco Instruments Inc. [www.veeco.com/pdfs.php/5]

Chapter 3:

A Kelvin Probe Biosensor

3.1: Introduction

In this work, a high-resolution, high-sensitivity, label-free and potentially high-speed biosensing approach is demonstrated for detecting immobilized target biomolecules on a solid support under ambient conditions. Using the scanning probe technique known as Kelvin Probe Microscopy it is possible to successfully devise a sensor for charged biomolecules. The tool works by measuring the difference in work function between a fixed substrate and a movable probe (The Kelvin Probe⁽²⁻⁴⁾). The probe is brought close to the substrate and if there is any difference in surface potential (or work function) between the probe and the substrate they exert a mutual force on one another. By modulating the applied potential on the probe until this force is extinguished, it is possible to determine the local potential of a surface.

Because many biological molecules have a native state which includes the presence of charge centers (e.g. the negatively charged backbone of DNA) the formation of highly specific complexes between biomolecules will often be accompanied by local changes in charge density. This is reflected in the molecule's isoelectric point. At a pH above the isoelectric point, the molecule will take on a negative charge while below the

isoelectric point the charge will be positive. However, on a surface, it is unlikely that the biological molecules are existing in a charged state which begs the question, “What is the source of the potential measured on a surface?”

When the Kelvin Probe measures a surface, it is actually measuring the potential energy map of the surface. Regions of low potential are regions that are attractive to an electron. When speaking about a molecule, the attraction that an electron feels to that molecule is termed the *electronegativity*. Unfortunately, there are not tables of electronegativities for biological molecules. However, there are similar measurements for biological molecules which are the pKa and isoelectric point. These are essentially measures of the proton affinity of a biological molecule. To first order, it is reasonable to assume that electronegativity is the opposite of proton affinity. As a result, we expect that the potential measured on a surface should correlate with pKa/isoelectric point of the bound biological molecule (Table 3.1-1).

Table 3.1-1: Proposed mechanism for observed potential. It is expected that the measured potential should correlate with the isoelectric point or pKa.			
↓	↑	↓	↓
A low potential is measured	This correlates with a large electronegativity	This is equivalent to a low proton affinity	This is equivalent to a low isoelectric point

In this work it is indeed demonstrated that the isoelectric point directly correlates with the measured surface potential (Fig 3.1-1). Molecules with a low isoelectric point show a negative potential while molecules with a large isoelectric point show a positive potential as expected. The density of molecular packing also affects the measured

potential in an apparently linear fashion. This linear effect on potential is inferred from the fact that double stranded DNA shows a potential that is twice that of single stranded DNA.

By spatially resolving the variation in surface potential it is possible to determine the presence of a specific bound target biomolecule on a surface without the aid of special chemistries or any form of labeling. The Kelvin Probe presented here is based on an AFM nanoprobe offering high resolution (<10nm), sensitivity (<50nM), speed (>1100µm/sec) and the ability to resolve as few as three nucleotide mismatches in a target DNA sequence.

Dip Pen Nanolithography is the tool used to pattern biological features onto a solid supports in analogy to current microarray technology (Fig 3.1-2). DNA microarrays were developed in the early 1990's reaching their modern form by 1995^(1, 5-8). Despite more than a decade of innovation, modern microarrays have remained amazingly similar to the original designs. In the interim, major growth has been seen in the microarray industry that has grown up around this exciting technology⁽⁹⁻¹²⁾. Microarrays are basically an evolution on the DNA dot blot and spotting techniques in which porous membranes were used to immobilize DNA probes^(6, 13-16). In modern microarrays, DNA probes are immobilized on a solid support and detection is achieved by utilizing fluorescently tagged target molecules. In the past decade improved manufacturing and microscopy has allowed considerable miniaturization compared to the original design⁽¹⁷⁾. Current manufacturing approaches (particularly photolithographic⁽⁵⁾) could push feature size down to the micron scale, though in practice, features are on the order of 10µm or larger due to limits in detection and manufacturing⁽¹¹⁾.

In this work, the feasibility of a manufacturing approach (Dip Pen Nanolithography) that can produce features at the submicron scale is verified. In addition a detection scheme based on Kelvin Probe Microscopy is demonstrated which is simultaneously high-resolution, high-sensitivity, high-speed and label-free. This detection scheme is used effectively to specifically detect the presence of proteins and single stranded DNA sequences on surfaces using features as small as 250nm.

Previous work using Kelvin Probe to detect biomolecules has been carried out by several groups, most notably by Cheran, Thompson *et al*⁽¹⁸⁻²¹⁾. They successfully detected proteins and DNA arranged in an array with features on the order of 100 μ m using a custom made Kelvin Probe with a pixel size of 100nm. Hansen *et al*⁽²²⁾ detected immobilized DNA features on the order of 1000 μ m using a commercially available Kelvin Probe system. Laoudj *et al*⁽²³⁾ used porous membranes as a substrate to detect the presence of immobilized proteins at the cm scale. These previous results reflect the correlation between measured surface potential and isoelectric point, although the correlation was not explicitly recognized. Additionally, these previous results have demonstrated that the potential associated with double-stranded DNA has twice the magnitude of single-stranded DNA as expected.

In the work presented here the resolution of the bio-Kelvin Probe measurements has been greatly improved (<10nm) by using an AFM nanoprobe which has allowed a decrease in feature size by 2-3 orders of magnitude compared to the state of the art in commercial microarrays. This improved resolution can be fully realized by utilizing dip-pen nanolithography (DPN) to create features. Using the DPN technique described by Demers and Ginger⁽²⁴⁾, thiol modified oligo-nucleotides have been patterned on gold

substrates. The features reported here are sub-micron and successful measurements of biological interaction on features as small as 250nm have been achieved genuinely pushing this technology into the nanoscale. Additionally, using DPN to pattern these features provides a route to creating fully functional arrays of biomolecular markers which can be assayed by Kelvin Probe in analogy to conventional fluorescent microarrays.

- Figures for Section 3.1

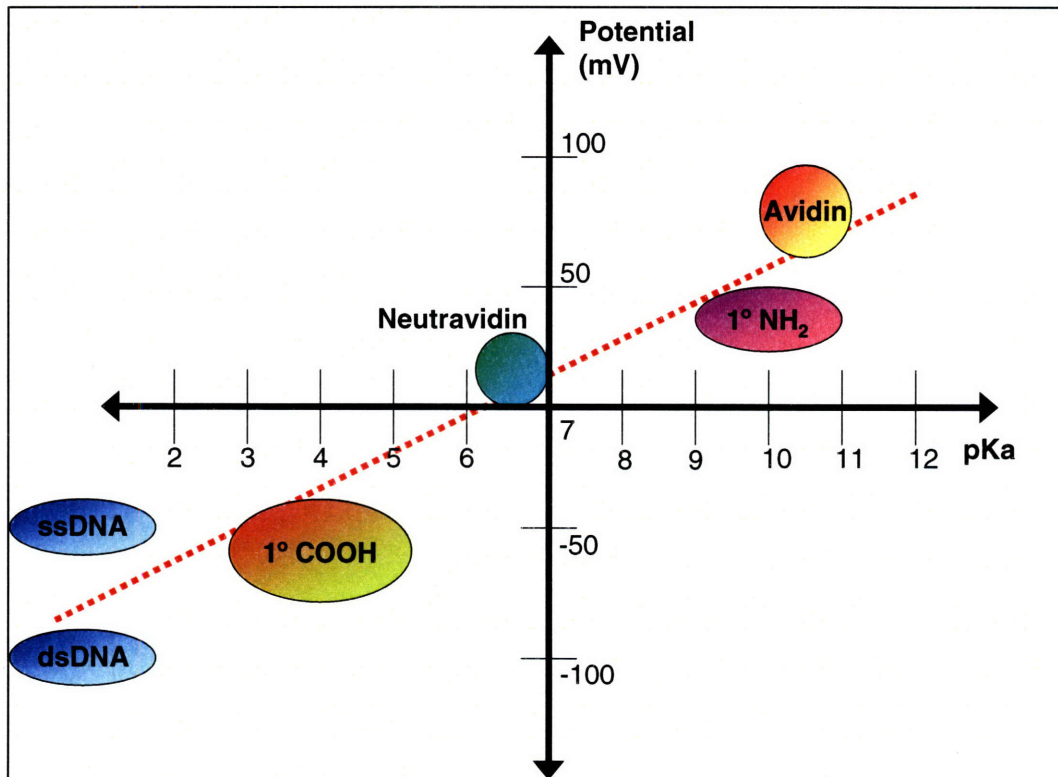


Figure 3.1-1: Correlation between measured surface potential and pKa. Using the Kelvin Probe, different molecule immobilized on surfaces were measured. There is a clear correlation between pKa and measured potential as expected. It is important to note that the measured potential is a function of pKa and molecule density. This is why ssDNA and dsDNA have the same pKa but different measured potentials. The surface density is not generally accounted for in this plot, the molecules are merely as dense as possible. (Notes: (1) avidin and neutravidin are actually listed in terms of their isoelectric points rather than pKa. (2) the primary carboxylic acid is from MHA; primary aliphatic acids typically have a pKa of 3-5. (3) the primary amine is from 3-aminopropyl tri-methoxysilane patterned on silica; primary aliphatic amines typically have a pKa of 9-11. (4) the pKa of the DNA backbone is approximately 0.)

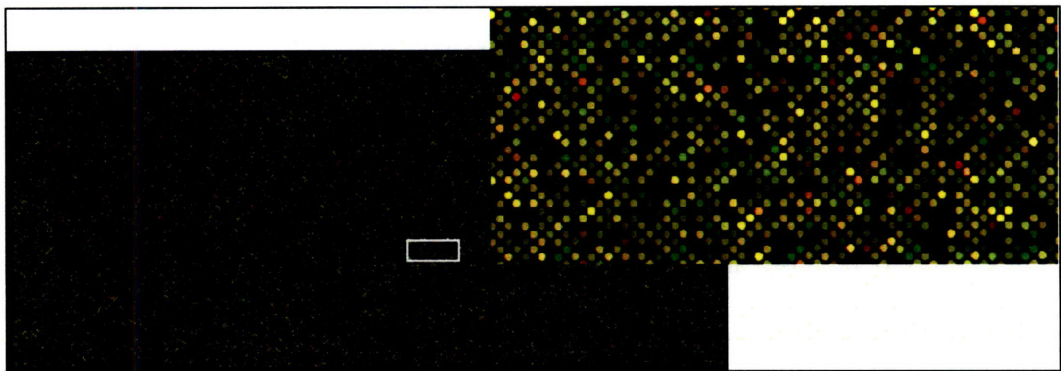


Figure 3.1-2: A DNA Microarray. This is an image of a DNA microarray. Each spot on the array is a different DNA probe sequence. The fluorescent spots are points where a fluorescently tagged target cDNA sequence has bound. Multiple fluorescent inks can be used to distinguish cDNAs from different experiments.
(From: <http://learn.genetics.utah.edu/units/biotech/microarray/>)

3.2: Patterning Biological Molecules

There are numerous ways to pattern molecules onto a solid support, including spotting^(15, 16) and photolithographic growth⁽¹⁾; the technique used here is based on Dip Pen Nanolithography⁽²⁵⁾. DPN is a good choice for this work because it can quite easily pattern features that are 100's - 1000's of nanometers in size (and smaller). At this scale, it is expected that hundreds of thousands of biological molecules will be present in a single feature. This quantity of molecules is quite sufficient to get a signal from a Kelvin Probe, but it is small enough spatially that fluorescence is extremely limited as a detection technique. Additionally, DPN is a quick and easy technique that is extremely amenable to laboratory scale process optimization. There are certainly other patterning techniques that may be more amenable to large scale patterning, most notably photolithographic patterning, which offer the prospect of massively parallel feature creation.

In this work, two types of biomolecular systems are investigated. The first is the idealized biotin-avidin system which serves as a surrogate for any general antibody-protein interaction. The second is the DNA-DNA system using oligonucleotides from anthrax and malaria. Patterning biotin is a multi-step process that starts with patterning an MHA linker molecule which can be used as a handle to bind biotin. Patterning DNA is achieved through the direct binding of thiol-modified single stranded DNAs to a gold substrate. Once patterned, these molecules become the highly specific probe which will target the analyte molecule which is to be detected using Kelvin Probe.

- *Antibody Patterning*

The antibody-protein system explored in this work is the biotin-avidin system. While biotin can not be strictly defined as an antibody, it serves a similar chemical purpose in that it specifically and strongly binds a target protein. It is possible to pattern biotin directly onto a gold substrate using a thiol-modified biotin molecule, but for this work, a multi-step binding procedure was adopted that will likely be more amenable to other antibody-protein systems (Fig 3.2-1). A detailed accounting of this patterning protocol can be found in Appendix 3.A.

The first step in antibody patterning is to pattern mercaptohexadecanoic acid (MHA) on a clean gold substrate. MHA is a good choice because it is likely the single most amenable molecule to Dip Pen Nanolithography. The result of MHA patterning is carboxylate terminated patterns that can be used as a handle for binding the antibody of interest. After MHA patterning, it is also necessary to passivate the background gold with a self-assembled monolayer that will resist protein and antibody attachment. A good choice for this purpose is a methoxy PEG thiol which produces a pegylated background which is highly hydratable and provides a poor surface for non-selective protein adsorption. In order to accomplish the desired antibody binding, the MHA is activated using carbodiimide chemistry which allows for the spontaneous formation of amides and esters with any primary amines or alcohols on the target antibody.

In this work the target antibody is actually a biotin molecule which has been functionalized with a primary amine (Fig 3.2-2). Biotin is a very simple molecule to pattern in this fashion because it has no extraneous functional groups which might

interfere with the binding protocol. Once patterned, the patterned biotin features are measured using the Kelvin Probe in order to get a baseline measurement. This measurement will be discussed in the 'Detection' section of this chapter.

- *Thiol-Modified DNA Patterning*

DNA detection is a biomolecular system which is extremely amenable to Kelvin Probe analysis. This is largely because DNA molecules have a phosphate backbone which exhibits a large negative charge with an isoelectric point of roughly zero. Another advantage of DNA analysis is that it is quite easy to pattern single stranded DNA on a solid support. In this work, DNA was patterned through the direct Dip Pen Nanolithography of thiol modified DNA molecules (Fig 3.2-3). The two DNA sequences used are 15-mers that are actually short sections of genes taken from anthrax and malaria proteins. These thiol modified molecules can be patterned in a fashion that is described by Demers and Ginger⁽²⁴⁾ and is described in detail in Appendix 3.B.

Just like any dip pen created pattern, DNA can be patterned into a variety of shapes including dots and lines (Fig 3.2-4). It is also important to note that the ability to pattern multiple DNA inks on the same substrate has been demonstrated using anthrax and malaria inks. This ability to write with multiple inks is necessary if this technology is going to be expanded to nanoarray style formats.

While Dip Pen Nanolithography is a useful tool for laboratory scale prototyping, scaling up DNA detection to the level of nanoarrays with millions of DNA probes is probably not feasible using DPN. A better technique would probably be

photolithographic feature creation (Fig 3.2-5). Photolithographic techniques can likely operate at the submicron scale and provide the massively parallel approach to device creation that is needed for nanoarrays.

- *Figures for Section 3.2*

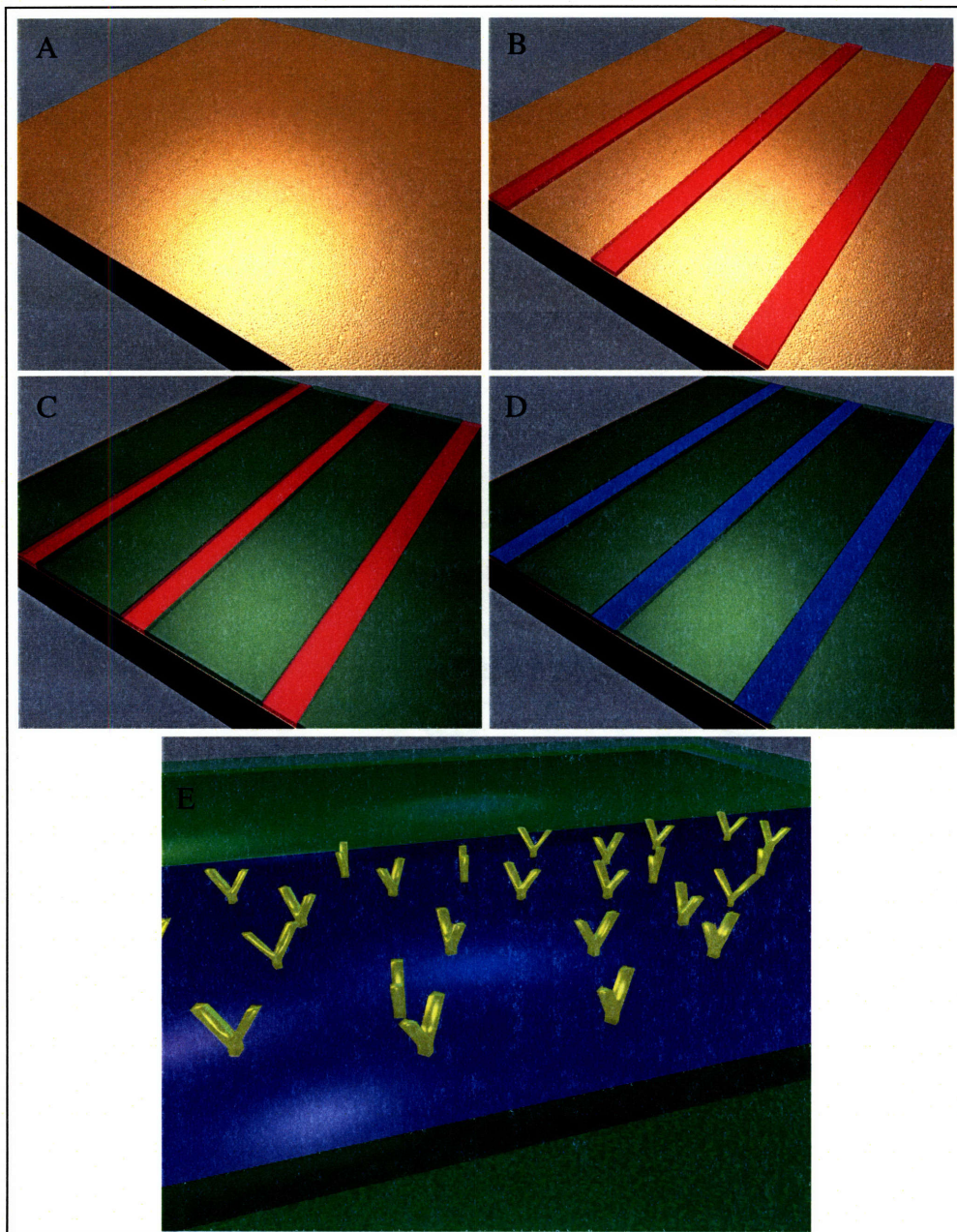
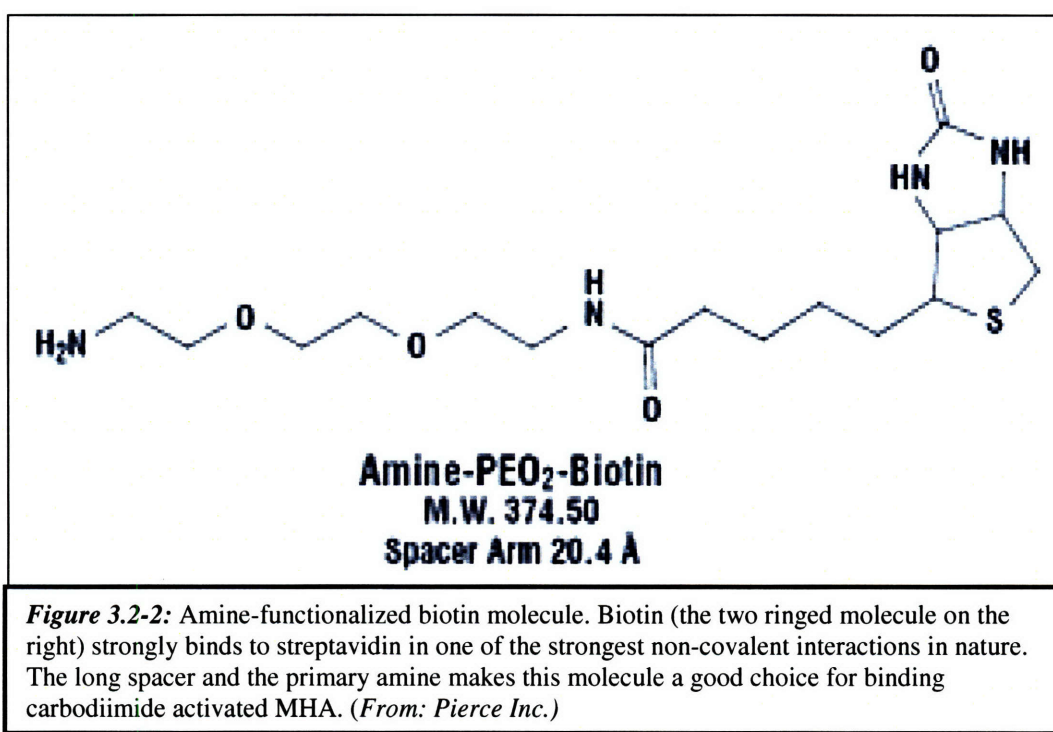
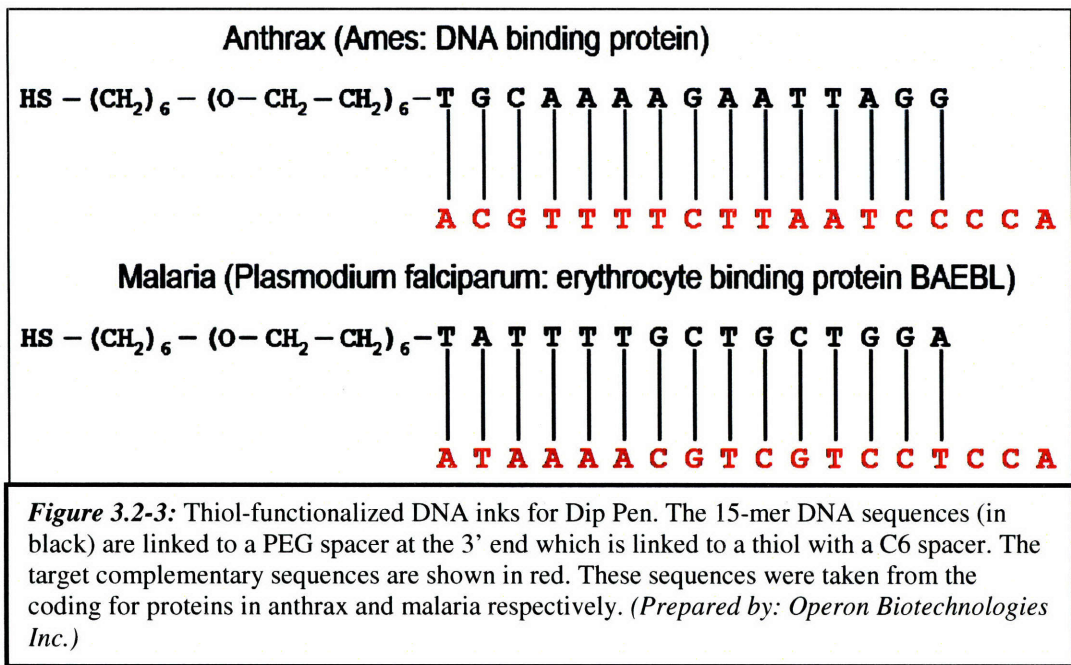
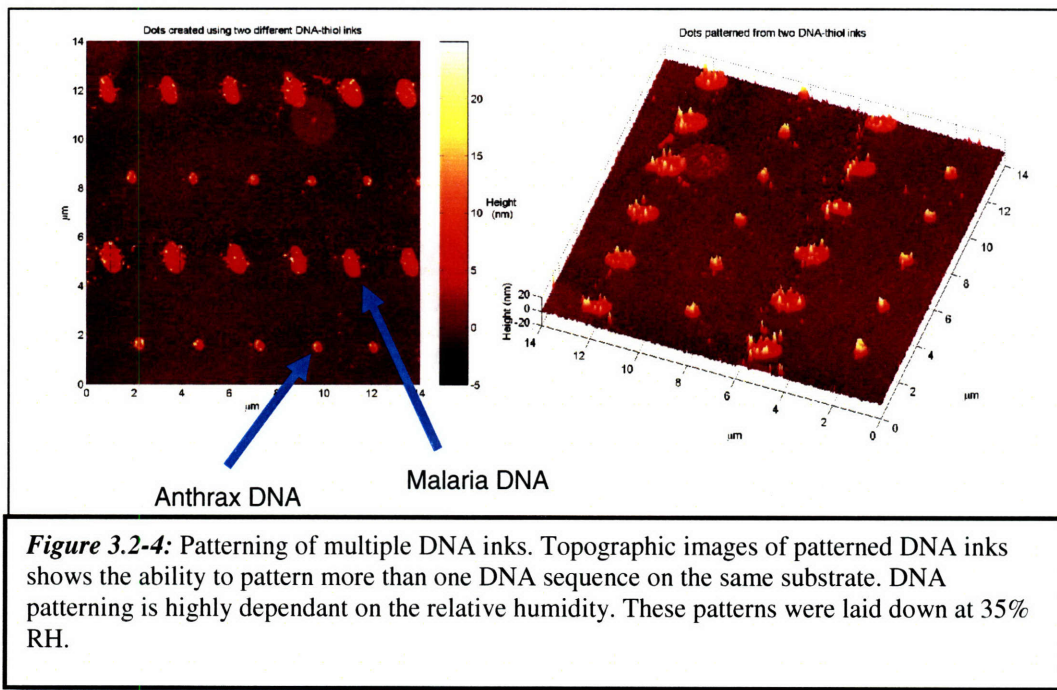


Figure 3.2-1: Schematic protocol for patterning antibodies. (A) Start with a clean gold substrate suitable for dip pen nanolithography. (B) Using dip pen, pattern MHA or another appropriate thiolated molecule. (C) Backfill the unpatterned gold with a thiolated molecule that will resist non-selective protein adsorption (e.g. Methoxy Peg Thiol). (D) Chemically activate the MHA so that it will bind the antibody of interest (e.g. carbodiimide activation). (E) Expose the activated substrate to antibodies which will spontaneously pattern.







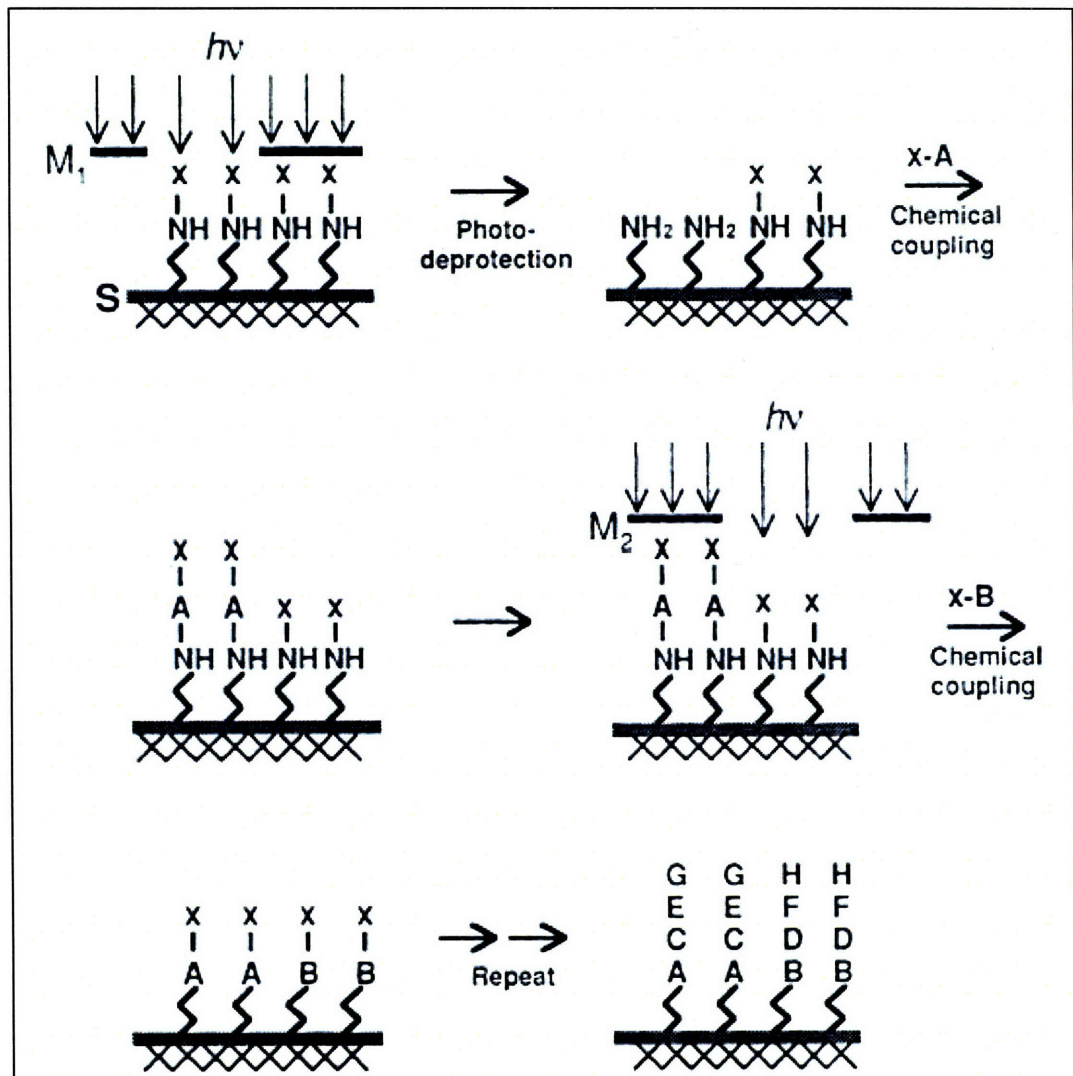


Figure 3.2-5: Spatially addressable photolithographic chemical patterning. Combining mask steps (M1, M2, ...) with photolabile protecting groups provides an elegant route to patterning a variety of molecules including DNA's and polypeptides. (From: Fodor et al. *Science*, 1991⁽¹⁾)

3.3: Detection of bound target analyte molecules

The Kelvin Probe Biosensor presented in this work is based on a conducting AFM tip operating in the vibrating capacitor mode. The AFM nanoprobe approach offers high resolution, high sensitivity and high speed. In order to make a Kelvin Probe measurement, the AFM performs what is known as an interleave scan (Fig 3.3-1). The concept of an interleave scan is that the AFM makes two passes for each scan line. The first pass is a topographic scan operating in tapping mode. For the second pass, the tip is lifted to a set height above the sample surface and scans across the surface following the topography at a constant height. This height control offered by the AFM electronics is a major advantage because Kelvin Probe measurements on small features are highly dependant on the scan height. As the tip is lifted away from the surface, it no longer interacts with the material directly below the tip. Rather, it begins to sample an increasing part of the surface. This causes an averaging affect in the recorded potential, muddying the measurement from any single feature.

For this work, analyte detection is a two part process. The first Kelvin Probe measurement is made after the probe molecule has been patterned. This provides a baseline measurement for the surface potential. The second Kelvin Probe measurement is made after exposure to the target analyte and is compared to the baseline. The difference between the baseline scan and the final scan is the signal provided by the sensor.

This differential approach to scanning has two rather interesting attributes that make it particularly useful for biosensing. The first advantage is that knowing the initial and final potential values can give some quantitative information about the number of

molecules present in a probe feature and the number of target molecules that bind a probe feature. Another useful aspect of this scanning is that it is possible to evaluate the quality of the probe patterning during the baseline scan. One of the most common and insidious manufacturing defects in fluorescent microarrays is when a feature is simply left off a surface⁽¹¹⁾. In a fluorescence system, this will result in a negative spot; potentially a false negative. Because Kelvin Probe measures a native property of the bound biomolecules it can just as easily detect the probe molecules as the target analyte, allowing for simple quality control during manufacturing. A detailed accounting of the Kelvin Probe biosensing can be found in Appendix 3.C.

- *Protein Detection*

The first system tested was the idealized binding between the molecule biotin and the glycoprotein avidin. This system is designed to serve as a model for more general protein microarray approaches. At neutral pH, it is expected that avidin will have a large positive charge because it has an isoelectric point of 10.5. Using DPN, mercaptohexadecanoic acid (MHA) was patterned on gold substrates and then carbodiimide activation was used to cross link amine functionalized biotin with the MHA's carboxylate terminus. Measuring the surface potential before and after exposure to avidin clearly reveals the presence of avidin binding (Fig 3.3-2). As expected, the avidin binding results in a significant increase in surface potential on the patterned features. When this signal is compared to what is seen in the topographic image, it is clear that Kelvin Probe is superior approach to detecting target analyte binding.

When the neutral counterpart to avidin (the deglycosolated 'neutravidin') is put through the same procedure, only a minor change in potential is observed (Fig 3.3-3). This is expected because the isoelectric point of neutravidin is only 6.5 which corresponds to having almost no charge near neutral pH. A more quantitative analysis can be found in Figure 3.3-4 where sections have been taken through the potential images. While avidin-biotin is an illustrative system to work with, it has limited technological relevance. A more interesting system is using DNA as the probe and target molecules.

- *DNA Detection*

A biological system that is more interesting than biotin-avidin and is quite amenable to Kelvin Probe is DNA hybridization. Because of DNA's negatively charged phosphate backbone, it can be readily resolved using Kelvin Probe. The isoelectric point of the DNA backbone is roughly zero which means that under almost any conditions, DNA should be negatively charged. Additionally, the difference in charge between a single stranded DNA and a double stranded DNA should be a factor of two.

The first system tested was to observe what happened when an anthrax-thiol ink was patterned and subsequently exposed to its complement. As expected, a doubling of the surface potential is observed when an anthrax probe is exposed to its complement (Fig 3.3-5). This is confirmation of the ability of this system to detect a target analyte, but also a confirmation that the signal observed is directly correlated with the isoelectric point of the bound molecule. In a second experiment, a patterned anthrax probe was exposed to a malaria complement which should result in no signal. As expected, there

was no change measured in the surface potential signal when an anthrax probe is exposed to a malaria complement and vice versa (Fig 3.3-6). A more quantitative analysis of this experiment reveals clearly that there is a doubling of the surface potential signal when the correct complement is used and no signal change when the incorrect complement is used (Fig 3.3-7). This experiment shows that the Kelvin Probe biosensor exhibits target specificity but also may be useable to gain some quantitative information about the concentration of target analyte present in solution.

In order to address the question of quantitative analysis, some characterization of the DNA binding system was performed as well. This characterization is discussed in the next section.

- *Figures for Section 3.3*

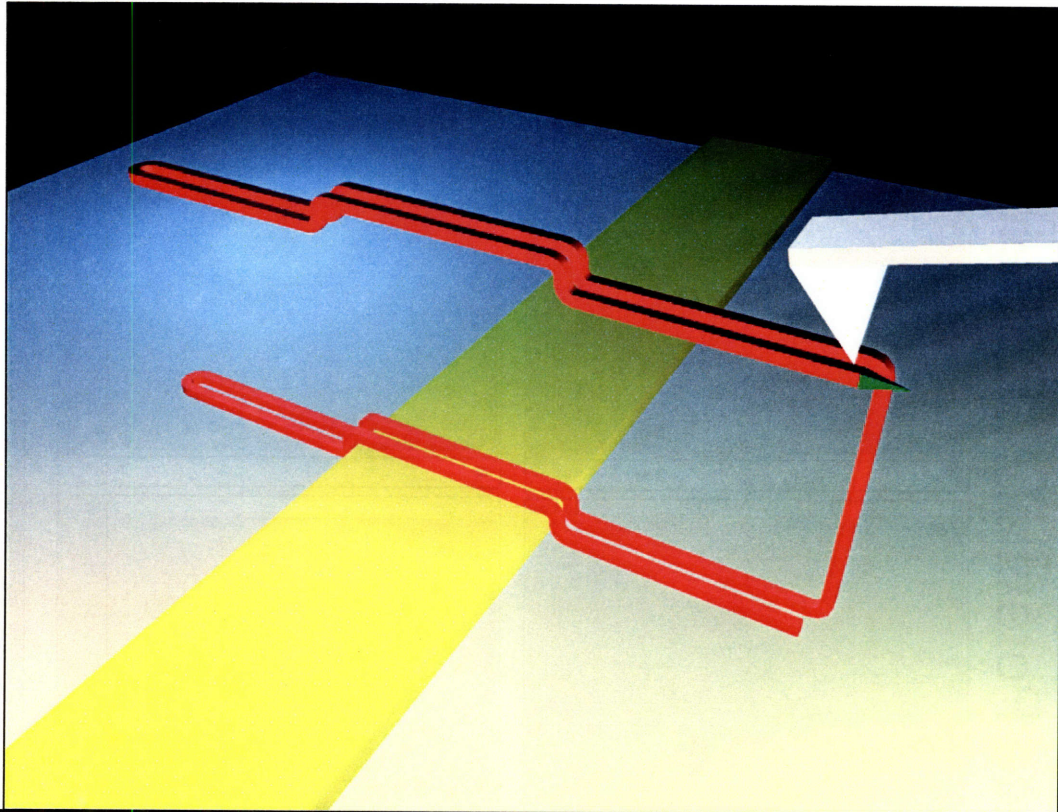
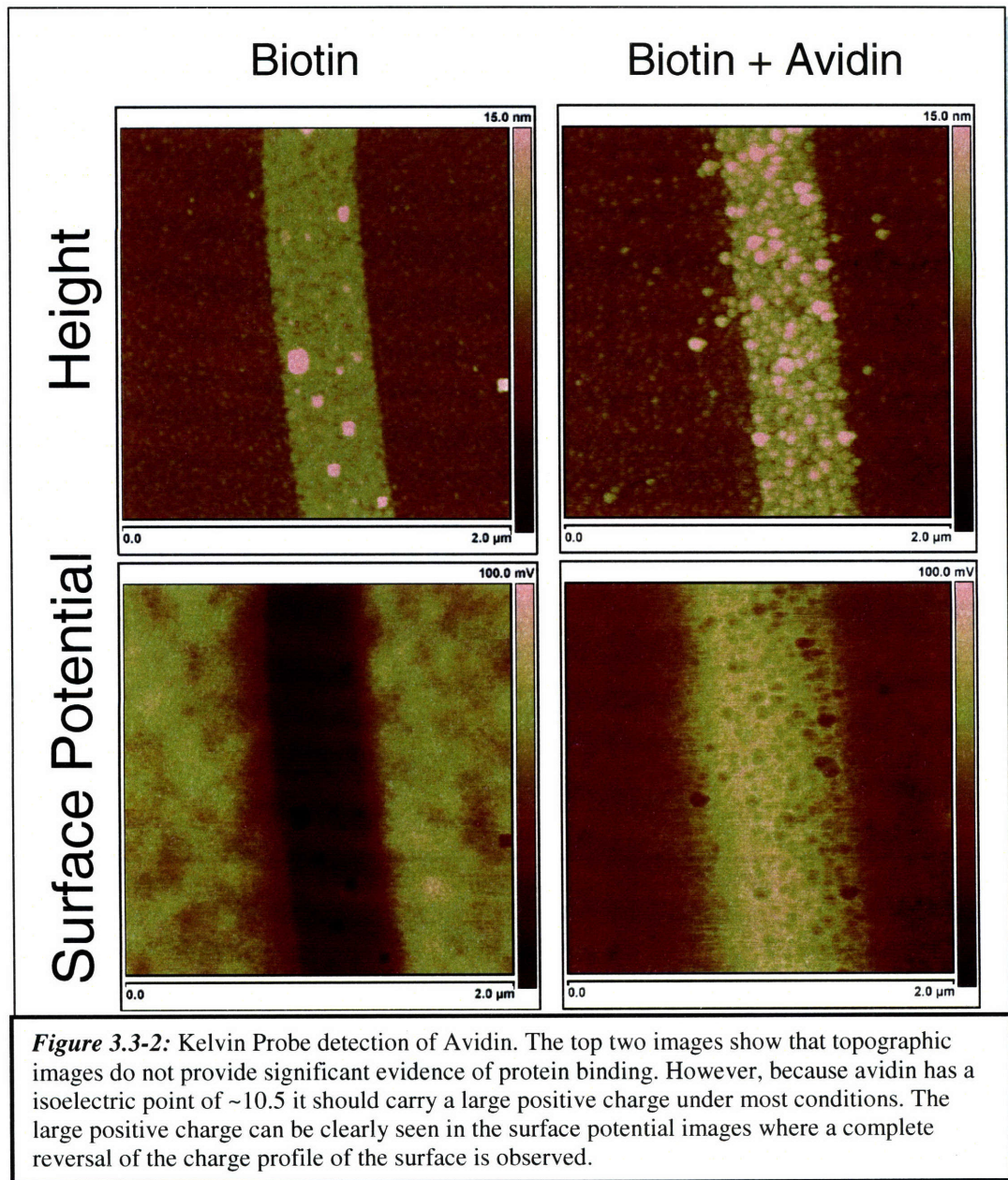


Figure 3.3-1: An AFM tip operating in interleave scan mode. Interleave scanning allows for precise non-contact measurements to be made of a feature of interest. The first scan determines the surface topography and the interleave scan traces this topography to maintain a constant distance between substrate and tip. Surface potential measurements are non-contact and are performed in interleave mode. The lift height used in this work is 15nm unless otherwise stated.



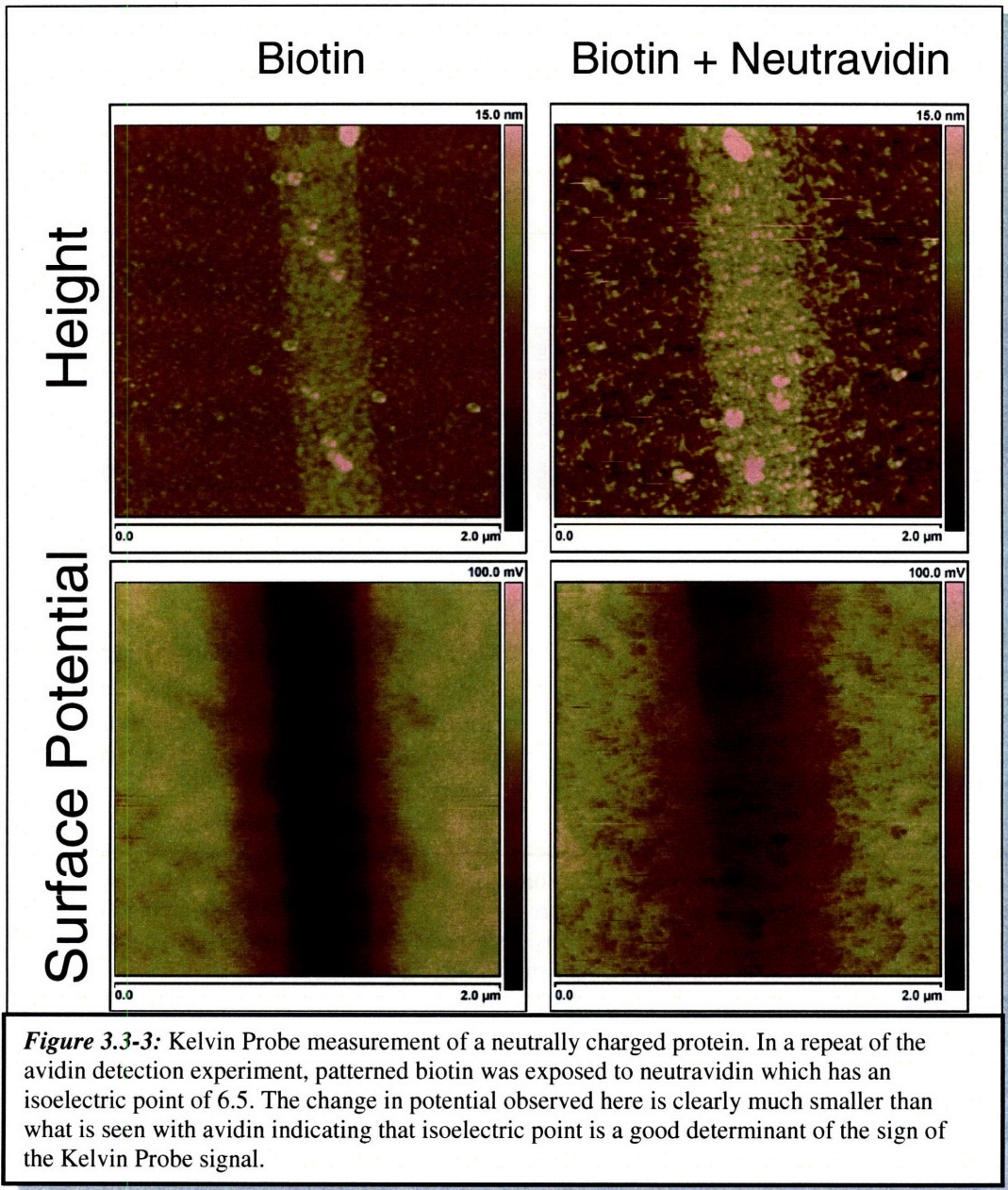
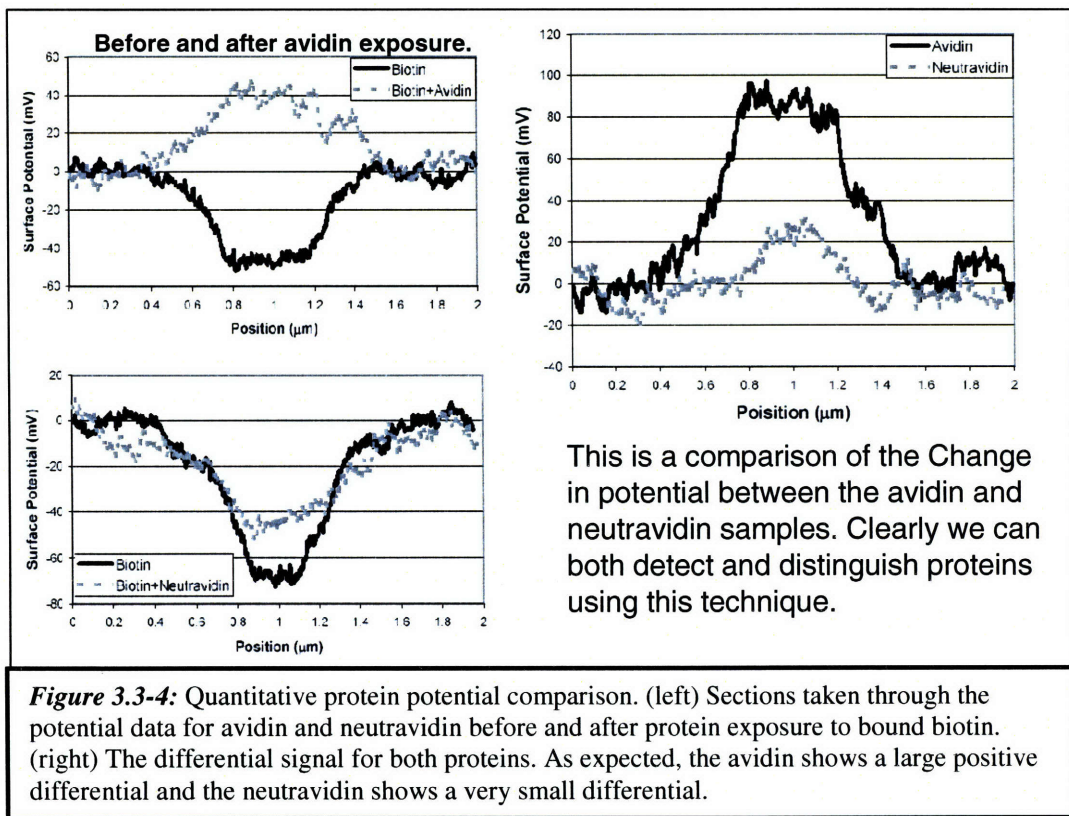
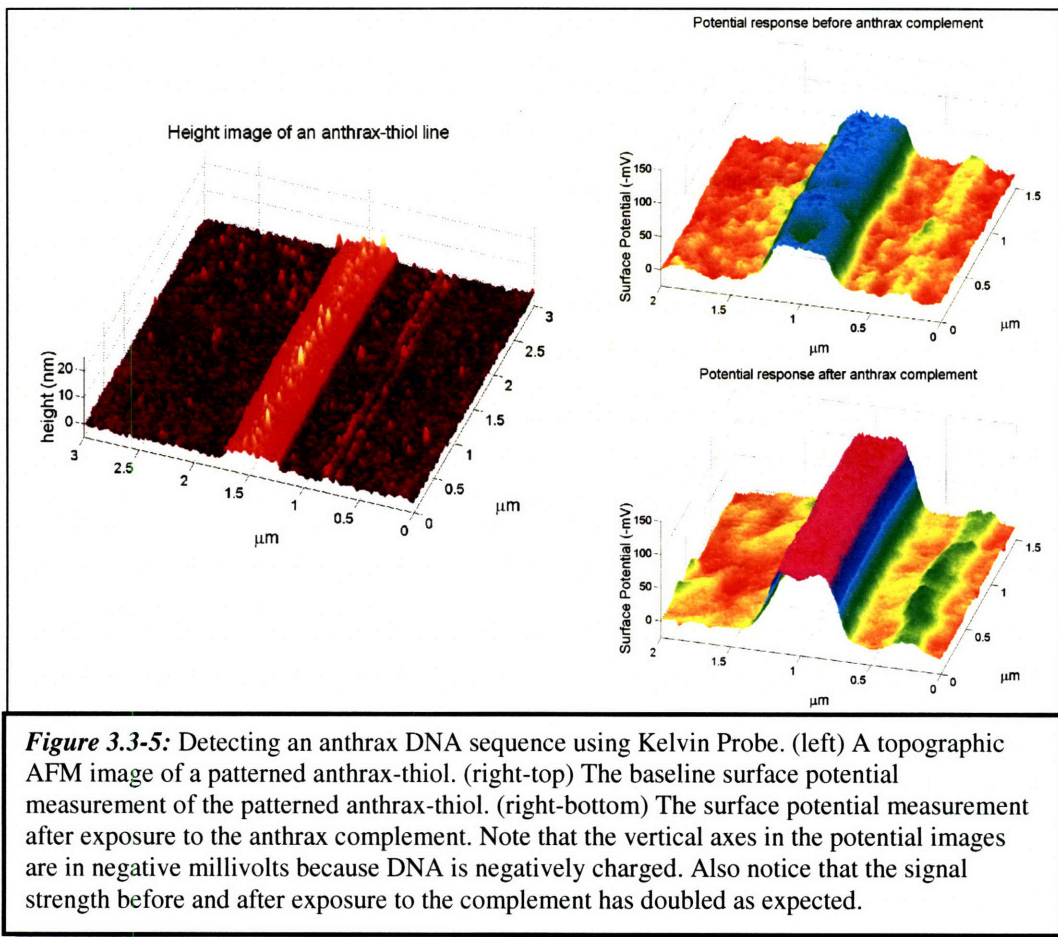
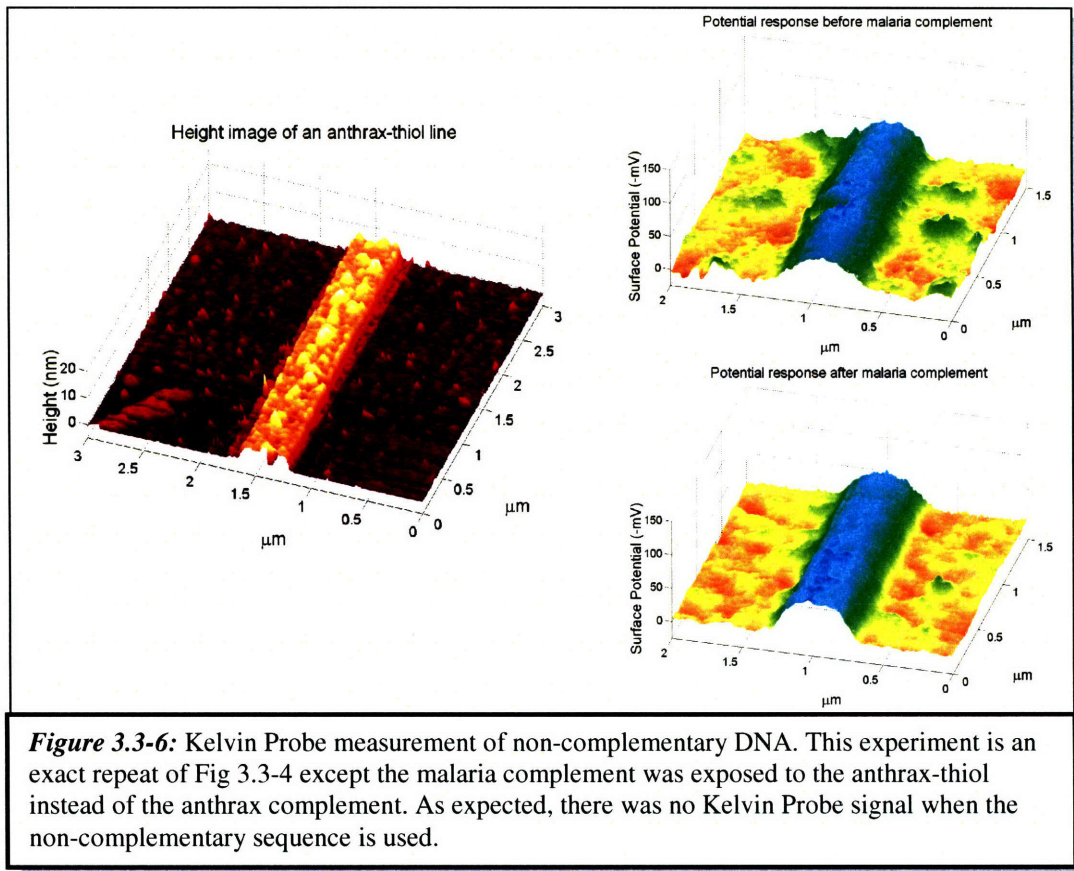


Figure 3.3-3: Kelvin Probe measurement of a neutrally charged protein. In a repeat of the avidin detection experiment, patterned biotin was exposed to neutraavidin which has an isoelectric point of 6.5. The change in potential observed here is clearly much smaller than what is seen with avidin indicating that isoelectric point is a good determinant of the sign of the Kelvin Probe signal.







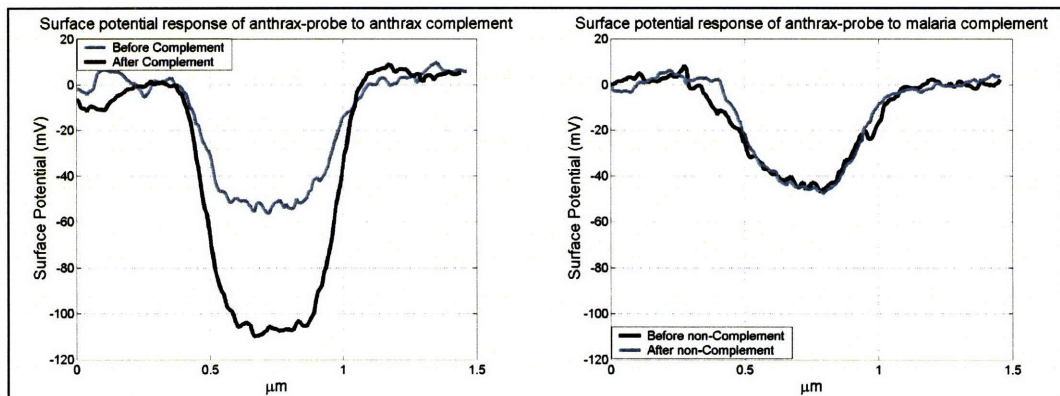


Figure 3.3-7: A quantitative comparison of Kelvin Probe measurements. (left) Clearly the signal from a complementary DNA sequence results in a doubling of signal intensity. (right) No signal change is observed when a non-complementary sequence is used. This doubling signifies that there is almost a perfect 1:1 correspondence between probe molecules and target molecules. It is possible that this relation could be used to gain additional quantitative information about the target molecule.

3.4: Characterization of DNA detection

The Kelvin Probe Biosensor could be characterized in any number of ways, but for this work the characterization focused on several aspects of the binding itself and also on the ability of Kelvin Probe to be pushed to its limits. The system was first tested for its ability to resolve different concentrations of target analyte and for its ability to resolve base pair mismatches in the target analyte. The system was also tested for its ability to resolve very small probe features. The Kelvin Probe itself was characterized using different scan heights to determine just how important scan height is in signal resolution. Also, the Kelvin Probe was tested at different scan rates to determine how scalable this approach would be to large scale integration.

- *Concentration*

The first test of the system was a series of experiments to determine how signal strength relates to target DNA concentration. Given that it is expected that there will be a doubling of surface potential when full complementarity is achieved, it is possible to determine how complete a signal is for a given concentration. The result of this experiment was that the system gives full signal strength at concentrations as low as tens of nanomolar (Fig 3.4-1). These concentrations are not going to break any records for sensitivity but it is still highly sensitive. This is not a single molecule detection scheme, but rather an ensemble measurement subject to mass-action limitations. However, DNA detection schemes have the advantage that they can incorporate polymerase chain

reaction which limits the importance of detection at very high sensitivities. Still, even at 10 nanomolar, the 1 microliter of solution used only has 10 femtomoles of target analyte present which is a very small amount.

- *Base Pair Mismatches*

The system was also tested for its ability to resolve base pair mismatches in a complementary sequence. This is a good test for what sort of specificity could be achievable in a large scale array. It was found in this work that the system could resolve as few as three mismatches (Fig 3.4-2). For a label-free detection approach, this really is quite a remarkable level of specificity⁽²⁶⁾⁽²⁷⁾.

- *Feature Size & Maximum Lateral Resolution*

It is also useful to characterize the ability of the Kelvin Probe system to measure features of various dimensions, specifically small features. From the data presented so far, it is clear that there is some sort of boundary region over which the signal forms. The boundary forms because the tip is not in direct contact with the surface, thus there is an averaging effect on the potential measured which is most obvious near the edge of a feature. This edge effect results in a boundary of roughly 150-200 nm over which the signal attains its maximum value. By treating the boundary region as one half the minimum feature size for which detection would be most quantitative, a feature size of roughly 250nm can be treated as a lower limit for quantitative detection. Manufacturing

and detecting binding on such features was accomplished quite easily (Fig 3.4-3). However, due to limitations from the law of mass-action, a full doubling of the signal intensity is not observed. It is certainly possible to detect even smaller features at the expense of quantitative information. At these dimensions, the feature density is already 1000's of times better than the state of the art in commercial microarrays which typically use 10 μ m features.

The maximum lateral resolution of the Kelvin Probe technique was also explored by finding the smallest possible surface feature that the technique was able to distinguish. It was found that the technique could see surface features smaller than 10nm giving a Kelvin Probe signal with a full width half maximum (FWHM) of ~6nm (Fig 3.4-4). This incredibly small resolution could allow for the creation of incredibly dense nanoarrays that go far beyond anything in use today.

- *Scan Height*

One major advantage of using an AFM for this work is the ability of the tool to control scan height. In this experiment, the importance of this advantage was characterized. It was found that an increase in scan height resulted in a considerable drop-off in signal strength (Fig 3.4-5). This result clearly shows that scanning close to the surface is essential to attain high sensitivity. In fact, for each doubling of scan height, it was found that roughly 25% of the signal strength was lost. Additionally, as the scan height was increased, a significant loss of resolution was observed. This is likely due to an averaging effect that occurs because as the tip is lifted further of the surface, it

samples a larger portion of the surface at any given moment. For these measurements a scan height of 15nm was used which is close enough to give high resolution but not so close as to be concerned with crashing the tip or experiencing Van der Waals interactions.

This characterization reveals that any attempt to scale up this approach will require strong feedback controls for probe height. This scale-up does not necessarily need to have all the controls found in a laboratory AFM, but certain parts of the system would have to be incorporated in order to gain useful results. A detailed accounting of this experiment can be found in Appendix 3.D.

- *Scan rate*

Whenever a scanning probe technique is suggested as a tool for large scale detection, a major question is whether or not it will be fast enough to give useful results. In this experiment the effect of scan rate on signal fidelity was characterized (Fig 3.4-6). While it is expected that the topographic image will blur at higher scan rates, it was interesting to note that the surface potential signal saw no deleterious effects from an increased scan rate over a range from 1 μ m/sec to 256 μ m/sec, and it was even possible to resolve micron scale features at scan speeds as high 1172 μ m/sec.

This ability to scan at high speeds is likely due to the fact that Kelvin Probe is a non-contact technique. As long as the AFM probe has a high enough resonant frequency to sample surface features during each pass, it should be scalable to very high scan rates. At the scan rates presented here the tool could already analyze an array with 1 million sub-micron features in about one thousand seconds. These are analysis speeds on par with

fluorescent microarrays. With an optimized tool, rather than the laboratory system used here, these numbers could probably be improved by orders of magnitude. A detailed accounting of this experiment can be found in Appendix 3.E.

- *Figures for Section 3.4*

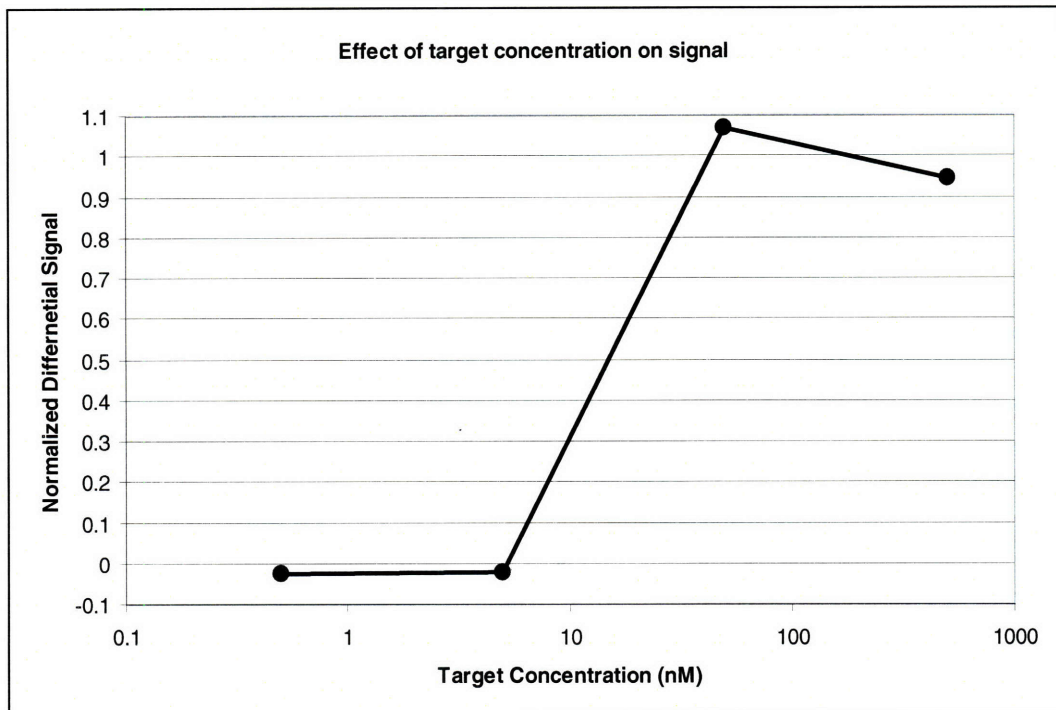
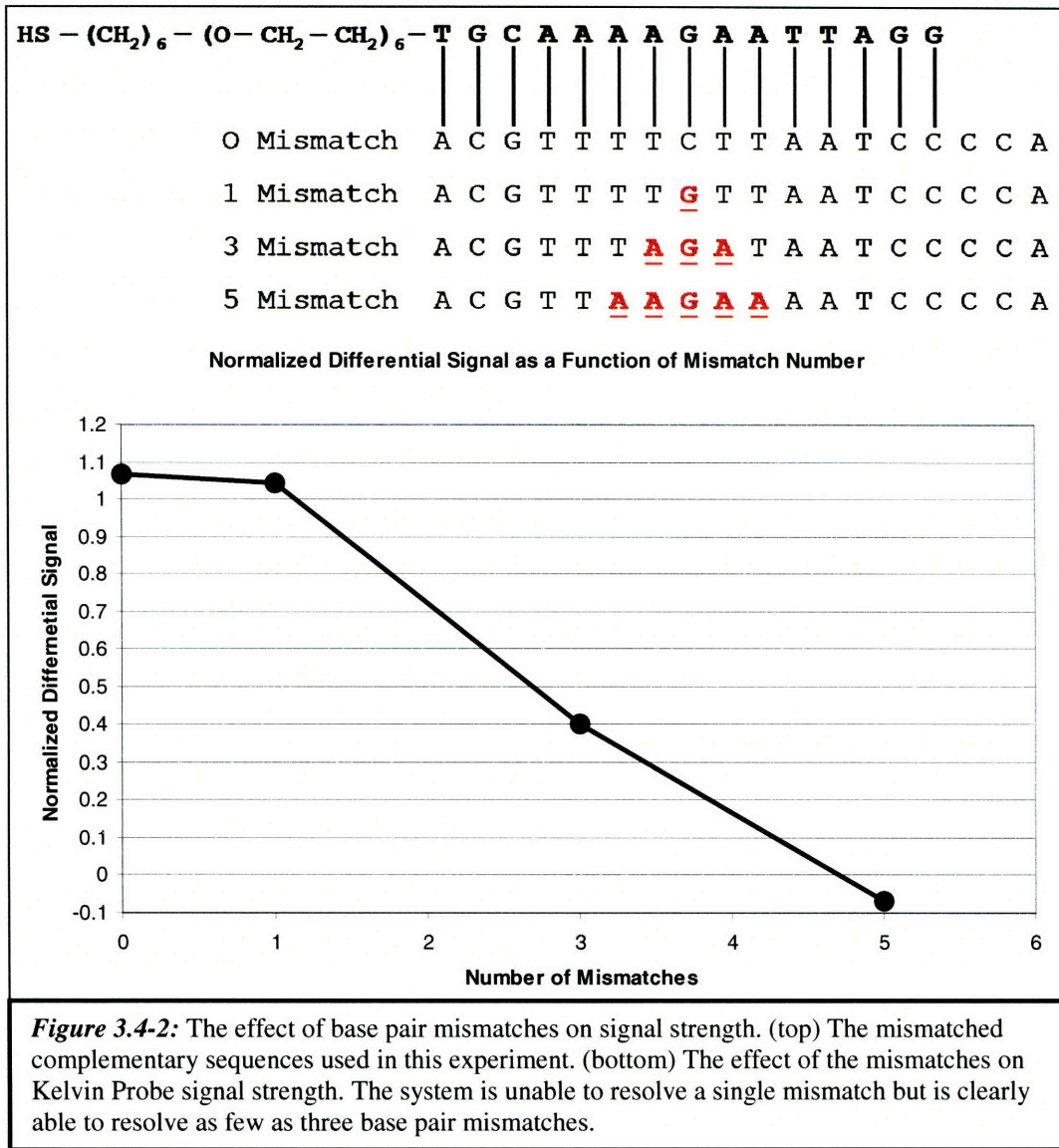


Figure 3.4-1: The effect of target concentration on Kelvin Probe signal. Due to mass-action limitations, it is expected that as the concentration of target molecule decreases, so will the signal strength. As it turns out, the signal on features 1 μ m in diameter is good down to about 50nMolar which is quite sensitive for a label-free ensemble measurement.



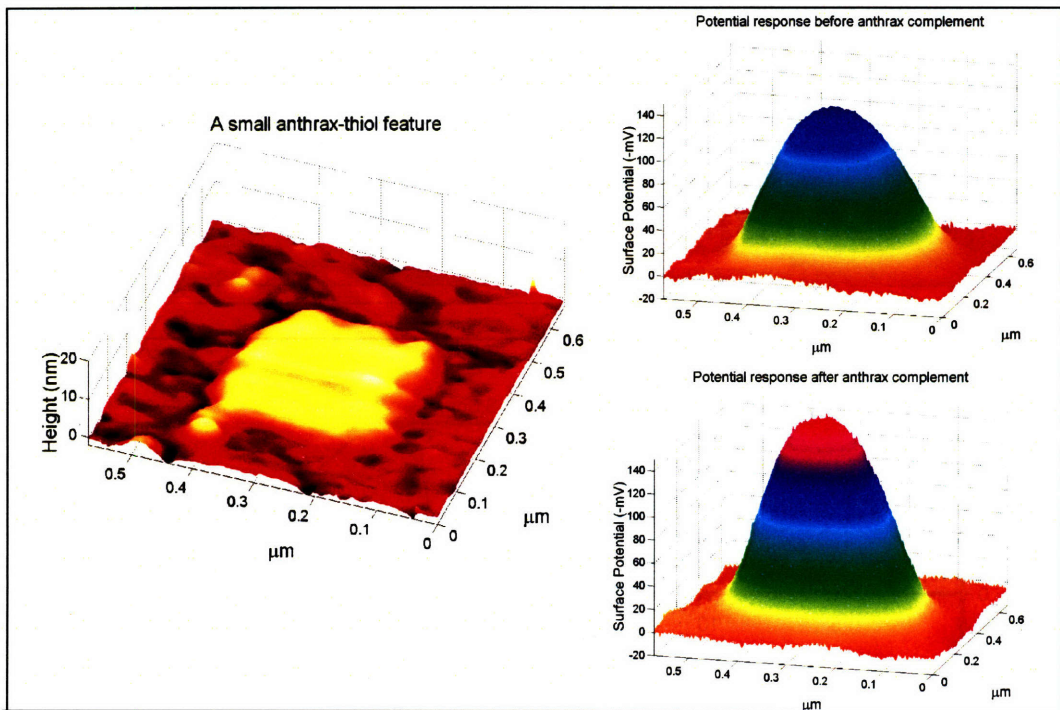
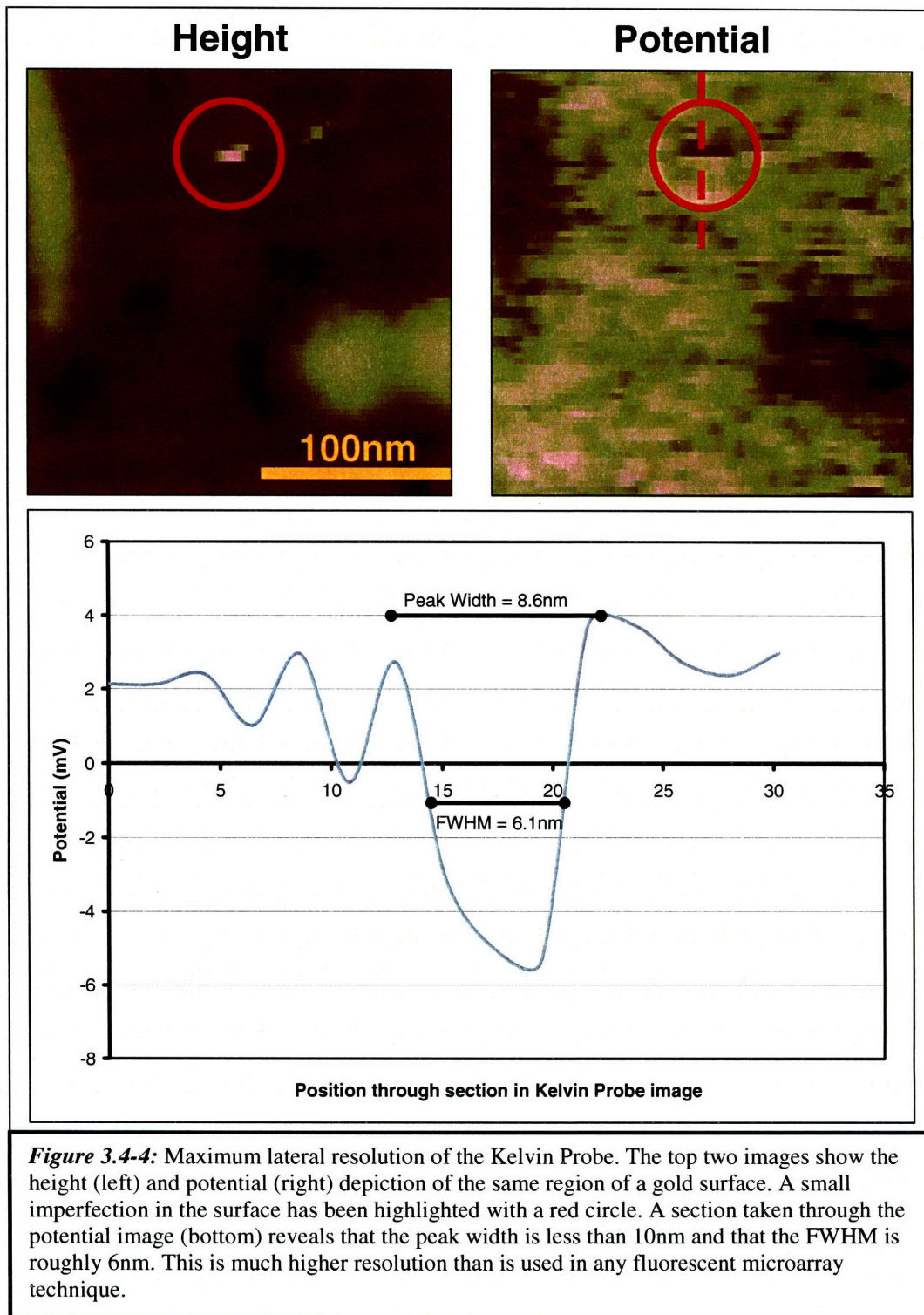
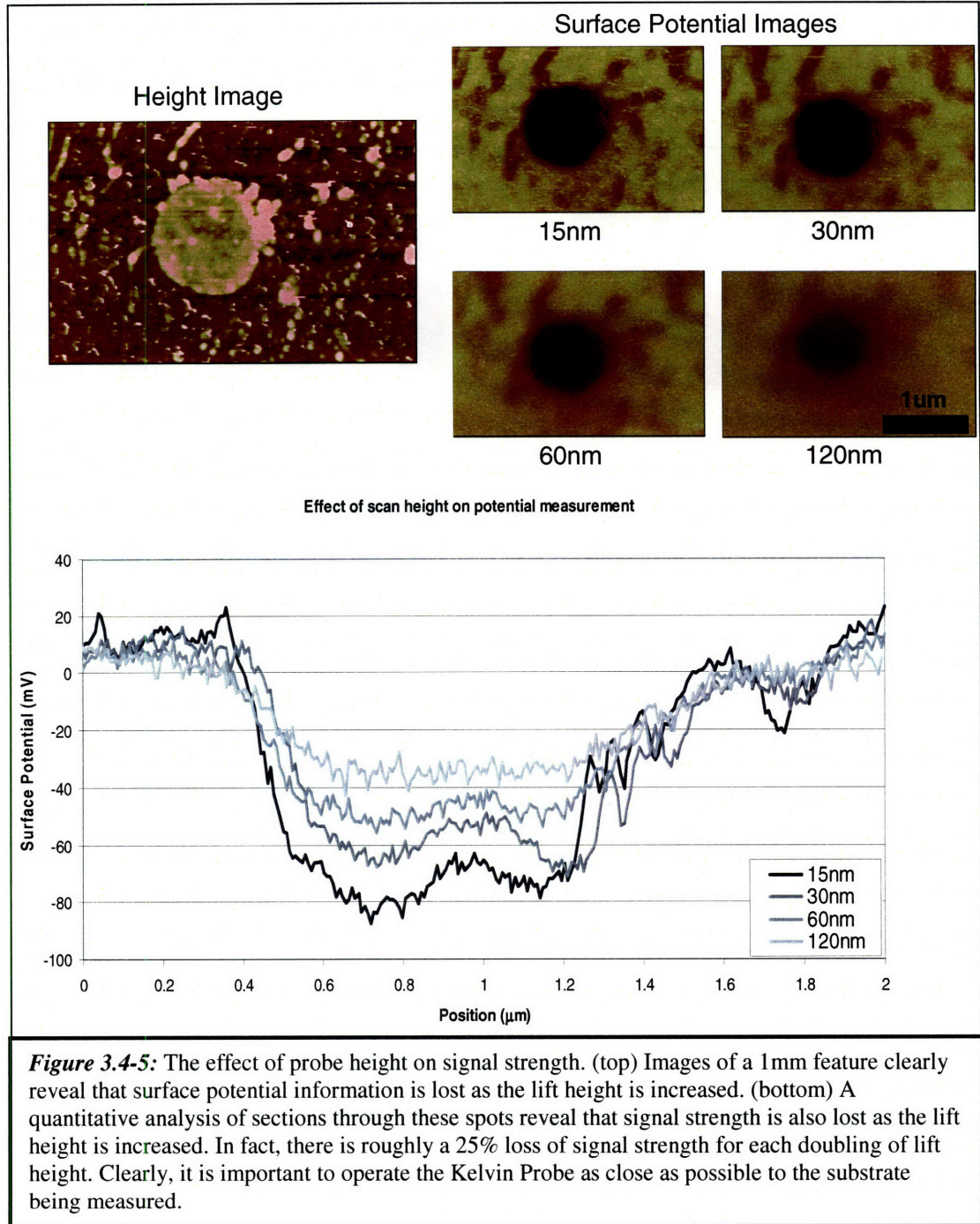
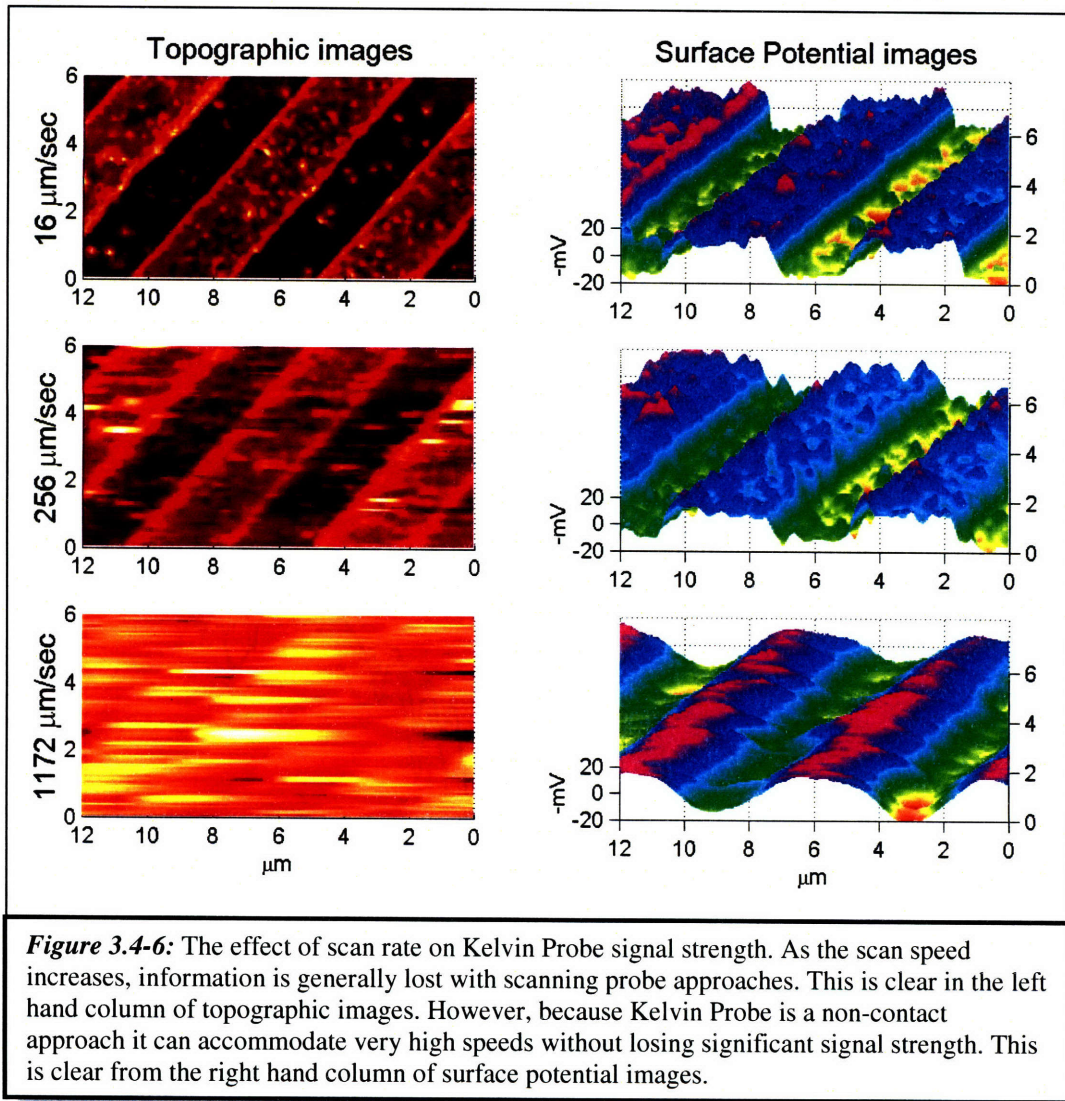


Figure 3.4-3: The ability of Kelvin Probe to resolve nanoscale features. (left) A topographic AFM image of a 250nm anthrax thiol feature. (right-top) The baseline surface potential signal from the anthrax probe feature. (right-bottom) The final surface potential signal after exposure to an anthrax complement. Clearly it is quite easy for the Kelvin Probe to resolve features at this small scale. However, even at this dimension mass-action limitations cause the signal to be less than doubled.







3.5: Discussion & Recommendations for Future Work

This work presents techniques for building and detecting sub-micron and even nanoscale label-free biological features immobilized on a solid support using dip pen nanolithography and Kelvin Probe. In this work, the Kelvin Probe used is actually the conducting nanoprobe of an Atomic Force Microscope (AFM) and the substrates are immobilized biological molecules on a gold surface. Kelvin Probe is a useful biosensing tool because it is simultaneously label-free, high resolution, highly sensitive and potentially high speed. In this work it is demonstrated that the isoelectric point directly correlates with the measured surface potential. Molecules with a low isoelectric point show a negative potential while molecules with a large isoelectric point show a positive potential as expected.

Kelvin Probe has several advantages as a biomolecular detection technique. The first is that it is a non-contact technique that can be carried out under ambient conditions. Because it is non-contact, this detection approach can operate at high speed while maintaining signal fidelity unlike other scanning probe techniques that require substrate contact. Kelvin Probe also has the advantage that it requires no labeling to detect a biomolecule because it is measuring a native property of the target molecule. Using a nanoscale AFM tip for detection confers high lateral resolution on the order of nanometers. Additionally, the distance between the AFM tip and the substrate can be made very small (down to a few nanometers) without worrying about making contact with the surface due to the feedback controls afforded by the AFM controller. This work

demonstrates the highly sensitive detection of surface immobilized biomolecules on features that are as small as a couple hundred nanometers.

This technology is most relevantly comparable to modern DNA microarrays in which $\sim 10\mu\text{m}$ biological features are fluorescently detected on a solid support. The state of the art in microarrays can regularly produce devices with 10^6 features per square centimeters. The features presented in this work are 250nm-1.0 μm which corresponds to feature densities 100 to 1000 times greater than current microarrays. Increased density has two primary advantages. The first, and most obvious, is that greater feature density makes it possible to detect a larger number of target molecules. The second advantage of increased feature density is that less target material is needed to trigger a particular feature. This can be interpreted as an increase in sensitivity.

In terms of feature manufacturing, it is instructive to note that while this work has shown the ability of DPN to create sub-micron DNA features for Kelvin Probe detection, any manufacturing technique can be adapted to Kelvin Probe measurements. One of the most interesting approaches could be massively parallel photolithographic manufacturing which has the promise of producing sub-micron features quite rapidly⁶. Regardless of the manufacturing technique, the Kelvin Probe should maintain its inherent advantages, most notably label-free detection and high resolution.

The most pressing concern with using scanning probe techniques is the speed of a measurement. In this work it was shown that feature fidelity was unhindered at scan rates as high as 256 $\mu\text{m}/\text{sec}$ and speeds as high as 1172 $\mu\text{m}/\text{sec}$ can be attained. At this speed, an array with 10^6 sub-micron features would take on the order of 1000sec to scan which is on par with fluorescent microarray systems. It may be possible to go to even higher

speeds by employing a ‘millipede’⁽²⁸⁾ style detection system with multiple AFM tips simultaneously measuring a sample. These parallel measurements could greatly reduce collection times, but would require many independent cantilevers. Another approach would be the use of so-called high speed AFM technology⁽²⁹⁾. These systems are capable of TV frame rates which would eliminate speed concerns with a Kelvin Probe measurement. Due to the fact that the surface potential measurement is a truly non-contact measurement, the Kelvin Probe is a perfect candidate for high speed AFM measurements.

Another potential advantage of Kelvin Probe Biosensing that invites further study is the ability of this technique to acquire dynamic data about the concentration of analyte present in solution. Fluorescence has not been able to provide high quality quantitative data because the fluorescent yield of a fluorophore is so sensitive to its local chemical environment. It is likely that measurements of isoelectric points will not have this same sensitivity and so may be able to overcome this hurdle. This would be a tremendous advantage over conventional fluorescent microarray approaches.

This work has demonstrated the feasibility of using a Kelvin Probe detection scheme for sensing biological molecules in an array format at the sub-micron scale. By measuring native properties of biological molecules we are free to avoid labeling chemistry that can limit the efficiency of label-based measurements. The next challenge comes from building a dedicated a device to perform these sorts of measurements, but in the meantime, any multimode AFM is capable of providing useful results.

Appendix 3.A: Antibody Patterning

As described previously, Antibody patterning is a multistep process that bears more than a passing resemblance to covalent virus patterning (Appendix 2.B). Essentially in this protocol, in lieu of patterning M13 phage via its terminal amine, an antibody is being patterned through a primary amine.

A schematic depiction of this process was shown in figure 3.2-1.

Dip Pen Nanolithography:

Pattern MHA using DPN - See Appendix 2.B

Backfilling:

Backfill using methoxy PEG Thiol - See Appendix 2.B

Activation:

Similarly to covalently patterning viruses, for patterning antibodies the patterning used is based on carbodiimide chemistry. However, because the biotin derivative used has no carboxylate groups (Fig 3.2-2) it can be added directly to the carbodiimide solution with the MHA rather than after a rinse step.

The activation was accomplished by first exposing the backfilled substrate to a solution of EDC (25mM) and S-NHS (50mM) in HEPES for 15 minutes as a pre-activation. This was subsequently rinsed briefly with HEPES. It was then exposed to a solution containing the biotin-amine (100mM) in the original carbodiimide solution. The exposure lasts for one hour.

After the exposure, the sample is rinsed in HEPES

At this point the antibody (in this case biotin) has been patterned. It can now be used to pattern any protein in the avidin family.

Appendix 3.B: DNA Dip Pen Nanolithography

DNA was patterned using the technique described by Demers and Ginger⁽²⁴⁾.

The thiolated DNA inks used in this work (Fig 3.2-3) were supplied by Operon Biotechnologies Inc. The gold substrates were prepared in the fashion described in Appendix 2.A.

The DNA ink is a 1mM solution of thiolated-DNA and 300mM magnesium chloride in dimethylformamide. The MgCl₂ is important because it allows the DNA to pack tightly on the surface by compensating for the negatively charged DNA backbone. However, the magnesium ions must be removed in order to get a good Kelvin Probe image.

The first step is coating the AFM tip with ink. An NP (or NP-S) tip by VEECO is cleaned in Pirhana (3:1::H₂SO₄:H₂O₂ – Caution: extremely dangerous, use proper PPE) for 60 seconds. The tip is then silanized to promote ink adhesion (1mM 3-aminopropyl trimethoxy silane in toluene) for 1 hr. The tip is rinsed in toluene and allowed to air dry. Once dry, the tip is dipped in the DNA solution for 5-10 seconds and allowed to dry.

DNA dip pen is carried out in a fashion which is similar to dip pen with MHA which is described in Appendix 2.B. However, DNA has certain characteristics for dip pen nanolithography that make a challenge molecule to pattern.

Writing with DNA is highly humidity dependant. At relative humidities below 30%, the ink will hardly right at all. At relative humidities above 40%, the ink will come off in globs and it is quite difficult to pattern nanoscale features. Based on experience, 35% relative humidity is the most versatile, but even then it can be a little finicky.

The easiest feature to write is a dot which can be created even at higher humidities by merely touching the tip to the surface but not moving it. The length of time the tip is in contact with the surface will determine the dot size through ink diffusion. At high humidities, the tip need not touch the surface for more than a second. The writing presented in this work was all done at relative humidities between 30% and 40%.

Once patterned, it is necessary to backfill the unpatterned gold background. The backfill molecule chosen for this application is octadecane thiol (ODT). This molecule was chosen because it creates a highly hydrophobic background while DNA is highly hydrophilic. Also, because it is a relatively small and simple molecule, it will create a decent monolayer very quickly. The solution used is 1mM ODT in ethanol and the patterned sample is immersed for 5 minutes followed by a brief rinse in ethanol. The sample was then rinsed in TBS for 30 minutes to facilitate ion exchange (sodium for magnesium) followed by a 15 minute rinse in DI water to remove as much sodium as possible.

Appendix 3.C: Kelvin Probe Biosensing Protocol

Once probe molecules have been patterned and backfilled (Appendix 3.A and appendix 3.B), the patterned substrate is now ready to detect target molecules.

The first step is to take a baseline Kelvin Probe measurement of the patterned target molecule. This was accomplished using a Veeco Multimode AFM with a Nanoscope IV controller. MESP conducting tips (Veeco) were mounted in an MMEFCH tip holder (Veeco) which is capable of controlling the tip voltage.

The AFM is operated in tapping mode and interleave mode. Performing a Kelvin Probe scan requires several settings in the AFM software. First, an image should be optimized in typical tapping mode. Then the system needs to be changed to interleave mode. This is done by changing several settings in the interleave menu.

First, interleave mode should be set to 'Lift'. Then the scan height should be set, in this work 15nm was used. Then the input feedback should be changed to 'Potential'. Then the data type on channel two should be set to 'Potential' and the line direction for all channels should be set to 'Retrace'. It is important that the line directions are in retrace because otherwise the lifting and dropping of the tip for the interleave scans will hurt imaging.

Some tuning can be done of the interleave drive amplitude and drive phase. In this work, these settings were always run at 6000mV and 0° respectively. Image tuning can be done using the interleave gains, but these were generally found to have little influence on image quality and in general the proportional gain was set to 1 and the integral gain was set to 1.5.

Frequently, running an interleave scan will hurt the quality of the topographic image, this can be avoided by lowering the scan rate or adjusting the Proportional and integral gains. Typical scan rates used are between 1 $\mu\text{m}/\text{sec}$ and 10 $\mu\text{m}/\text{sec}$. Once the image quality is satisfactory, the baseline potential scan can be completed.

Once the baseline potential image has been acquired the next step is exposing the patterned substrate to the target molecule. In this work, two different types of target molecule are used, proteins (avidin, neutravidin) and DNA. The exposure solution is different in the two cases and is described below.

For protein, the solution used was a 5 μM solution of the target protein in HEPES buffer. The protein concentration used is much higher than what is necessary given the nature of the biotin-avidin couple, but for proof of concept, it is appropriate. After exposure to the target protein solution the samples were rinsed with HEPES.

For DNA, the exposure solution is 1.5mM MgCl_2 in TBS with whatever concentration of DNA is desired. The MgCl_2 is used to again compensate the charge of the DNA backbone so it can pack more easily. After the target DNA exposure it is necessary to soak the sample in TBS for half an hour to facilitate ion exchange (Na^+ for Mg^{2+}) followed by a water soak to remove as much sodium as possible.

Once dry, the exposed sample can be imaged using Kelvin Probe as described previously. This scan will provide the final signal that can be compared to the baseline to determine if target detection has actually occurred.

Appendix 3.D: Scan Height Characterization of Kelvin Probe

Characterization of the effect of scan height has revealed that it is very important when performing Kelvin Probe measurements. This characterization was done by patterning a 1 μ m diameter spot on a gold substrate using the procedure described in Appendix 3.B.

A series of Kelvin Probe scans were performed using the procedure described in Appendix 3.C for the baseline scan.

When each scan was complete, the 'Scan Height' setting in the interleave pulldown menu could be adjusted to whatever setting was desired. Once complete, the various scans could be compared and sections could be taken to gather quantitative data.

Appendix 3.E: Scan Rate Characterization of Kelvin Probe

It turns out that Kelvin Probe is able to achieve very high scan rates largely because it is a non-contact technique. In this work, scan rate was tested over a range of speeds from $1\mu\text{m}/\text{sec}$ to $1172\mu\text{m}/\text{sec}$.

The samples used to test the Kelvin Probe scan rate were actually microcontact printed samples that were created on silicon substrates. The microcontact printing protocol is described in Appendix 2.F.

Once printed, the samples were mounted on the AFM and scanned using the protocol described in Appendix 3.B for a baseline scan. After each image was complete, the scan rate was increased roughly by a factor of 4.

Very high scan rates are not possible with a very large field on the J scanner so the field had to be adjusted to achieve scans as fast as $1172\mu\text{m}/\text{sec}$. At this rate, the field size was roughly $12\mu\text{m}$.

3.Ref: References

1. **Fodor, S. P. A., R. P. Rava, X. H. C. Huang, A. C. Pease, C. P. Holmes, and C. L. Adams.** 1993. Multiplexed Biochemical Assays with Biological Chips. *Nature* **364**:555-556.
2. **Besocke, K., and S. Berger.** 1976. Piezoelectric Driven Kelvin Probe for Contact Potential Difference Studies. *Review of Scientific Instruments* **47**:840-842.
3. **Zisman, W. A.** 1932. A New Method of Measuring Contact Potential Differences in Metals. *Review of Scientific Instruments* **3**:367-368.
4. **Kelvin, L.** 1898. The Contact Electrification of Metals. *Philosophy Magazine* **46**:82-120.
5. **Fodor, S. P. A., J. L. Read, M. C. Pirrung, L. Stryer, A. T. Lu, and D. Solas.** 1991. Light-Directed, Spatially Addressable Parallel Chemical Synthesis. *Science* **251**:767-773.
6. **Ekins, R., F. Chu, and E. Biggart.** 1989. Development of Microspot Multi-Analyte Ratiometric Immunoassay Using Dual Fluorescent-Labeled Antibodies. *Analytica Chimica Acta* **227**:73-96.
7. **Schena, M., D. Shalon, R. W. Davis, and P. O. Brown.** 1995. Quantitative Monitoring of Gene-Expression Patterns with a Complementary-DNA Microarray. *Science* **270**:467-470.
8. **Drmanac, R., S. Drmanac, Z. Strezoska, T. Paunesku, I. Labat, M. Zeremski, J. Snoddy, W. K. Funkhouser, B. Koop, L. Hood, and R. Crkvenjakov.** 1993. DNA-Sequence Determination by Hybridization - a Strategy for Efficient Large-Scale Sequencing. *Science* **260**:1649-1653.
9. **Schena, M., R. A. Heller, T. P. Theriault, K. Konrad, E. Lachenmeier, and R. W. Davis.** 1998. Microarrays: biotechnology's discovery platform for functional genomics. *Trends in Biotechnology* **16**:301-306.
10. **Ramsay, G.** 1998. DNA chips: State-of-the-art. *Nature Biotechnology* **16**:40-44.
11. **Dufva, M.** 2005. Fabrication of high quality microarrays. *Biomolecular Engineering* **22**:173-184.
12. **Marshall, A., and J. Hodgson.** 1998. DNA chips: An array of possibilities. *Nature Biotechnology* **16**:27-31.
13. **Ekins, R., and F. Chu.** 1992. Multianalyte Microspot Immunoassay - the Microanalytical Compact-Disk of the Future. *Annales De Biologie Clinique* **50**:337-353.
14. **Ekins, R. P., and F. W. Chu.** 1991. Multianalyte Microspot Immunoassay - Microanalytical Compact-Disk of the Future. *Clinical Chemistry* **37**:1955-1967.
15. **Frank, R.** 1992. Spot-Synthesis - an Easy Technique for the Positionally Addressable, Parallel Chemical Synthesis on a Membrane Support. *Tetrahedron* **48**:9217-9232.
16. **Ekins, R. P., and F. W. Chu.** 1995. Miniaturized Microspot Multianalyte Immunoassay Systems. *Immunoanalysis of Agrochemicals* **586**:153-174.
17. **Bier, F. F., and F. Kleinjung.** 2001. Feature-size limitations of microarray technology - a critical review. *Fresenius Journal of Analytical Chemistry* **371**:151-156.

18. **Cheran, L. E., S. Sadeghi, and M. Thompson.** 2005. Scanning Kelvin nanoprobe detection in materials science and biochemical analysis. *Analyst* **130**:1569-1576.
19. **Cheran, L. E., M. Chacko, M. Q. Zhang, and M. Thompson.** 2004. Protein microarray scanning in label-free format by Kelvin nanoprobe. *Analyst* **129**:161-168.
20. **Thompson, M., L. E. Cheran, M. Q. Zhang, M. Chacko, H. Huo, and S. Sadeghi.** 2005. Label-free detection of nucleic acid and protein microarrays by scanning Kelvin nanoprobe. *Biosensors & Bioelectronics* **20**:1471-1481.
21. **Cheran, L. E., M. E. McGovern, and M. Thompson.** 2000. Surface immobilized biochemical macromolecules studied by scanning Kelvin microprobe. *Faraday Discussions*:23-34.
22. **Hansen, D. C., K. M. Hansen, T. L. Ferrell, and T. Thundat.** 2003. Discerning biomolecular interactions using Kelvin probe technology. *Langmuir* **19**:7514-7520.
23. **Laoudj, D., C. Guasch, E. Renault, R. Bennes, and J. Bonnet.** 2005. Surface potential mapping of dispersed proteins. *Analytical and Bioanalytical Chemistry* **381**:1476-1479.
24. **Demers, L. M., D. S. Ginger, S. J. Park, Z. Li, S. W. Chung, and C. A. Mirkin.** 2002. Direct patterning of modified oligonucleotides on metals and insulators by dip-pen nanolithography. *Science* **296**:1836-1838.
25. **Piner, R. D., J. Zhu, F. Xu, S. H. Hong, and C. A. Mirkin.** 1999. "Dip-pen" nanolithography. *Science* **283**:661-663.
26. **Storhoff, J. J., R. Elghanian, R. C. Mucic, C. A. Mirkin, and R. L. Letsinger.** 1998. One-pot colorimetric differentiation of polynucleotides with single base imperfections using gold nanoparticle probes. *Journal of the American Chemical Society* **120**:1959-1964.
27. Based on a discussion with J. Leighton Read of Alloy Ventures.
28. **Vettiger, P., M. Despont, U. Drechsler, U. Durig, W. Haberle, M. I. Lutwyche, H. E. Rothuizen, R. Stutz, R. Widmer, and G. K. Binnig.** 2000. The "Millipede" - More than one thousand tips for future AFM data storage. *Ibm Journal of Research and Development* **44**:323-340.
29. **Hansma, P. K., G. Schitter, G. E. Fantner, and C. Prater.** 2006. Applied physics - High-speed atomic force microscopy. *Science* **314**:601-602.

Conclusions and Closing Remarks:

In this work, we have exploited the interactions that occur between biological molecules and inorganic surfaces. These interactions were studied in three forms: the biomolecular interaction of proteins with crystal defects, the templated patterning of genetically programmed viruses and the sensing of immobilized biological molecules using Kelvin Probe Microscopy. These three projects have all achieved considerable success and have provided considerable opportunity to learn about the overlap of materials science and biochemistry. Additionally, this process of pursuing a PhD has allowed for becoming more intimately aware of scientific inquiry in general.

As is usually the case at the end of PhD experience, each project has considerable room for future work which could help to elucidate the phenomena and mechanisms involved. I have done my best to provide suggestions for what would be the most obvious next step for future study. It is almost always true that research is never really finished; rather it is passed on to the next researcher to take in his or her own direction. What does remain from one researcher to the next is the persistent knowledge that builds into better and better results. This knowledge is often assembled from a series of ‘constructive failures’ which I have certainly experienced. The best example would be my first project on biomolecular recognition of crystal defects. I had to iterate basically every step of that

work in order to find conditions that created what I wanted. In the end, the knowledge that I found most exciting from that work was not the specific defect binding, but the overall approach to diffuse selection. In general, what I found most enjoyable about my PhD experience was getting to be a part of the great scientific enterprise, even if my role was small. That being said, I would like to take a moment to reflect on where this enterprise came from.

Francis Bacon is the father of the scientific method (sometimes referred to as the Baconian method), which is no small feat. He receives little fanfare for this contribution which was in many ways necessary to allow the Enlightenment. Francis Bacon's most important work is his *Novum Organum* (The New Organon[‡]- 1620) in which he lays out the Baconian approach to observing nature. The text is lengthy and too long to summarize here, but I feel that there is one part that is particularly worth mentioning. The first book of the *Organon* is a listing of aphorisms favored by Bacon. The third aphorism reads:

Human knowledge and human power meet in one; for where the cause is not known the effect cannot be produced. Nature to be commanded must be obeyed; and that which in contemplation is as the cause is in operation as the rule.

The sentiment that *Nature to be commanded must be obeyed* is such a powerful statement of the underlying principle of the scientific method that I believe it is worth noting. As Prof. Lionel Kimerling has commented, research is a balance between arrogance and humility; the arrogance to believe that nature can be commanded and the humility to realize that we do not get to decide the ground rules. The scientific method is an attempt

[‡] An *Organon* is an instrument for acquiring knowledge.

through an iterative project of hypothesis and experimentation to interpret the governing dynamics of nature to the best of our ability.

The researcher must be willing to fail, because failure is constructive and a critically important part of scientific inquiry. I have had the opportunity to experience this process first hand during my time at MIT and for that I thank everyone who made it possible.